UNIVERSIDAD NACIONAL AUTÓNOMA DE MEXICO
DOCTORADO EN CIENCIAS (FÍSICA)

Quantum Information Aspects in Holography

TESIS
QUE PARA OPTAR POR EL GRADO DE:
DOCTOR EN CIENCIAS

PRESENTA:
YAITHD DANIEL OLIVAS ARCOS

TUTOR PRINCIPAL:
DR. ALBERTO GÜIJOSA HIDALGO
INSTITUTO DE CIENCIAS NUCLEARES (UNAM)

COMITÉ TUTORAL:
DR. MARIANO CHERNICOFF MINSBERG
FACULTAD DE CIENCIAS (UNAM)

DR. JOSÉ DAVID VERGARA OLIVER
INSTITUTO DE CIENCIAS NUCLEARES (UNAM)

CIUDAD DE MÉXICO, MÉXICO, NOVIEMBRE 2022

Compendio de la tesis:

“Quantum Information Aspects in Holography”

Resumen

Durante las últimas décadas, la correspondencia AdS/CFT ha demostrado ser una excelente herramienta para obtener resultados de teorías cuánticas de campo (TCC) fuertemente acopladas en términos de cálculos gravitacionales. El diccionario holográfico relaciona observables en una TCC con entidades gravitacionales significativas abarcando un amplio espectro de aplicaciones. De esta gama de aplicaciones, un elemento destacado es la conexión entre la teoría de la información cuántica y la gravedad. En esta tesis se presenta una serie de trabajos que exploran la relación entre los conceptos de información cuántica y cantidades geométricas en el bulto gravitacional. En esencia, nuestro trabajo se ocupa de tres de ellos: la entropía de entrelazamiento, la complejidad y la matriz de densidad reducida, que están relacionadas con los subespacios de codimensión dos, uno y cero en el bulto gravitacional, respectivamente.

Contenido de la tesis:

Capítulo 1: Introducción breve a la correspondencia holográfica. En este capítulo se pretende presentar de manera didáctica las herramientas matemáticas y físicas necesarias para comprender el origen de la correspondencia holográfica.

Capítulo 2: En este capítulo se pretende presentar los conceptos fundamentales de la teoría de la información cuántica haciendo énfasis en su traducción holográfica. Se presentan todos los conceptos utilizados en los artículos de investigación listados.

Capítulo 3: Se presenta una exposición breve de todos los artículos publicados durante el curso del doctorado. En particular, se explica cómo las herramientas del capítulo 2 ayudaron al desarrollo de cada investigación. Adicionalmente, se incluyen las conclusiones correspondientes.

Agradecimientos académicos

Quiero expresar mi profundo agradecimiento al Dr. Alberto Güijosa, mi tutor, por aceptarme como su estudiante de doctorado y guiarme en el transcurso de mis estudios. Por siempre haber estado disponible para resolver todas mis dudas además de apoyar y enriquecer mis ideas. Su perspectiva completa y acertada sobre la investigación ha sido invaluable para mí. Su dedicación y apoyo han sido fundamentales en mi formación académica y estoy agradecido de haber tenido la oportunidad de trabajar con él.

A mi comité tutoral conformado por el Dr. José David Vergara Oliver y el Dr. Mariano Chernicoff Minsberg por brindarme una guía complementaria en mis estudios y estar siempre disponibles para resolver mis dudas. Sus conocimientos y experiencia en el área han sido fundamentales para mi desarrollo académico, su apoyo ha sido esencial en la realización de mi investigación.

A mis sinodales, el Dr. José Antonio García Zenteno, el Dr. Saúl Noe Ramos Sánchez, el Dr. Rodolfo Patricio Martínez y Romero, y el Dr. Héctor Hugo García Compean, por haber aceptado revisar esta tesis. Su valiosa contribución en la revisión y evaluación de mi trabajo ha sido fundamental para su mejora y perfeccionamiento.

A los miembros, trabajadores y colaboradores del Instituto de Ciencias Nucleares de la UNAM. El ambiente académico, científico y de colaboración que ofrecen ha sido esencial para mi desarrollo. Estoy agradecido por las oportunidades y los recursos que se me brindaron, así como por la amistad y el apoyo que recibí de todos los miembros de la institución.

Agradecimientos

A Alberto Güijosa por brindarme su amistad. Recuerdo que desde que fui a hablar contigo la primera vez me sentí muy cómodo y en confianza. Tu sabiduría y consejos siempre han sido valiosos para mí y me han ayudado a superar muchos obstáculos en mi vida. No puedo describir lo mucho que he aprendido de ti en los últimos años, me has ayudado a crecer no solo académicamente sino también personalmente. Tu bondad y generosidad son un ejemplo para mí y siempre estaré agradecido por la amistad que hemos construido juntos. Muchas gracias, Alberto.

A mi madre, Diana María Carolina Arcos Martínez, por su constante apoyo y presencia en mi vida. Siempre has sido mi sostén, brindándome las herramientas necesarias para enfrentar las dificultades de la vida con valentía y determinación. Aprecio tu respeto hacia mis decisiones y pensamientos, y tu confianza en mi autonomía. Entiendo el gran sacrificio que has hecho para brindarme lo mejor, nunca olvidaré tu amor y dedicación incondicional. Muchas gracias, mamá.

A mis abuelos Eduardo Arcos y María de Lourdes Martínez por su apoyo constante e incondicional en mi vida. Siempre han estado atentos a mi bienestar tanto físico como emocional. Aprecio los valores y enseñanzas que me han transmitido, y estoy agradecido por la influencia positiva que han tenido en mi vida.

A mis amigos de la facultad, del PCF, del ambiente del baile y a todas esas personas que han tenido un impacto positivo en mi vida. Cada uno de ellos ha contribuido de manera significativa a mi crecimiento personal y desarrollo, ya sea a través de sus consejos, apoyo, risas, y compañía. Aprecio mucho la diversidad de perspectivas y experiencias que cada uno de ellos ha aportado a mi vida. Me han ayudado a ver el mundo desde diferentes ángulos, a aprender nuevas habilidades y enriquecer mi conocimiento.

Contents

List of Figures

Abstract

During the past decades, the AdS/CFT correspondence has proved to be an excellent tool for obtaining results from strongly coupled QFTs in terms of gravitational calculations. The holographic dictionary relates QFT observables with meaningful gravitational entities in an enormous range of applications. From that range of applications, a prominent item is the connection between Quantum Information Theory and Gravity. This thesis presents a series of papers exploring the relationship between quantum information concepts and geometrical quantities in the gravitational bulk. In essence, our work deals with three of them: entanglement entropy, complexity, and the reduced density matrix, which are related to codimension two, one and zero subspaces of the bulk, respectively.

Chapter 1

Introduction to the Holographic Correspondence

Nowadays, humanity possesses at least two physical theories (theoretical frameworks) that describe perfectly some of the phenomena around us. Essentially, it is possible to separate an enormous diversity of phenomena into two categories: the physics of massive, gravitating objects, and the physics of the microscopic world. The latter is known as particle physics, where it is possible to use the Standard Model to describe the basic building blocks of matter and their interactions. This framework has demonstrated a lot of success over the last decades. Even though the Standard Model can predict many phenomena, it has some limitations. The most notable is that it cannot describe gravity at the microscopic level. On the other hand, in the world of massive, macroscopic objects, the Theory of General Relativity emphasizes that gravity is a manifestation of spacetime curvature, massive objects curve spacetime, and curved spacetime tells the objects how to move.

1.1 A Brief Review of String Theory

This section includes a review of all the essential ingredients in String Theory needed to understand the holographic correspondence. For efficiency, the intention is not to present all the topics in a formal framework; instead, this chapter should be taken as a practical guide.

The knowledge of the fundamental constituents of matter has always been a central question in Physics. Since the beginning, it has been answered up to a certain level, first by postulating the existence of atoms and eventually by the discovery of all the fundamental particles and their interactions. The central hypothesis in String Theory is that all matter is made of strings. Those strings can vibrate in different frequencies depending on their energy, giving rise to all known fundamental particles.

1.1.1 Worldsheet formulation of String Theory

The first approach to tackle String Theory is to consider a bosonic string moving in spacetime. The aforementioned string is relativistically described by the Nambu-Goto action, which is a non-quadratic expression in the embedding functions $X^\mu(\tau, \sigma)$ which describe the path of the string through spacetime, with (τ, σ) parameters labeling points on the string worldsheet. Quantizing the Nambu-Goto action is challenging, so the traditional path is to work with the Polyakov action, which gives the same equations of motion, but can be expressed as a quadratic expression.

Bosonic String Theory is not the whole history. It contains at least three features that makes this theory incompatible with nature:

- The existence of a tachyon.
- The theory needs 26 spacetime dimensions to be mathematically consistent.
- The absence of fermionic states.

It is known that nature contains fermions. One way to induce the appearance of spacetime fermionic states in the Hilbert space of the theory is by including worldsheet fermionic degrees of freedom in the Polyakov action. This can be expressed in the following way:

$$S\left[X,\Psi\right]=-\frac{1}{2\pi}\int d^2\sigma\left[\frac{1}{2\alpha'}\partial^a X^\mu\partial_a X_\mu-i\Psi^\mu\gamma^a\partial_a\Psi_\mu\right], \tag{1.1}$$

with $\alpha'\equiv l_s^2$, and l_s is a parameter known as the string lenght. The previous formula is commonly known as the Ramond-Neveu-Schwarz action, where Ψ^μ represents a set of D Majorana spinors. The equations of motion obtained from the previous action are

$$\partial^a\partial_a X^\mu=0, \tag{1.2}$$
$$\gamma^a\partial_a\Psi^\mu=0, \tag{1.3}$$

whose solutions can be expressed in terms of $X(\tau+\sigma)$ (left) and $X(\tau-\sigma)$ (right) components and for the bosonic field and $\Psi(\tau+\sigma)$ (left) and $\Psi(\tau+\sigma)$ (right) for the fermionic field. In the case of the bosonic fields, the only set of compatible boundary conditions demand the fields to be periodic. The fermions boundary conditions in the case of closed strings are either of the following:

$$\Psi^\mu(\sigma+2\pi,\tau)=\Psi^\mu(\sigma,\tau)\qquad\text{Ramond,} \tag{1.4}$$
$$\Psi^\mu(\sigma+2\pi,\tau)=-\Psi^\mu(\sigma,\tau)\qquad\text{Neveu-Schwarz.} \tag{1.5}$$

The combinations of periodic and anti-periodic boundary conditions for the left- and right-moving fermionic modes allows the creation of different sectors in the case of a closed string:

- R-R sector
- R-NS sector
- NS-R sector
- NS-NS sector

In the case of an open string, a right-moving mode can be converted into a left-moving mode and vice-versa. Then, the allowed sectors for this case are

- R sector
- NS sector

The identification of the possible boundary conditions for each case (open and closed string) allows the decomposition of the fields in the following form:

$$\Psi^\mu(z)=\sum_{r\in Z+\Delta}\frac{\Psi^\mu_r}{z^{r+\frac{1}{2}}}, \tag{1.6}$$
$$\tilde{\Psi}^\mu(z)=\sum_{r\in Z+\tilde{\Delta}}\frac{\tilde{\Psi}^\mu_r}{z^{r+\frac{1}{2}}}, \tag{1.7}$$

where $z=e^{i(\sigma-\tau)}$, while Ψ^μ_r and $\tilde{\Psi}^\mu_r$ refer to the left and right field modes respectively. As a consequence of the OPE, the previously mentioned operator modes satisfy

$$\{\Psi^\mu_r,\Psi^\nu_s\}=\eta^{\mu\nu}\delta_{r,-s}, \tag{1.8}$$
$$\{\tilde{\Psi}^\mu_r,\tilde{\Psi}^\nu_s\}=\eta^{\mu\nu}\delta_{r,-s}. \tag{1.9}$$

This field decomposition allows in turn the construction of the full Hilbert Space of each sector. In the case of the Neveu-Schwarz sector all the states are bosons, while in the Ramond sector the states are spacetime fermions. Among all the states thus constructed in the Hilbert Space, only a small subset represent physical states compatible with the constraints of the theory.

1.1.2 Open String Spectrum

The open string spectrum refers to the physical states inside the previously described Hilbert Space. Those states must satisfy the following physical constraints imposed at the quantum level:

$$L_{n>0}^{X,\Psi} \left|\text{physical}\right\rangle = 0, \tag{1.10}$$

$$\left(L_0^{X,\Psi} - A_\Delta^{X,\Psi} + A_\Delta^{\text{total}}\right) \left|\text{physical}\right\rangle = 0, \tag{1.11}$$

$$G_{n\geqslant 0} \left|\text{physical}\right\rangle = 0, \tag{1.12}$$

where L_n and G_n are respectively the Fourier (or Laurent) modes of the worldsheet stress-energy tensor and supercurrent. The first and the second condition arise from imposing $T_{ab} = 0$ at the quantum level, meaning that small changes in the fixed metric cannot change physical amplitudes. While the third, arises from imposing the nullification of the supercurrent, that is, $J_a = 0$.

Taking into account the previous quantum conditions, it is possible to identify the physical states in the Neveu-Schwarz and Ramond sectors. Starting with the NS sector, eq.(1.11) gives rise to the on-shell mass condition

$$m^2 = \frac{N - \frac{1}{2}}{\alpha'} \qquad \text{where} \qquad N = 0, \frac{1}{2}, 1, \frac{3}{2}, \cdots \tag{1.13}$$

Therefore, it is possible to clasify all the states depending on the mass obtained at each level. In the case of $N = 0$, the on-shell mass conditions gives rise to a tachyonic state. The second case of study involves $N = 1/2$, at this level only one oscillator mode acting on the ground state is possible. Therefore, the mass condition gives rise to a massless state that can be identified with a gauge vector boson. Application of (1.12) gives rise to the transverse polarization and the gauge transformation properties of the state. Continuous application of the on-shell mass formula to higher levels gives rise to more massive states.

In the Ramond sector, the on-shell mass formula gives the following expression

$$m^2 = \frac{N}{\alpha'} \qquad \text{where} \qquad N = 0, 1, 2, \cdots . \tag{1.14}$$

Given the fact that in this sector all the states are fermions, at $N = 0$ a state is found describing a Dirac fermion (satifies the Dirac equation) with zero mass. Such a state is named Gaugino emphasizing the supersymmetry relation with the gauge boson found in the NS sector.

1.1.3 Closed String Spectrum

In the case of the closed string, an additional condition is needed for the physical states. This conditon arises from the reparametrization invariance under contant shift of the spatial string coordinate. At the quantum level, this condition can be expresed as

$$\left(L_0^{\text{total}} - \tilde{L}_0^{\text{total}}\right) \left|\text{physical}\right\rangle = 0. \tag{1.15}$$

The previous relation can be translated to

$$m^2 = \frac{4}{\alpha'}(N - \Delta) = \frac{4}{\alpha'}(\tilde{N} - \tilde{\Delta}). \tag{1.16}$$

Hence, all the closed string states must be balanced tensor products of left-movers and right-movers. The NS sector can be divided into two components NS_- and NS_+. Each sector is characterized by the eigenvalue obtained when applying $(-1)^F$ over the physical states, where F is the fermion number operator. Therefore, the level matching condition (1.15) can be applied only if the sectors $(\text{NS}_-, \text{NS}_-)$ or $(\text{NS}_+, \text{NS}_+)$ are paired. The main characteristic of the $(\text{NS}_-, \text{NS}_-)$ sector is that, at $N = 0$, it contains a tachyonic state. While the $(\text{NS}_+, \text{NS}_+)$ sector contains the

$$\epsilon_{\mu\nu} \psi^\mu \tilde{\psi}^\nu \left|0, 0, k\right\rangle, \tag{1.17}$$

which describes the massless Supergravity bosonic fields, $g_{\mu\nu}, B_{\mu\nu}$ and ϕ.
In the same manner, the Ramond sector can be divided into two components depending on the eigenvalue obtained when applying the fermionic number operator over the state, R_- and R_+. The following list contains all possible pairings, together with the physical states in each sector:

- (R_+, R_+). Contains states describing antisymetric tensor fields $C(x)$, $C_{\mu\nu}(x)$ and $C^+_{\mu\nu\lambda\rho}(x)$.
- (R_-, R_-). Contains states describing $\hat{C}(x)$, $\hat{C}_{\mu\nu}(x)$ and $C^-_{\mu\nu\lambda\rho}(x)$.
- (R_+, R_-). Contains states describing $C_\mu(x)$ and $C_{\mu\nu\lambda}(x)$.
- (R_-, R_+). Contains states describing $\hat{C}_\mu(x)$ and $\hat{C}_{\mu\nu\lambda}(x)$.

All the fields previous listed are known as Ramond-Ramond fields. Those fields systematically emerge from decomposing the most general Ramond-Ramond state into a direct sum of anti-symmetric tensors.

The last set of possible combinations corresponds to pairing the NS and Ramond sectors in the following way:

- (NS_+, R_+).
- (R_+, NS_+).
- (NS_+, R_-).
- (R_-, NS_+).

All the previous sectors contain states describing dilatino and gravitino fields, only differing in the fermionic number eigenvalue of each state. The null states generated in this sectors lead to an equivalence relation between the states. This relation can be translated to spacetime supersymmetry. Up to this point, we have constructed the string spectrum first by acting with the creation and annihilation operators obtained in the NS and Ramond expansions. Then, we imposed the constraints at the quantum level leaving only those elements representing physical states. Now, it is essential to emphasize that consistency at one loop (modular invariance) requires a further truncation of the previously obtained string spectrum. This truncation, known as GSO projection, gives rise to the various string theories that exist.
Essentially, the GSO projection reduces the whole physical Hilbert space by selecting those elements with a specific eigenvalue for the fermionic number operator. This truncation is defined by the following operation

$$|\text{physical}\rangle_{\text{NS}} \longrightarrow P_{\text{GSO}} \, |\text{physical}\rangle_{\text{NS}} \,, \tag{1.18}$$

where

$$P_{\text{GSO}} = \frac{1}{2}\left[1 \pm (-1)^F\right] \tag{1.19}$$

where the sign is chosen differently for the right-moving modes on the type IIA or IIB string theories. The definition of the GSO projection operator is the same in the NS and Ramond sectors; the only difference is the definition of the fermionic number operator.

1.1.4 Type IIB String Theory and low energy limit

All the previous sections were devoted to an introduction of the main ingredients needed to establish the various types of string theories that exist. In particular, this thesis will focus on a specific string theory known as Type IIB string theory. This theory, after the GSO projection, has the following states divided into the previously defined sectors:

- $\phi(x)$ dilaton field
- $h_{MN}(x)$ graviton field
- $B_{MN}(x)$ Kalb-Ramond field
- $C(x)$ axion field

- $C_{MN}(x)$ Ramond-Ramond 2-form
- $C^{+}_{MNLP}(X)$ Ramond-Ramond 4-form
- $\lambda_s(x)$ first dilatino field
- $\lambda'_s(x)$ second dilatino field
- $\chi_{Ms}(x)$ first gravitino field
- $\chi'_{Ms}(x)$ second gravitino field

Notice here that, since the massless spectrum contains two gravitino fields, the metric field can be connected to these states via two different supersymmetry transformations, as inferred from the theory's name. Type IIB string theory aims to be a candidate theory to correctly describe the interactions of the fundamental constituents of matter, strings. As such, it represents a theory that can be seen as the UV completion of the actual theories that describe the quantum nature of matter and their interactions. Hence, to make contact with those theories, it is important to study its low energy limit, meaning that we have to explore energies $E \ll \frac{1}{l_s}$. In this limit, the effective action is expected to take the following form:

$$S_{\text{IIB,eff}} = S_{\text{SUGRA}} + S_{\alpha'}, \tag{1.20}$$

In the previous expression, $S_{\text{sugra,IIB}}$ refers to the Type IIB Supergravity action in ten dimensions and $S_{\alpha'}$ the corrections coming from String Theory that can be omitted in the low energy limit. The explicit form of the bosonic part of the action takes the following form:

$$S_{\text{sugra,IIB}} = S_{\text{NS}} + S_{\text{R}} + S_{\text{CS}}, \tag{1.21}$$

where

$$S_{\text{NS}} = \frac{1}{2\kappa_{10}^2} \int d^{10}x \sqrt{-G} e^{-2\Phi} \left(R + 4\partial_\mu \Phi \partial^\mu \Phi - \frac{1}{2}|H_3|^2 \right), \tag{1.22}$$

$$S_{\text{R}} = -\frac{1}{4\kappa_{10}^2} \int d^{10}x \sqrt{-G} \left(|F_1|^2 + |\tilde{F}_3|^2 + \frac{1}{2}|\tilde{F}_5|^2 \right), \tag{1.23}$$

$$S_{\text{CS}} = \frac{1}{4\kappa_{10}^2} \int C_4 \wedge H_3 \wedge F_3. \tag{1.24}$$

where H and F denote the field strengths of B and C fields, respectively. Notice that, in the previous expression the fields with a tilde above should be taken as the specific combinations:

$$\tilde{F}_3 = F_3 - C_0 \wedge H_3, \tag{1.25}$$

$$\tilde{F}_5 = F_5 - \frac{1}{2} C_2 \wedge H_3 + \frac{1}{2} B_2 \wedge F_3 \tag{1.26}$$

A supersymmetric field theory is characterized by a set of transformations that relate bosons with fermions and vice versa. The parameter used in these transformations is fermionic, i.e., it is a constant non-commutative number. Promoting the global supersymmetry to a local symmetry gives the fermionic parameter spacetime dependence. Therefore, adding gauge fields is necessary to keep the theory's invariance under such transformations. The resulting theory, is known as Supergravity or in the specific case of this theory: Type IIB Supergravity described by (1.21). Supersymmetric field theories have a high degree of symmetry. Therefore, they have a lot of restrictions over their parameters. In d dimensions, imposing a particle spectrum of $d \leq$ at most spin two generates a condition over the dimension of the spacetime. It restricts its value to 10 or 11. In the case of $d = 10$, any supersymmetric theory admits a maximum of two sypersymmetric charges, i.e., $\mathcal{N} = 2$. The solution to the equations of motion given by (1.21) represents coherent states of the associated particles (which are in turn particular modes of oscillation of the string), such as background profiles where the string can propagate consistently.

1.2 The AdS/CFT correspondence

A solution to the Type IIB supergravity equations of motion was found by Horowitz and Strominger in 1991 [12]. The explicit solution describes an extended object with a horizon surrounding it. The detailed background profiles for the fields are given by

$$ds^2 = \frac{1}{\sqrt{H(r)}}\left[-f(r)dt^2 + dx_1^2 + \cdots + dx_p^2\right] + \sqrt{H(r)}\left[\frac{dr^2}{f(r)} + r^2 d\Omega_{8-p}^2\right] \qquad \text{(metric)}, \tag{1.27}$$

$$e^{\phi} = g_c H(r)^{\frac{3-p}{4}} \qquad \text{(dilaton)}, \tag{1.28}$$

$$C_{01\ldots p} = \frac{1}{\zeta g_c}\left[1 - \frac{1}{H(r)}\right] \qquad \text{(RR field)}, \tag{1.29}$$

where

$$H(r) = 1 + \zeta\left(\frac{L}{r}\right)^{7-p}, \tag{1.30}$$

$$f(r) = 1 - \left(\frac{r_h}{r}\right)^{7-p}, \tag{1.31}$$

$$L^{7-p} = r_h^{7-p}\left(\frac{\zeta}{1-\zeta^2}\right). \tag{1.32}$$

In the previous expressions, r_h refers to the location of the horizon of the given solution and ζ to the non-extremality parameter. It is straightforward to calculate the RR-charge of the given object by just integrating over a closed surface containing it. Such calculation gives the following result:

$$q = \frac{(7-p)\Omega_{8-p}}{(2\pi)^{7-p} g_c}\left(\frac{L}{l_c}\right)^{7-p}. \tag{1.33}$$

Therefore, it is possible to understand L as a parameter that controls the charge of the extended object. Given the similarities with black holes this object was named black p-brane. In the extremal case, with $p = 3$, and taking $r_h \to 0$, $\zeta \to 1$ con L^{7-p} fixed, the given solution acquires the following form:

$$ds^2 = \frac{1}{\sqrt{H(r)}}\left[-dt^2 + dx^2 + dy^2 + dz^2\right] + \sqrt{H(r)}\left[dr^2 + r^2 d\Omega_5^2\right], \tag{1.34}$$

$$e^{\phi} = g_c, \tag{1.35}$$

$$C_{0123} = \frac{1}{g_c}\left[1 - \frac{1}{H(r)}\right], \tag{1.36}$$

where,

$$H(r) = 1 + \left(\frac{L}{r}\right)^4, \tag{1.37}$$

$$L^4 = c_p g_c N l_c^4. \tag{1.38}$$

In such a case, the mass and the charge are given by

$$M = \frac{N V_p}{(2\pi)^p g_c l_c^{p+1}} \qquad \text{y} \qquad q = N. \tag{1.39}$$

Analyzing the low-energy limit, i.e., $E << \frac{1}{l_c}, \frac{1}{L}$, the form of the metric simplifies drastically, giving the following expression:

$$ds^2 = \frac{r^2}{L^2}\left(-dt^2 + dx^2 + dy^2 + dz^2\right) + \frac{L^2}{r^2}dr^2 + L^2 d\Omega_5^2. \tag{1.40}$$

The resulting metric can be trivially identified with the $AdS_5 \times S_5$ metric in Poincaré coordinates. The AdS_{d+1} is a maximally symmetric solution to Einstein's equations with a negative cosmological

constant, $\Lambda = -\frac{d(d-1)}{2L^2}$. The previous statement implies that the curvature tensor can be trivially expressed in terms of the metric, $g_{\mu\nu}$, giving the following expression:

$$R_{\mu\nu\rho\sigma} = -\frac{1}{L^2}\left(g_{\mu\rho}g_{\nu\sigma} - g_{\mu\sigma}g_{\nu\rho}\right). \tag{1.41}$$

This spacetime contains the maximum number of Killing vectors that generate its isometries. In other words,

$$\dim\left[\mathrm{Iso}(AdS_{d+1})\right] = \frac{(d+1)(d+2)}{2}. \tag{1.42}$$

In fact, the AdS_{d+1} isometry group is isomorphic to the conformal group in $(d+1)$ dim, $SO(d,2)$, to be discussed below. The AdS_{d+1} spacetime can be understood as a submanifold of co-dimension one in a Minkowski space with $(2,d)$ signature. The following relation determines such embedding:

$$-X_{-1}^2 - X_0^2 + \sum_{i=1}^{d} X_i = -L^2. \tag{1.43}$$

In the previous relation, X_i are the Minkowski space coordinates with $(2,d)$ signature. Different embedding solutions represent different coordinate systems that describe the AdS_{d+1} spacetime.

Analyzing another string theory system is convenient at this point: a stack of coincident N $D3$-branes. Dp-branes are solitonic objects where the strings can end. Such a condition is imposed by applying Dirichlet boundary conditions over the ends of the string in a specific subset of the spacetime coordinates,$\{x_k\}_{k=p+1}^{9}$. The massless open string theory spectrum contains states that describe particles related to a scalar, spinorial, and vector fields. Additionally, Dp-branes are charged over RR fields. Therefore, type IIB string theory can only sustain stable Dp-branes with $p = -1, 1, 3, 5, 7, 9$. The bosonic part of the Dp-brane action, in a supergravity background, can be described by

$$S_{\mathrm{Dp}} = S_{DBI} + S_{WZ}, \tag{1.44}$$

where, at the lowest order in the derivatives we obtain

$$S_{DBI} = -\frac{1}{g_s(2\pi)^p l_s^{p+1}}\int d^{p+1}x e^{-\Phi}\sqrt{-\det\mathbb{P}\left[G_{\alpha\beta} + (2\pi F_{\alpha\beta} + B_{\alpha\beta})\right]}, \tag{1.45}$$

$$S_{WZ} = -\frac{1}{(2\pi)^p l_s^{p+1}}\int \mathbb{P}\exp\left(2\pi F_2 + B_2\right)\wedge \oplus_n C_n. \tag{1.46}$$

In the previous expression, $\mathbb{P}$ refers to the pull-back of the metric to the Dp-brane worldvolume. It is possible to generalize the aforementioned action to the case where the system contains N coincident Dp-branes. In the low-energy limit and taking $p = 3$, we obtain

$$S_{DBINA} \approx NT_{D3}V_3 + \frac{1}{4\pi g_s}\int d^4x\,\mathrm{Tr}\left[F^2 + (D\Phi)^2 + [\Phi,\Phi]^2 + \cdots\right]. \tag{1.47}$$

This action matches precisely with the action that describes the Super-Yang-Mills theory with $\mathcal{N} = 4$ supersymmetry and $U(N)$ as gauge group, if the identification $g_{YM}^2 = (2\pi)g_s$ is performed. This supersymmetric theory is also a conformal field theory; in other words, its β function equals zero. Hence, it is a fixed point in the renormalization group flow.

At this time, it is convenient to emphasize some fundamental properties of the conformal field theories. A conformal field theory, CFT, is a subclass of quantum field theory in which the Poincaré symmetry group is extended to include the conformal group. In simple terms, a conformal transformation is a change of coordinates that leaves invariant the form of the metric up to a scale factor, i.e.,

$$g'_{\mu\nu}(x') = \Omega(x)g_{\mu\nu}(x). \tag{1.48}$$

Rewriting this expression in terms of an infinitesimal change of the coordinates, $x'^{\mu} = x^{\mu} + \epsilon^{\mu}$, eq. (1.48) imposes a condition over the parameters of the transformation

$$\partial_{\mu}\epsilon_{\nu} + \partial_{\nu}\epsilon_{\mu} = \frac{2}{d}(\partial \cdot \epsilon)\eta_{\mu\nu}. \tag{1.49}$$

The set of parameters giving a solution to the previous equation characterizes the different conformal transformations. Such transformations are classified in the following way:

- $\epsilon^{\mu} = a^{\mu}$ translations
- $\epsilon^{\mu} = \omega_{\mu\nu}x^{\nu}$ rotations and boosts.
- $\epsilon^{\mu} = \lambda x^{\mu}$ scale transformation.
- $\epsilon^{\mu} = b^{\mu}x^2 - 2x^{\mu}(b \cdot x)$ special conformal transformation.

This set of coordinates gives rise to the conformal transformation which are elements of the $SO(2, d)$ group.

As previously explained, Dp-branes are charged with respect to RR fields. Consequently, a stack of N Dp-branes has a total charge that is the sum of the individual elements, i.e., $q = N$. Furthermore, in the case of $p = 3$, the configuration has the following mass:

$$M = \frac{NV_3}{(2\pi)^3 g_s l_s^4}. \tag{1.50}$$

Considering the previous arguments, it is possible to imagine a relationship between the black 3-brane and the stack of coincident N $D3$-branes. Such a relationship is motivated by the fact that both objects have the same RR charge and mass. The conclusion is that both things are different incarnations of the same physical object. The formalism in terms of Supergravity is under control only in the regime where $g_s N >> 1$, while the description in terms of the stack of $D3$-branes is safe in the opposite regime, i.e., $g_s N << 1$. In the low-energy limit, the black 3-brane describes two decoupled systems: the throat and its exterior. In the external system, the effective description is free supergravity fields. On the other hand, in the system described by the stack of $D3$-branes, closed strings decouple from the branes, generating a description in terms of free supergravity fields. Therefore, it is straightforward to equate that component in both subsystems. Identifying the remaining systems, it is possible to conclude the following:

Type IIB String Theory on $AdS_5 \times S^5$ with N units of RR-flux through S^5	$\equiv$	$\mathcal{N} = 4$ SYM with $SU(N)$ gauge group on Minkowski $3 + 1$

Maldacena discovered this astounding equivalence in 1997 [2]. It is important to emphasize that both objects are different, i.e., on the left side is a string theory, while on the right side is a conformal field theory without gravity. This is not the only difference; on the string theory side is a formalism with more dimensions than on the right. The holographic correspondence has been investigated through the years, finding many different examples of it. In the following list it is possible to see some examples of Maldacena's correspondence:

1. $AdS_3 \times \mathbb{S}^2 \times \chi_4$ dual to $SCFT_2$. Here $SCFT_2$ is a superconformal field theory that lives on the world volume generated by the $D1/D5$ system, which has Q_1 $D1$-branes and Q_5 $D5$-branes wrapped throught the χ_4 factor of the metric.

2. $NAdS_2$ dual to $NCFT_1$. The SYK model is a quantum mechanical system with N Majorana fermions interacting randomly [23]. In the IR regime, the model develops an approximate conformal symmetry. This theory is equivalent to the Jackiw-Teitelboim model, a two-dimensional gravitational model containing a scalar field (dilaton field) [24].

3. $T\overline{T}$ deformation dual to AdS with a radial cutoff. The $T\overline{T}$ models comprise a broad class of deformations of a CFT_2 that is possible to solve exactly [25]. On the gravitational side, the coupling, μ, acts as an IR cutoff that removes the asymptotic part of the AdS [26].

4. $\mathcal{N} = 4$ SYM deformed by a θ term at finite temperature is dual to an anisotropic Schwarzschild-AdS black hole.

A more general statement about the correspondence goes as follows:

Statement Any CFT defined on $\mathbb{R}\times\mathbb{S}^{d-1}$ is totally equivalent to a quantum gravity theory defined on a asymptotically $AdS_{d+1} \times M$ spacetime, where M is a compact manifold, see figure (1.1).

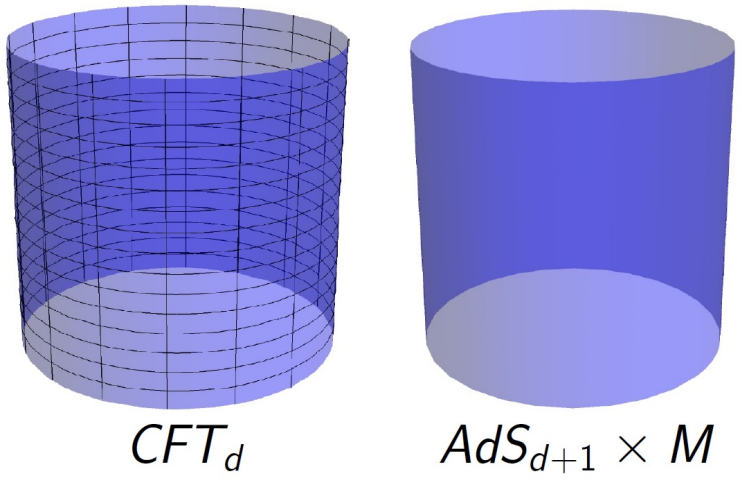

Figure 1.1: Graphical representation of the holographic correspondence. On the left side, the geometry in which the CFT is defined, and on the right side, the geometry, including the interior, in which the gravitational theory is defined.

The dictionary that translates observables between both sides can be described by the following bijective map:

$$\phi : \mathcal{H}_{QG} \to \mathcal{H}_{CFT}. \tag{1.51}$$

As a consequence of this map, any CFT observable must have an image on the gravity side. This does not mean that the mapping must be trivial, i.e., objects described easily in one language can be described on the other side by a very complex structure.

1.3 Anisotropic Black Branes: the Mateos-Trancanelli model

The Mateos-Trancanelli model (MT model) is a IIB supergravity solution whose effective action in five dimensions is

$$S = \frac{1}{16\pi G_N}\int_{\mathcal{M}} d^5x\sqrt{-g}\left[R + \frac{12}{L^2} - \frac{1}{2}\left(\partial\phi\right)^2 \frac{1}{2}e^{2\phi}\left(\partial\chi\right)^2\right] + S_{\text{GH}}\,, \tag{1.52}$$

where ϕ, χ and $g_{\mu\nu}$ are the dilaton field, the axion field and the metric respectively. The Newton constant involved, G_N, refers to its five-dimensional version. Additionally, the Gibbons-Hawking term has been added considering the presence of a smooth space-like or time-like boundary. A solution of the equations of motion derived from the action (1.52) takes the form

$$ds^2 = L^2 e^{-\phi(r)/2}\left[-r^2\mathcal{F}(r)\,\mathcal{B}(r)dt^2 + \frac{dr^2}{r^2\mathcal{F}(r)} + r^2\left(dx^2+dy^2+\mathcal{H}(r)dz^2\right)\right], \tag{1.53}$$

where

$$\chi = az, \qquad \phi = \phi(r), \qquad \mathcal{H} = e^{-\phi}, \tag{1.54}$$

the 4-tuple (t, x, y, z) refers to the coordinates in a Minkowski spacetime assigned to the boundary gauge theory, r is the radial coordinate of AdS, and L is identified as its radius of curvature. The above solution contains an event horizon located at r_h such that $\mathcal{F}(r_h)$ and satisfies that it is asymptotically AdS_5. For values other than zero, the parameter a generates an anisotropic direction on both sides of the duality. At the same time, for $a = 0$, the contributions of the axion and dilaton fields are extinguished, thus recovering the isotropic solution. The dual boundary theory corresponds to $\mathcal{N} = 4$ SYM with gauge group $SU(N)$, deformed by a θ term dependent on the anisotropic coordinate. In the case $a = 0$ the boundary theory reduces to $\mathcal{N} = 4$ SYM with a $SU(N)$ gauge group without θ term. The functions $\mathcal{F}$, $\mathcal{B}$, $\mathcal{H}$ and the dilaton value ϕ can be determined analytically for small values of a. In this thesis, we will only consider terms up to quadratic order in a to avoid technical complications in a first analysis. The explicit form of these functions is

$$\mathcal{F} = 1 - \frac{r_h^4}{r^4} + \frac{a^2}{24r^4r_h^2}\left[8r^2r_h^2 - 2r_h^2(4+5\log 2) + (3r^4+7r_h^4)\log\left(1+\frac{r_h^2}{r^2}\right)\right] + \mathcal{O}(a^4), \tag{1.55}$$

$$\mathcal{B} = 1 - \frac{a^2}{24r_h^2}\left[\frac{10r_h^2}{r^2+r_h^2} + \log\left(1+\frac{r_h^2}{r^2}\right)\right] + \mathcal{O}(a^4), \tag{1.56}$$

$$\phi = -\frac{a^2}{4r_h^2}\log\left(1+\frac{r_h^2}{r^2}\right) + \mathcal{O}(a^4)\,. \tag{1.57}$$

Imposing regularity on the horizon in the Euclidean solution, the temperature is found to be

$$T = \frac{r_h}{\pi} + \frac{(5\log 2 - 2)}{48\pi}\frac{a^2}{r_h} + \mathcal{O}(a^4)\,. \tag{1.58}$$

The Bekenstein-Hawking entropy can be found by calculating the area of the horizon, obtaining

$$S = \frac{r_h^3}{4G_N}\left(1+\frac{5a^2}{16r_h^2}\right)V_3 + \mathcal{O}(a^4)\,. \tag{1.59}$$

where V_3 is the spatial volume in the gauge theory. Using standard holographic renormalization techniques [27], the following expression is obtained for the energy-momentum tensor [188, 29]

$$T_{ij} = \mathrm{diag}(E, P_{xy}, P_{xy}, P_z)\,, \tag{1.60}$$

where

$$E = \frac{3\pi^2N^2T^4}{8} + \frac{N^2T^2}{32}a^2 + \mathcal{O}(a^4) \tag{1.61}$$

is the black brane energy density and

$$P_{xy} = \frac{\pi^2N^2T^4}{8} + \frac{N^2T^2}{32}a^2 + \mathcal{O}(a^4)\,, \tag{1.62}$$

$$P_z = \frac{\pi^2N^2T^4}{8} - \frac{N^2T^2}{32}a^2 + \mathcal{O}(a^4) \tag{1.63}$$

are the pressures along the transverse and longitudinal directions to the anisotropic direction. So, the mass of the black brane turns out to be

$$M = E\,V_3 = \left(\frac{3\pi^2 N^2 T^4}{8} + \frac{N^2 T^2}{32} a^2\right) V_3 + \mathcal{O}(a^4)\,, \tag{1.64}$$

It can be seen that the mass of the isotropic solution increases due to the presence of anisotropy maintaining the same temperature, in other words, we have

$$M(a) = M(0) + \frac{V_3}{2}\left(P_{xy} - P_z\right) + \mathcal{O}(a^4)\,. \tag{1.65}$$

1.4 Magnetic Black Branes: the D'Hoker-Kraus model

The D'Hoker-Kraus model [30] (DK) is a magnetic black brane solution of Einstein-Maxwell gravity in five dimensions. The action for this model is

$$S = \frac{1}{16\pi G_N}\int d^5x\sqrt{-g}\left(R + 12 - F_{MN}F^{MN}\right)\,. \tag{1.66}$$

For very large values of the electromagnetic field ($B/T^2 >> 1$) the solution takes the form

$$ds^2 = -3(r^2 - r_H^2)dt^2 + \frac{dr^2}{3(r^2 - r_H^2)} - \frac{B}{\sqrt{3}}\left(dx^2 + dy^2\right) + 3r^2 dz^2\,. \tag{1.67}$$

With field strength $F = B\,dx \wedge dy$. The Hawking temperature and Bekenstein-Hawking entropy corresponding to the black brane solution are

$$T = \frac{3r_H}{2\pi}\,, \quad S = \frac{3V_3 B^{\,2}}{4G_N}\,. \tag{1.68}$$

In this expression V_3 is the volume in 3 dimensions. The mass of the solution is

$$M_B = \int T dS = \frac{V_3}{16\pi G_N} \times 3B^2\,. \tag{1.69}$$

Chapter 2

Quantum Information Theory and Holography

2.1 Entanglement Entropy

A property that clearly distinguishes quantum from classical mechanics is quantum entanglement. In simple terms, quantum entanglement can be characterized as the degree of uncertainty that the components of a given quantum system share. Concretely, given $|\Psi\rangle \in \mathcal{H}_1 \otimes \mathcal{H}_2$, we say that the state is entangled if it is not possible to write it in the following way:

$$|\Psi\rangle = |\Psi_1\rangle \otimes |\Psi_2\rangle \,, \tag{2.1}$$

where $|\Psi_i\rangle \in \mathcal{H}_i$ with $i = 1, 2$. In order to understand better the previous scenario it is convenient to consider a simple case where $\mathcal{H}_i$ is the Hilbert space of a two-level system. In this case, a complete basis for the Hilbert space is given by $\{|0\rangle \otimes |0\rangle \,, |0\rangle \otimes |1\rangle \,, |1\rangle \otimes |0\rangle \,, |1\rangle \otimes |1\rangle\}$. Therefore, an example of a non-entangled state is

$$|\Psi\rangle = \frac{1}{2} \left(|0\rangle + |1\rangle\right) \otimes \left(|0\rangle - |1\rangle\right) , \tag{2.2}$$

while an entangled state is for instance

$$|\Psi\rangle_{EPR} = \frac{1}{\sqrt{2}} \left(|1\rangle \otimes |0\rangle - |0\rangle \otimes |1\rangle\right) . \tag{2.3}$$

The previous state is known as EPR state [1]. It is possible to generalize the concept of an entangled state to the case where the quantum system admits a decomposition of the following form:

$$\mathcal{H} = \mathcal{H}_1 \otimes \cdots \otimes \mathcal{H}_N, \tag{2.4}$$

where N represents the number of components the system has. This last generalization is suitable when defining entangled and non-entangled states in the context of a CFT or more generally, a QFT.

Consider a CFT placed on a lattice, so assigning a Hilbert space to every point on it is possible. Therefore, the full Hilbert space is given by

$$\mathcal{H} = \otimes_\alpha \mathcal{H}_\alpha, \tag{2.5}$$

where α runs in such a way that it enumerates all the points on the lattice. A state will be entangled if it is impossible to write it as a product of states. From this perspective, is possible to consider a division of the degrees of freedom into two subsets: A and A^c. These subsets share a boundary

denoted by ∂A, see figure (2.1). The total Hilbert space can be expressed in the following way:

$$\mathcal{H} = \mathcal{H}_A \otimes \mathcal{H}_{A^c}. \tag{2.6}$$

At this stage, it is suitable to eliminate the UV cutoff and consider the CFT as a continuum theory.

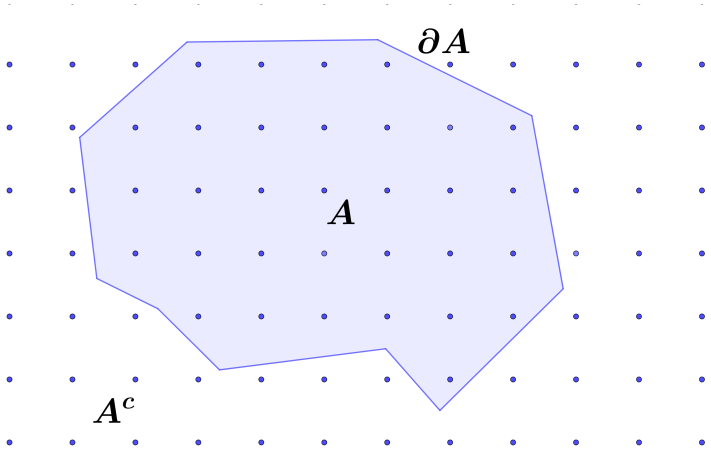

Figure 2.1: Spatial separation of the degrees of freedom in a lattice QFT. Both subsets, A and A^c, share the same boundary ∂A.

Within this limit we take the system to be described by a pure state $|\Psi\rangle \in \mathcal{H}$. Additionally, we consider an observer who can perform measures in the subset denoted by A. As a consequence of the fact that the total Hilbert space is factorized according to eq. (2.6), $|\Psi\rangle$ admits a Schmidt decomposition, i.e.,

$$|\Psi\rangle = \sum_k \sqrt{p_k}\, |k\rangle_A \otimes |k\rangle_{A^c}\,, \tag{2.7}$$

where p_k are non-negative numbers that satisfy $\sum p_k = 1$ and $\{|k\rangle_{A,A^c}\}$ is an orthonormal basis for each component. That the observer only has access to A means that they can only act with operators within that region. Such operations have the following form:

$$\mathcal{O}(x) = \mathcal{O}_A(x) \otimes \mathbb{I}, \qquad \text{with} \qquad x \in A. \tag{2.8}$$

Therefore, the expectation value of the previous operator can be expressed in the following form:

$$\begin{aligned} \langle \mathcal{O}(x) \rangle &= \sum_k p_k \, \langle k| \, \mathcal{O}_A(x) \, |k\rangle_A \\ &= \mathrm{Tr}_{\mathcal{H}_A} \left[\rho_A \mathcal{O}_A(x) \right], \end{aligned} \tag{2.9}$$

where,

$$\rho_A = \mathrm{Tr}_{A^c} \, |\Psi\rangle \, \langle\Psi| \tag{2.10}$$

$$= \sum_k p_k \, |k\rangle_A \, \langle k|_A \,. \tag{2.11}$$

Due to the lack of knowledge that the observer has over A^c, in general the previous density matrix describes a mixed state. Accordingly, all the $\{p_k\}$ allow determining the degree of uncertainty over the subsystem. The von Neumann entropy gives a good measure of this uncertainty, which uses these coefficients to return a number. The explicit expression is

$$\begin{aligned} S(A) &= -\,\mathrm{Tr}_{\mathcal{H}_A} \left(\rho_A \log \rho_A \right) \\ &= -\sum_k p_k \log p_k. \end{aligned} \tag{2.12}$$

This function gives a good measure also of the entanglement between the degrees of freedoom localized inside A from those in A^c. In particular, if

$$|\Psi\rangle = |\Psi_A\rangle\,|\Psi_{A^c}\rangle \qquad \text{(No entanglement)} \tag{2.13}$$

then

$$S(A) = 0. \tag{2.14}$$

2.2 Euclidean Formalism

The previously presented formula to calculate the EE is suitable in a system with a finite number of degrees of freedom. Nevertheless, in a CFT the number of degrees of freedom turns out to be infinite, making calculation with the standard definition intractable. The Feynman path integral is a handy tool established in the context of a QFT. Thus, it is useful to establish a path integral definition of the EE.

Calculating the expression given by eq. (2.12) can be a challenging task. However, a much simpler task is to calculate

$$S_n(A) = \frac{1}{1-n}\log \mathrm{Tr}_A\left(\rho_A^n\right). \tag{2.15}$$

These functions are known as Rényi entropies, and one can capitalize on them to calculate the EE by taking the following limit:

$$\begin{aligned} S(A) &= \lim_{n\to 1} S_n(A) \\ &= -\lim_{n\to 1}\partial_n \log \mathrm{Tr}_A\left(\rho_A^n\right). \end{aligned} \tag{2.16}$$

where to obtain the second equality from the first, it was necessary to use the L´Hôpital rule. Thus, all the difficulty is translated into finding a path integral expression for the Rényi entropies.

To motivate the origin of the path integral expression for the Rényi entropies, it is convenient first to consider a simple system instead of a CFT. This system is a quantum mechanical system that describes the state of a particle. The amplitude for finding a particle in $|x_f, t_f\rangle$ starting from $|x_i, t_i\rangle$ is given by

$$\langle x_f, t_f | x_i, t_i\rangle = \langle x_f|\, e^{-i\hat{H}(t_f - t_i)}\,|x_i\rangle\,, \tag{2.17}$$

where $\hat{H}$ is the Hamiltonian of the system. The path integral expression for the previous quantity is

$$\langle x_f, t_f | x_i, t_i\rangle = \int_{x(t_i)=x_i}^{x(t_f)=x_f} \mathcal{D}x(t)\exp\left[i\int_{t_i}^{t_f} dt L(x,\dot{x})\right]. \tag{2.18}$$

where $L(x,\dot{x})$ is the Lagrangian of the system. On the other hand, eq. (2.17) can be rephrased by taking the time interval to be $[T, 0]$ and the spatial points y and x, giving the following:

$$\langle x, 0 | y, T\rangle = \langle x|\, e^{i\hat{H}T}\,|y\rangle \tag{2.19}$$

$$= \sum_n \psi_n(x)\psi_n^*(y)e^{iE_nT}, \tag{2.20}$$

Notice that to reach the second line from the first, it was necessary to insert an identity matrix expressed as a sum over an entire basis. In eq. (2.19) $\psi_n(x) = \langle x|n\rangle$. Thus, after doing a Wick rotation by taking $T = -i\tau$ and $\tau \to -\infty$, we obtain

$$\langle x, 0 | y, -\infty\rangle = \lim_{\tau\to-\infty}\psi_0(x)\psi_0^*(y)e^{E_0\tau}. \tag{2.21}$$

From this expression it is clear that is possible to express $\psi_0(x)$ in the following way:

$$\Psi(x) = \int^{x(0)=x} \mathcal{D}x(\tau) e^{-I_E}. \tag{2.22}$$

by absorbing the factors in front $\psi_0(x)$ in a normalization constant and using eq. (2.18). Notice that in the previous expression we have changed $\psi_0(x) \to \Psi(x)$.

A similar procedure gives a conjugated ground state wave function; the expression is

$$\Psi^*(x) = \int_{x(0)=x} \mathcal{D}x(\tau) e^{-I_E}. \tag{2.23}$$

Notice from this expression that it is mandatory to sum over all the positions in the distant future. To be able to discuss a reduced density matrix, consider a system with only two degrees of freedom associated with two particles whose positions are x_A y x_B respectively. Additionally, suppose that the state to consider is the ground state, $|\Omega\rangle$. Thus, given a state in the total system, $|x_A, x_B\rangle$, the matrix elements of the reduced density matrix are given by

$$\langle x_A| \rho_A |x'_A\rangle = \int dx_B \langle x_A, x_B|\Omega\rangle \langle \Omega|x'_A, x_B\rangle . \tag{2.24}$$

Substituting the ground state wave function in the previous expression, it is straightforward to obtain

$$\langle x_A| \rho_A |x'_A\rangle = \frac{1}{Z} \int dx_B \int_{\mathcal{M}_\epsilon^+ \cup \mathcal{M}_\epsilon^-} \mathcal{D}y_A(\tau) \mathcal{D}y_B(\tau) e^{-I_E(y_A, y_B)}, \tag{2.25}$$

where $\mathcal{M}_\epsilon^+$ and $\mathcal{M}_\epsilon^-$ refer to the regularized upper and lower half-line respectively, i.e.,

$$\mathcal{M}_\epsilon^+ = \{\tau \in \mathbb{R} | \epsilon \leq \tau\}, \tag{2.26}$$
$$\mathcal{M}_\epsilon^- = \{\tau \in \mathbb{R} | \tau \leq -\epsilon\}, \tag{2.27}$$

and Z is a normalization factor.

The boundary conditions on region are

$$y_A(\epsilon) = x'_A, \quad y_B(\epsilon) = x_B \quad \text{on} \quad \partial\mathcal{M}_\epsilon^+, \tag{2.28}$$
$$y_A(-\epsilon) = x_A, \quad y_B(-\epsilon) = x_B \quad \text{on} \quad \partial\mathcal{M}_\epsilon^-. \tag{2.29}$$

Thus, performing the integral over x_B and taking $\epsilon \to 0$, we obtain

$$\langle x_A| \rho_A |x'_A\rangle = \frac{1}{Z} \int \mathcal{D}y_A(\tau) \mathcal{D}y_B(\tau) e^{-I_E(y_A, y_B)} \delta\left(y_A(0^+) - x'_A\right) \delta\left(y_A(0^-) - x_A\right). \tag{2.30}$$

In the previous expression, the Dirac delta functions fix the desired boundary conditions. Notice that the notation $0^\pm = \lim_{\epsilon \to 0} \pm\epsilon$ has been implemented. The relation observed in eq. (2.30) is the path integral representation for the matrix elements of the reduced density matrix. The procedure to obtain a parallel expression in the case of a continuum CFT is morally similar and does not contribute to a new physical feature. Hence, to generalize eqs. (**??**), (2.23) and (2.30) the following substitution is needed:

$$\hat{x} \to \hat{\phi}(\vec{x}), \tag{2.31}$$
$$|x\rangle \to |\phi(\vec{x})\rangle , \tag{2.32}$$
$$\Psi(x) \to \Psi[\phi(\vec{x})]. \tag{2.33}$$

With this replacement, the formula to compute the ground state wave function acquires the following form:

$$\Psi[\phi(\vec{x})] = \langle \phi(\vec{x})|\Omega\rangle \tag{2.34}$$

$$= \int_{(t,\vec{x})\in\mathcal{M}_\epsilon^-}^{\phi(-\epsilon,\vec{x})=\phi(\vec{x})} \mathcal{D}\phi(t,\vec{x}) e^{-I_E(\phi)}. \tag{2.35}$$

In the same way, conjugate expression is

$$\Psi^*[\phi'(\vec{x})] = \langle \Omega|\phi'(\vec{x})\rangle \tag{2.36}$$

$$= \int_{\phi(\epsilon,\vec{x})=\phi'(\vec{x})}^{(t,\vec{x})\in\mathcal{M}_\epsilon^+} \mathcal{D}\phi(t,\vec{x}) e^{-I_E(\phi)}. \tag{2.37}$$

The QFT generalization requires a modification of the aforementioned boundary conditions over $\mathcal{M}_\epsilon^+$ and $\mathcal{M}_\epsilon^-$. Thus,

$$\mathcal{M}_\epsilon^+ = \{(\tau,\vec{x}) \in \mathbb{R}^{d+1} | \epsilon \leq \tau, x \in \mathbb{R}^d\}, \tag{2.38}$$

$$\mathcal{M}_\epsilon^- = \{(\tau,\vec{x}) \in \mathbb{R}^{d+1} | \tau \leq -\epsilon, x \in \mathbb{R}^d\}. \tag{2.39}$$

Additionally, with the replacement given by eqs. (2.31),(2.32) and (2.33) the reduced density matrix acquires the following form:

$$\rho_A[\phi_a^A(\vec{x}), \phi_b^A(\vec{x})] = \frac{1}{Z}\int \mathcal{D}\phi(t,\vec{x}) e^{-I_E(\phi)} \prod_{\vec{x}\in A} \delta\left(\phi(0^+,\vec{x}) - \phi_a^A(\vec{x})\right) \delta\left(\phi(0^-,\vec{x}) - \phi_b^A(\vec{x})\right). \tag{2.40}$$

In this formula, Z refers to the CFT partition function. Also, from eq. (2.40) it is feasible to obtain $\mathrm{Tr}_A\, \rho_A^n$ by multiplying in a specific form n ρ_A factors. Schematically, the objective is to obtain an expression for

$$\rho_A^n = \underbrace{\rho_A \cdots \rho_A}_{n \text{ times}} \tag{2.41}$$

Concretely, the multiplication of two factors is performed by identifying the upper boundary condition of the first factor with the lower boundary condition of the second factor and summing over this repeated index. The specific way to do this is by integrating over this boundary condition. Repeating the previous step N times and then taking the trace, we obtain

$$\mathrm{Tr}_A\, \rho_A^n = \frac{1}{Z_1}\int_{(t,\vec{x})\in\mathcal{R}_n} \mathcal{D}\phi(t,\vec{x}) e^{-I_E(\phi)} \equiv \frac{Z_n}{Z_1^n}, \tag{2.42}$$

where $\mathcal{R}_n$ refers to the replica manifold obtained from the gluing of the boundary conditions. Notice that the previous formula includes a definition for the partition function in the replica space, Z_n. This notation is convenient because it emphasizes a correct normalization for the case $n = 1$, i.e., the relevant case for ρ_A. Thus, calculating the EE has become a task of calculating a path integral expression given by eq. (2.42). The cases where this is impossible are minimal, knowing exact results only in the context of a $1+1$ CFT.

2.3 Holographic Entanglement Entropy

The entanglement entropy is an essential quantity in any quantum theory because it has a wide range of applications, for example, as an order parameter to diagnose phase transitions related

to the confinement in a gauge theory [147]. For this reason, it is extremely valuable to have a holographic description for it in terms of a geometrical quantity in a gravitational theory.

Ryu and Takayanagi proposed a recipe to calculate EE [148] using a geometric measure in a static gravitational theory. Subsequently, Hubeny, Rangamani, and again Takayanagi generalized the prescription to include time-dependent gravitational dynamics. To describe their recipe, first it is convenient to introduce a group of definitions.

Definition. Let R be a spatial region located in the boundary of an asymptotically AdS space. A Hubeny-Rangamani-Takayanagi (HRT) surface for R is a codimension two bulk spatial submanifold with boundary, γ_R, with the following properties:

- γ_R and R have the same boundary, i.e., $\partial\gamma_R = \partial R$.
- The area of γ_R is extremal under small variations of its location in the spacetime, provided the variations respect $\partial\gamma_R = \partial R$.
- γ_R is homologous to R, i.e., a codimension-one submanifold must exist, such that $\partial H_R = \gamma_R \cup R$.
- There is no other surface of strictly smaller area obeying the above three properties.

Definition Let R be a spatial region located in the boundary of an asymptotically AdS geometry. The domain of dependence related to R, $D[R]$, is defined as the set of events located in the boundary such that every inextensible causal curve that passes through them also intercepts R.

Definition Let R be a spatial region located in the boundary of an asymptotically AdS geometry. The entanglement wedge of R, $W[R]$, is defined as the domain of dependence of $D[H_R]$, see figure (2.3).

Considering the previous definitions, it is important to emphasize that the causal wedge and the entanglement wedge, in general, are not the same object. In [31], it was demonstrated that for manifolds that obey the null-energy condition, it is fulfilled that

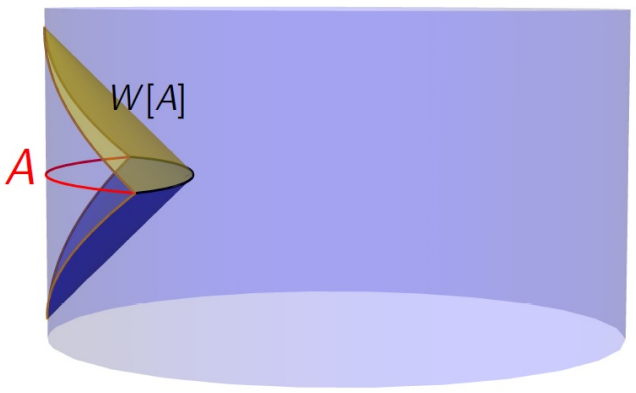

Figure 2.2: Entanglement wedge associated to a boundary spatial region (red).

$$C[R] \subset W[R], \tag{2.43}$$

namely, the entanglement wedge reaches dipper into the gravitational bulk. Once all the tools have

been established, it is straightforward to state the holographic prescription to compute the EE.

RT/HRT/Engelhardt-Wall formula. Let ρ be a CFT state. The von Neumann entropy associated to the state reduced to the spatial region R, ρ_R, satisfies

$$S(\rho_R) = \frac{\left\langle \hat{\text{Area}}(\gamma_R) \right\rangle}{4G_N} + S(\rho_{H_R}). \tag{2.44}$$

In this formula, $S(\rho_{H_R})$ is the contribution to the EE given by the quantized fields on the homology surface H_R and $\left\langle \hat{\text{Area}}(\gamma_R) \right\rangle$ is the area expectation value. The expression (2.44) is also known as generalized entropy. At this point, it is suitable to emphasize the relevance of each term. The first term arose as the first proposal to holographically calculate EE in the classical approximation [10, 11]. In the case of a static spacetime, there exists a preferred foliation in time; therefore, the extremality condition automatically translates to the statement of finding the surface with minimal area. This contribution is dominant in the regime of a big number of colors $\mathcal{O}(N^2)$ in the CFT, which corresponds to small G_N in the bulk. The second term represents the first quantum corrections which are of order $\mathcal{O}(N^0)$ and were first calculated in [17]. In general, formula (2.44) is expected to be valid at any N [86], as long as γ_R satisfy the extremality condition.

2.3.1 Entanglement Entropy of an Interval in a two-dimensional CFT

The validity of the RT formula has been verified a significant number of times; see review papers [80, 32, 33]. As an example, this section is concerned with reviewing the EE calculation for a spatial interval in a two-dimensional CFT using both approaches.

See [34] for an introduction to the topic. In a CFT_2, there is not much freedom for selecting spatial regions because, in this case, the intervals and their union are the only spatial regions that can exist. Thus, for this example, we selected an interval defined on $t = 0$. For simplicity, it is considered that the interval is centered at the origin of the spatial coordinate and that the total state is the vacuum, $|\Omega\rangle$. Therefore, the interval to consider is

$$I = \{z = x + it \in \mathbb{C}| \quad -\frac{l}{2} \leq \text{Re}\, z \leq \frac{l}{2}, \quad \text{Im}\, z = 0\}, \tag{2.45}$$

where l refers to the total interval length. In order to regularize the UV divergences we use the following regularized version of the interval with an auxiliary parameter ϵ, namely,

$$I_\epsilon = \{z = x + it \in \mathbb{C}| \quad -\frac{l}{2} + \epsilon \leq \text{Re}\, z \leq \frac{l}{2} - \epsilon, \quad \text{Im}\, z = 0\}. \tag{2.46}$$

Using the conformal transformation

$$\xi = \frac{z + \frac{l}{2}}{z - \frac{l}{2}}, \tag{2.47}$$

it is possible to map the interval I_ϵ to the semi-real negative axis in the new coordinates. Additionally, performing the transformation

$$\omega \equiv \tau + i\varphi = \frac{1}{2\pi} \log \xi, \tag{2.48}$$

all the points in the complex plane with coordinates ξ such that $0 \leq \text{Re}\, \xi$, are mapped to the cylinder with radius equal to one and length equal to $\frac{1}{\pi} \log\left(\frac{l}{\epsilon}\right)$. Hence, the real positive axis with coordinates ξ is mapped to the line at $\varphi = 0$. In the ω coordinates, it is easy to build a replica space. For example, for $n = 2$, the upper opening of the first cylinder and the lower opening of the second cylinder build together a big cylinder with two times the original circumference. Thus, gluing together n copies will generate a cylinder with n times the original circumference. The

partition function in $\mathcal{M}_n$ is mapped to the cylinder partition function, namely,

$$Z[\mathcal{M}_n] = \langle\Omega| e^{-\beta\hat{H}} |\Omega\rangle , \tag{2.49}$$

where $\beta = \frac{1}{\pi}\log\left(\frac{l}{\epsilon}\right)$ is the cylinder's regularized length and $\hat{H}$ Hamiltonian of the system that generates translation in τ.

$$\hat{H} = \frac{2\pi}{n}\left(L_0 + \overline{L}_0 - \frac{c}{12}\right), \tag{2.50}$$

where $L_0 + \overline{L}_0$ is the dilatation transformation in the complex plane. Thus, using the fact that both L_0 and $\overline{L}_0$ annihilate the vacuum, it is possible to simplify (2.49). The result obtained from this procedure is

$$\log Z[\mathcal{M}_n] = \frac{c}{6n}\log\left(\frac{l}{\epsilon}\right). \tag{2.51}$$

Using (2.42) and (2.16),

$$S(I_\epsilon) = \frac{c}{3}\log\left(\frac{l}{\epsilon}\right). \tag{2.52}$$

The final result for the EE of an interval has a simple form fixed by the symmetries of the theory. It is important to emphasize that since the result is too simple, it does not contain specific information about the theory. It only contains the CFT central charge, which counts the total number of degrees of freedom. In this sense, the result obtained is considered a universal feature of the theory.

2.3.2 Entanglement Entropy of an Interval using the RT/HRT prescription

This section contains the gravitational calculation to obtain the EE of a spatial interval in a two-dimensional CFT, using holography. The point is to compare with the calculation explained in the previous section using CFT methods. To achieve this, we use the same configuration for the interval; namely, its length is l, it is centered on the origin, and the $t = 0$ slice contains all the points included in the interval. Since the CFT state is the vacuum, the following bulk metric will be used:

$$ds^2 = \frac{L^2}{z^2}\left(-dt^2 + dz^2 + dx^2\right), \tag{2.53}$$

describing pure AdS. Notice that the scenario is time-independent. Thus, the gravitational computation only involves the $t = 0$ slice. In this case, the metric simplifies giving

$$ds^2 = \frac{L^2}{z^2}\left(dz^2 + dx^2\right). \tag{2.54}$$

For large N, following the RT/HRT prescription, it is desired to find a codimension-two surface, namely, a curve. This curve must share its boundary with the interval, i.e., the curve must be anchored on the interval endings. The last desired property involves finding the curve with minimal area. In this case, the functional area takes the following form:

$$L[\gamma_I] = \int ds \frac{L}{z(s)}\sqrt{z'^2(s) + x'^2(s)}. \tag{2.55}$$

A geodesic is a curve that minimizes the area functional with the specified boundary conditions. A convenient parametrization of this curve is the following:

$$x(s) = \frac{l}{2}\cos s, \tag{2.56}$$

$$z(s) = \frac{l}{2}\sin s, \tag{2.57}$$

where $s \in [\frac{2\epsilon}{l}, \pi - \frac{2\epsilon}{l}]$. Notice that the parameter ϵ regularizes the curve's length. A straighforward calculation reveals that

$$L[\gamma_I] = L \int_{\frac{2\epsilon}{l}}^{\pi - \frac{2\epsilon}{l}} \frac{ds}{\sin s} \tag{2.58}$$

$$= 2L \log\left(\frac{l}{\epsilon}\right). \tag{2.59}$$

Thus, the EE is

$$S(I_\epsilon) = \frac{c}{3} \log\left(\frac{l}{\epsilon}\right). \tag{2.60}$$

To arrive at the previous expression, we used the famous relation between the central charge of a given CFT and the AdS curvature radius, $c = \frac{3L}{2G_N}$. This result coincides exactly with the result obtained using CFT methods.

2.4 Differential Entropy, Kinematic Space and Integral Geometry

This section will be focused on the basic concepts needed to introduce the reader to the field of integral geometry in the context of the AdS_3/CFT_2 correspondence. As explained before, AdS/CFT can relate geometrical quantities with quantum information measures. Thus, it is reasonable to make progress on finding a complete dictionary to connect both sides of the holographic duality. Given a boundary state and a spatial region, the reduced density matrix of this region contains all the information needed to know every physical aspect inside the entanglement wedge [35, 36]. By definition, the RT/HRT surface contains IR gravitational information. The IR/UV connection establishes that IR effects in the bulk are directly connected to UV information in the CFT [39, 37]. A closed spatial curve in the bulk is a geometric object that can be defined without the need of a regularization parameter meaning that is related to the UV bulk information. From this perspective and taking into consideration the holographic correspondence as a primary guide, it is natural to ask: what type of CFT information is encoded in a closed curve in the bulk?. Additionally: does this information have a clear interpretation? The differential entropy formula provides the answer to these questions. The first implementation of the differential entropy formula was given in [38].

Given an ordered[1] periodic family of spatial intervals, $\{I_i\}_{i=1}^N$, en la CFT_2, its differential entropy is defined as

$$E = \sum_{k=1}^{N} \left[S\left(I_k\right) - S\left(I_k \cap I_{k+1}\right)\right]. \tag{2.61}$$

In this formula, $S(I_k)$ refers to the EE of each interval I_k. It turns out that there is a convenient way to interpret the previous formula using a closed spatial curve in the bulk. A bulk closed spatial curve naturally defines a geodesic family whose endings reach the AdS boundary, therefore, defining a family of intervals in the boundary, see figure (2.4). To elaborate on this statement, take a closed spatial curve and consider an imaginary division into small segments. Each segment is characterized by an initial and final point inside the curve, those points are also used to show the division. Now, consider a geodesic tangent son each segment. Such geodesic automatically defines an interval in the boundary. Thus, the previously mentioned procedure defines an infinite family of intervals. It is straightforward to generalize the previous approach to the continuum by

[1]The term "ordered" refers to the ending points of each interval, namely, the initial goes before the final ending.

making the segments infinitesimally small. The expression of the differential entropy formula in the continuum limit is

$$E = -\oint d\lambda \frac{\partial S\left(\gamma_I(\lambda'), \gamma_D(\lambda)\right)}{\partial \lambda}\bigg|_{\lambda=\lambda'}, \tag{2.62}$$

where $I(\lambda) = [\gamma_I(\lambda), \gamma_D(\lambda)]$ is the family of intervals defined by the geodesics. In [14] it was shown that $E = \frac{A}{4G_N}$, namely, the differential entropy of a family of intervals is equal to the gravitational entropy of the hole delimitated by the family of geodesics, see section [14]. As a result, this new dictionary entry was known as hole-ography.

To better understand the previous construction, consider an interval member of the previously described family $I(\lambda) = [\gamma_I(\lambda), \gamma_D(\lambda)]$. This interval was generated by shooting a tangent geodesic from a point on the closed spatial curve. It is possible to associate a causal diamond, $D[I(\lambda_0)]$, to the such interval. Hence, it is natural to conclude that the local information of the closed curve in the bulk is associated with in the corresponding causal diamond in the CFT. To exemplify this interpretation, take in the bulk a circumference with radius R_0 and located in the $t = 0$ slice. All the causal diamonds generated from the family of tangent geodesics draw a strip whose width is equal to $2T_0$, where T_0 is the time that a ray takes to reach the boundary after being shot radially from any point in the circumference. The local observers in the CFT cannot access the IR information whose characteristic length is greater than $2T_0$, given that such information is causally restricted.

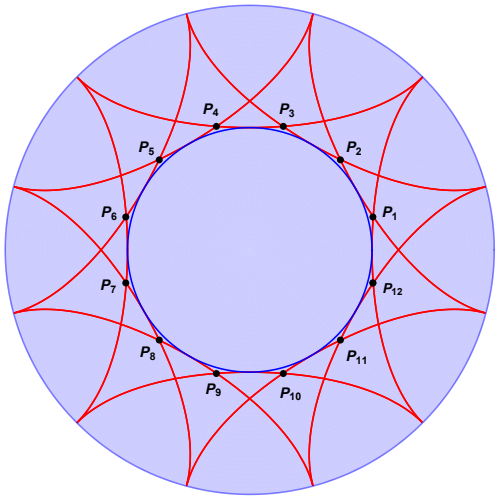

Figure 2.3: A convex closed curve in the bulk defines a family of intervals whose endpoints are connected to tangent geodesics in the bulk.

2.4.1 Equality between Differential Entropy and Gravitational Entropy

Hole-ography is based on the equality between the differential entropy formula and the gravitational entropy. Thus, this section will be concerned with the derivation of such a relation. The starting point is to consider the family of geodesics as objects that extremize the functional area. From this perspective, it is possible to use the usual tools coming from classical mechanics to justify equality.

Let $\gamma_B^\mu(\lambda)$ be a closed spatial curve in the bulk with generalized planar symmetry[2] and $\Gamma^\mu(\lambda, s)$ the set of tangent geodesics to $\gamma_B^\mu(\lambda)$ at each λ. As explained before, this family of geodesics

[2]Given an asymptotically AdS spacetime in $d+2$ dimensions, a codimension-two surface, γ_B^μ, will have planar symmetry if it is possible to find a parametrization of the following form:

$$\gamma_B^\mu(\lambda, \sigma^a) = \{q^i(\lambda, \sigma^a), y^a(\lambda, \sigma^a)\} = \{q^i(\lambda), \sigma^a\},$$

generates a set of boundary intervals denoted by $(\Gamma_I(\lambda), \Gamma_D(\lambda))$. Now, consider the following action:

$$S = \int_{s_i}^{s_f} ds \mathcal{L}(\gamma, \partial_s \gamma). \tag{2.63}$$

In this expression, $\mathcal{L}$ is the Lagrangian of a particular classical system. This Lagrangian depends on the coordinates γ^μ and their derivatives $\partial_s \gamma^\mu$. The specific form of the Lagrangian is not relevant for the rest of the section. All that we need is for it to satisfy the following properties:

1. The action defined by (2.63) is invariant under reparametrizations in s.

2. $\mathcal{L}$ is a homogeneous functions of degree one in its second argument, namely, $\mathcal{L}(\gamma, \alpha \partial_s \gamma) = \alpha \mathcal{L}(\gamma, \partial_s \gamma)$.

3. It is possible to write the Lagrangian as $\mathcal{L}(\gamma, \partial_s \gamma) = \partial_s \gamma^\mu p_\mu$, where, $p^\mu = \frac{\partial \mathcal{L}}{\partial(\partial \gamma^\mu)}$. Hence, p^μ is a homogeneous function of zero degree.

Additionally, if a family of solutions $\tilde{\Gamma}^\mu(\lambda, s)$ exist, from the equation of motion it is possible to demonstrate that

$$R(s) \equiv \oint d\lambda \left[\partial_\lambda \tilde{\Gamma}^\mu(\lambda, s)\right] p_\mu, \tag{2.64}$$

is conserved, namely, $\partial_s R = 0$. Now, with all the ingredients at hand it is elementary to establish the desired result by identifying

$$\gamma \to \gamma_I, \tag{2.65}$$

$$\partial_s \gamma \to \gamma_D, \tag{2.66}$$

$$\int_{s_i}^{s_f} ds \mathcal{L}(\gamma, \partial_s \gamma) \to S(\gamma_I, \gamma_D). \tag{2.67}$$

Therefore, let $\Gamma(s, \lambda)$ be a continuous family of solutions to the equation of motion where the endings are denoted by $\gamma_{I,D}(\lambda) = \Gamma(s_{I,D}, \lambda)$. From these observations it follows that

$$E = \oint d\lambda \frac{\partial S\left(\gamma_I(\lambda), \gamma_D(\lambda')\right)}{\partial \lambda'}\bigg|_{\lambda=\lambda'}, \tag{2.68}$$

$$= \oint d\lambda \underbrace{\frac{\partial \gamma_D^\mu}{\partial \lambda'}\bigg|_{\lambda=\lambda'}}_{\partial_{\lambda'} \tilde{\Gamma}^\mu} \underbrace{\frac{\partial S(\gamma_I, \gamma_D)}{\partial \gamma_D^\mu}\bigg|_{\lambda}}_{p^\mu\big|_{s_D}}, \tag{2.69}$$

$$= R(s_D). \tag{2.70}$$

The previous calculation reveals that the differential entropy and $R(s)$ are the same. Now, suppose that there exists a curve in the bulk, $\gamma_B(\lambda)$, such that it is tangent to every element in the family of solutions, $\Gamma(s, \lambda)$, at a given point, $s = s_B(\lambda)$. From this, it is possible to obtain the following conditions:

$$\Gamma^\mu(s_B(\lambda), \lambda) = \gamma_B^\mu(\lambda), \tag{2.71}$$

$$\partial_s \Gamma^\mu(s_B(\lambda), \lambda) = \alpha(\lambda) \gamma_B'^\mu(\lambda). \tag{2.72}$$

---

where, $\{q^i, y^a\}$ refers to a set of AdS_{d+2} coordinates with $q^i = \{t, x, z\}$ and $y^a = \{y^1, ..., y^{d-1}\}$. Also, $\{\lambda, \sigma^1, ..., \sigma^{d-1}\}$ is used as a particular parametrization of γ_B. An $aAdS$ spacetime will be said to have planar symmetry if all codimension-two surfaces have planar symmetry.

In the previous expression $\alpha(\lambda)$ is a positive function. Therefore, the following result is obtained when $R(s_B)$ is evaluated

$$R(s_B) = \oint d\lambda \partial_\lambda \Gamma^\mu(s_B, \lambda) p_\mu(\Gamma^\mu(s_B, \lambda), \partial_s \Gamma^\mu(s_B, \lambda)) \tag{2.73}$$

$$= \oint d\lambda \gamma'^\mu_B(\lambda) p_\mu(\gamma_B, \gamma'_B) \tag{2.74}$$

$$= \oint \mathcal{L}(\gamma_B, \gamma'_B) \tag{2.75}$$

where the reparametrization invariance was essential to obtain the final result. Additionally, to get the second line from the first, it was necessary to consider that p_μ is a homogeneous function of zero degree in its second variable. From the second to the third line, it was considered that $\mathcal{L}(\gamma, \partial_s \gamma) = \partial_s \gamma^\mu p_\mu$, where $p^\mu = \frac{\partial \mathcal{L}}{\partial(\partial \gamma^\mu)}$. This set of statements conclude the desired derivation. It is also possible to relax conditions (2.71) and (2.72) with the objective of considering more general alignment conditions.

To visualize the generalized alignment conditions, let us consider the following Lagrangian:

$$\mathcal{L}(\Gamma, \dot{\Gamma}) = \sqrt{g_{\mu\nu}(\Gamma) \dot{\Gamma}^\mu \dot{\Gamma}^\nu}. \tag{2.76}$$

Therefore, the momentum is given by

$$p_\mu = \frac{g_{\mu\nu} \dot{\Gamma}^\nu}{|\dot{\Gamma}|}. \tag{2.77}$$

With the help of the previous expression is possible to evaluate $R(s)$ explicitly. The result is

$$R(s) = \oint \frac{\gamma'_B \cdot \dot{\Gamma}}{|\dot{\Gamma}|}. \tag{2.78}$$

Thus, substituting the alignment condition it is possible to appreciate that the differential entropy and the gravitational entropy are going to be equal as long as the following condition is met

$$\gamma'_B \cdot \dot{\Gamma} = |\gamma'_B||\dot{\Gamma}|. \tag{2.79}$$

Notice that this condition is preserved if

$$\dot{\Gamma} = \alpha \gamma'_B + n, \tag{2.80}$$

where n is a null vector orthogonal to γ'_B. With the previous result it is possible to conclude that it is not mandatory for the geodesics to be tangent to reconstruct a given curve in the bulk, it is also possible to use geodesics that satisfy (2.80). In the rest of the text we will refer to this by the term null vector alignment or NVA.

2.4.2 Kinematic Space, Crofton formula and Integral Geometry.

According to the definition given by the expression (2.12), the entanglement entropy is a function that goes from all possible spatial regions to the real numbers. This means that seen as a function of the shape of a set, it is a highly complex object to work with, obtaining explicit results only when the considered region has a high degree of symmetry. An example of the above can be found in spherical spatial regions. As already emphasized above, analyzing a QFT using entanglement is critical to understanding the emergence of space-time via the holographic correspondence. In this series of ideas, it is convenient to focus on the entanglement entropy behavior of spherical regions. For the case of a CFT_2, the analysis is quite simplified because, in general, a spatial region can be seen as the union of spatial intervals. Then, "kinematic space" is defined as the set of all spherical

spatial regions or, when working in two dimensions, the set of all possible intervals [202]. Note that due to the holographic dictionary, the kinematic space can also be defined as the set of geodesics connecting two points on the boundary. This space inherits a Lorentzian structure and can be built naturally in each CFT without resorting to the holographic correspondence. The remainder of this section will focus on the context of the AdS_3/CFT_2 mapping.

It is convenient first to analyze the case at constant time since the geometry in the bulk is represented by the hyperbolic plane. The metric of the hyperbolic plane is given by

$$ds^2 = d\rho^2 + \sinh^2 \rho d\theta^2. \tag{2.81}$$

In this expression, it can be seen that the boundary of the hyperbolic plane is found when $\rho \to \infty$. In this coordinate system, the geodesics anchored on the boundary satisfy the following implicit equation:

$$\tanh^2 \rho \cos(\theta - \phi) = \cos \alpha, \tag{2.82}$$

where ϕ is the angle at the geodesic's deepest point, and α is half the opening angle that the geodesic subtends on the border. These two parameters characterize each geodesic, so the kinematic space, K, in this case, is two-dimensional and can be represented using ϕ and α. A result in integral geometry applied to the hyperbolic plane case states that the length of a closed curve γ is given by [202]

$$L[\gamma] = \frac{1}{4} \int_K \omega(\alpha, \phi) n_\gamma(\alpha, \phi). \tag{2.83}$$

In this expression, $\omega(\alpha, \phi)$ is a 2-form defined in kinematic space called the Crofton form, and $n_\gamma(\alpha, \phi)$ is the number of intersections that each geodesic has with the curve γ. In the case of the hyperbolic plane, the Crofton form is given by [202]

$$\omega(\alpha, \phi) = -\frac{1}{\sin^2 \alpha} d\alpha \wedge d\phi. \tag{2.84}$$

The Crofton form gives an appropriate measure in the space of geodesics, which, combined with n_γ, encodes the density of geodesics that traverse the curve. Two parameters characterize each geodesic, so a change of variables can be made so that the parameters in the kinematic space are the initial and final endpoints of the geodesic, that is, u and v. Using the formula for differential entropy (2.62), it is possible to find the relationship between Crofton's formula and entanglement entropy. Then the differential entropy can be rewritten as follows:

$$\begin{aligned} L[\gamma] &= -\int_0^{2\pi} du \frac{\partial S(u,v)}{\partial u}\bigg|_{v=v(u)} \\ &= -\int_0^{2\pi} du \left[\frac{\partial S(u,v)}{\partial u}\bigg|_{v=v(u)} - \frac{\partial S(u,v)}{\partial u}\bigg|_{v=u+\pi} \right] \\ &= \frac{2}{4} \int_0^{2\pi} du \int_{v(u)}^{u+\pi} dv 2 \times \frac{\partial^2 S(u,v)}{\partial u \partial v}. \end{aligned} \tag{2.85}$$

To go from the first equality to the second, a term has been added with differential entropy equal to zero, that is, that of a point (see below). To go from the second to the third equality, one more integral has been implemented, which through an extra derivative in v reproduces the previous terms. The first factor of 2 counts the number of intersections of the geodesic with the curve, while the second factor of 2 counts the two orientations of each geodesic. The advantage of this representation is that everything is expressed in terms of kinematic space variables, and therefore it is immediate to identify the corresponding Crofton form given by [202]

$$\omega(u, v) = \frac{\partial^2 S(u,v)}{\partial u \partial v} du \wedge dv. \tag{2.86}$$

Thus, it has been shown that the differential entropy formula provides a way to identify the corresponding Crofton form as the double derivative of the entanglement entropy. Because of this, given the intervals

$$A = (u - du, u), \qquad B = (u, v) \qquad \text{y} \qquad C = (v, v + dv), \tag{2.87}$$

it is possible to use a fundamental property of entanglement entropy, strong subadditivity, which states

$$S_{AB} + S_{BC} - S_B - S_{ABC} \geq 0, \tag{2.88}$$

to show that

$$S(u - du, u) + S(u, v + dv) - S(u, v) - S(u - du, v + dv) \approx \frac{\partial^2 S(u, v)}{\partial u \partial v} du dv \geq 0. \tag{2.89}$$

Crofton's formula is a fundamental piece from which other geometric elements and concepts can be derived. Given a convex curve in the bulk, the Crofton form integrates over a subregion of the kinematic space of codimension-zero, since it takes into account all the geodesics that intersect the curve. However, it is possible to think of a continuous transformation that turns the original curve into a point. In this way, the length of the curve is reduced until it reaches zero, which is equivalent in kinematic space to the reduction of the integration region until it collapses to a subregion of co-dimension one. It should be emphasized that the contraction of the aforementioned curve is always possible in the present context since there are no topological restrictions. Due to the previous construction, the geometric interpretation is clear and, at the same time, surprising. A point is identified in kinematic space as the curve that defines the set of geodesics that intersect the point; this curve is known as a point curve. All these geodesics are anchored throughout the boundary. Consequently, the definition of a point on the bulk translates into non-local information at the boundary.

Another important concept in geometry is the distance between points. To identify the region in kinematic space that correctly computes the distance between two points A and B, consider that they are infinitesimally far apart. The previous argument determines how each point corresponds to its respective point curve. Assuming that the separation between the points is zero, it is consistently held that the point curves coincide and therefore, the volume in the kinematic space will have measure zero. As A and B move apart, a region of co-dimension zero bounded by the point curves is generated; this is precisely the correct integration region that reproduces the distance between A and B. Each point within this region represents a geodesic that intersects the geodesic segment that joins the two points. This region between the curve points p_A and p_B will be denoted as $p_A \triangle p_B$. Then the kinematic formula for the distance between A and B is

$$\frac{l(A, B)}{4G_N} = \frac{1}{4} \int_{p_A \triangle p_B} \omega. \tag{2.90}$$

The last kinematic space formula involves the calculation of the interior volume Q whose boundary is a convex closed curve. In [149],the authors justified the following formula:

$$\frac{V(Q)}{4G_N} = \frac{1}{2\pi} \int_{G \subset K} \lambda_G \omega. \tag{2.91}$$

In this expression, G is the subset of the kinematic space of geodesics that traverse region Q and λ_G is the length of the geodesic segment that remains within region Q.

2.5 Entanglement of Purification

In section 5.3, it was detailed how a density matrix representing a pure state generates a density matrix representing a mixed state for some subsystem. In the field theory context, this was achieved by restricting an observer's measurements to a specific region of space, R. The entanglement entropy was used as a measure of the quantum correlations that the observer region has with

their surroundings. For a non-entangled state, this quantity turns out to be identically zero since there is complete separability between the state that describes the subregion and the state that describes the rest. Thinking the other way around, given a mixed state with a bipartition, ρ_{AB}, it is interesting to consider the possibility of purifying the state by allowing access to additional degrees of freedom. Then, a state $|\psi\rangle \in \mathcal{H}_{AA'} \otimes \mathcal{H}_{BB'}$ is said to purify the density matrix ρ_{AB} if the following happens:

$$\rho_{AB} = \mathrm{Tr}_{A'B'} \left(|\psi\rangle \langle\psi| \right). \tag{2.92}$$

The purifying state, $|\psi\rangle$, is an element of a larger Hilbert space since, in addition to containing the original degrees of freedom, AB, it contains additional information encoded in the bipartition $A'B'$. Due to the nature of the construction, there are an infinite number of possible purifications, so from a preliminary point of view, the concept of purification seems of little use. However, entanglement is an essential resource in protocols applicable to quantum computing; it is the currency that allows processes that are classically impossible to be carried out. From this perspective, one can choose from the infinite number of purifications one that involves the least possible entanglement. Then, the entanglement of purification [**?**] is defined by

$$E_P(\rho_{AB}) = \min_{\rho_{AB}} S(\rho_{BB'}). \tag{2.93}$$

In this expression, $\rho_{BB'} = \mathrm{Tr}_{AA'} \left(|\psi\rangle \langle\psi| \right)$ and the minimization process is performed with respect to all states $|\psi\rangle$ that satisfy the relation (2.92) and also with respect to all bipartitions $A'B'$. The entanglement of purification is a quantum information measure in which classical and quantum correlations are treated at the same level. Properties that relate entanglement of purification to mutual information and entanglement entropy are known; these are:

$$\frac{1}{2} I(A:B) \leq E_P(\rho_{AB}) \leq \min \left[S(\rho_A), S(\rho_B) \right] \tag{2.94}$$

$$E_P(\rho_{A(BC)}) \geq E_P(\rho_{AB}) \tag{2.95}$$

$$E_P(\rho_{A(BC)}) \geq \frac{1}{2} I(A:B) + \frac{1}{2} I(A:C) \tag{2.96}$$

On the gravitational side of the holographic correspondence, there is a geometric object that fulfills the same equalities listed above: the entanglement wedge cross-section. Specifically, suppose we have two non-overlapping subsystems, A and B, at the boundary of a d-dimensional, static, and asymptotically AdS space-time. Consider the constant-time slice of the entanglement wedge associated with the union of these regions, M_{AB}. The entanglement wedge boundary can be decomposed as follows:

$$\partial M_{AB} = A \cup B \cup \Gamma_{AB}^{min}, \tag{2.97}$$

where Γ_{AB}^{min} is the RT surface associated to the union between A y B. Additionally, Γ_{AB}^{min} can be separated as

$$\Gamma_{AB}^{min} = \Gamma_{AB}^{(A)} \cup \Gamma_{AB}^{(B)}. \tag{2.98}$$

Then, the entanglement wedge cross-section, Σ_{AB}^{min}, is defined as the minimal-area surface anchored to Γ_{AB}^{min} that separates the regions A and B. The cross-sectional area is given by

$$E_W(\rho_{AB}) = \frac{A(\Sigma_{AB}^{min})}{4G_N}. \tag{2.99}$$

This object correctly reproduces the inequalities (2.94), (2.95), and (2.96). In [152, 153] it was recently proposed that

$$E_P(\rho_{AB}) = E_W(\rho_{AB}). \tag{2.100}$$

2.6 Computational Complexity

Entanglement entropy plays a fundamental role in the emergence of classical spacetime from the holographic point of view. This can be appreciated in the Poincaré disk. In this geometry, it is possible to foliate the entire space using geodesics anchored on the boundary. Those geodesics have a specific regularized length whose value computes the entanglement entropies of the associated intervals. From this perspective, when calculating the entanglement entropies, a list of data is created, which has to be reproduced by the length of the corresponding geodesics. However, in general, it is unrealistic to expect that from a list of data produced by the entanglement entropies of different regions, a geometry can be found such that its extreme surfaces match all the data. The existence of entanglement shadows [150] and black hole interiors, in static situations [151], eliminates the possibility of reconstructing the complete geometry from the extremal surfaces because these cannot penetrate those regions. So, it is important to find other measures of information that allow us to probe regions where the entanglement entropy does not help us.

Computational complexity or circuit complexity is a concept in quantum computing that has the purpose of measuring the degree of difficulty of performing a specific task. Specifically, given two states $|\psi_R\rangle$, $|\psi_T\rangle \in \mathcal{H}$ and a set of elementary operations acting on a small number of qubits at the same time, the computational complexity is defined as the minimum number of elementary operations that build a unitary operator U that satisfies

$$|\psi_T\rangle = U\,|\psi_R\rangle\,. \tag{2.101}$$

In the case of a system of n qubits, U is a unitary matrix of $2^n \times 2^n$, and the set of elementary operations consists of operators that only act on two qubits at a time, that is, operators of the form

$$\mathcal{O}_{n-1,n} = \underbrace{I \otimes \cdots \otimes I \otimes G}_{n \quad \text{factors}}. \tag{2.102}$$

This operator, known as a gate, only acts on qubits $n-1$ and n. By restricting the number of gates that can be used to implement a unitary U operator, you limit the different types of operators that can be constructed. Therefore, the set of gates must meet a sufficiency criterion that allows you to build any type of operator available. The following definition characterizes this property:

Definition (Set of universal gates.) Let $\mathcal{G}$ be a finite set of gates. $\mathcal{G}$ is said to be universal or $\mathcal{G}$-universal if it is possible to use a subset of its elements to construct **any** unitary operator U to **any** given degree of precision.

Consequently, working with a discrete set of gates or elementary operations requires the implementation of a tolerance ϵ that measures the degree of precision with which the objective state is obtained, that is, Eq. (2.101) is replaced by

$$||\,|\psi_T\rangle - U\,|\psi_R\rangle\,|| < \epsilon, \tag{2.103}$$

for some notion of distance between states. An example of a $\mathcal{G}$-universal set contains the following gates:

1. The Toffoli gate, which maps $|x, y, z\rangle$ to $|x, y, z \bigoplus xy\rangle$, where $x, y, z \in \{0, 1\}$ and $\bigoplus$ represent modulo 2 addition.

2. The Hadamard gate, this gate maps $|0\rangle \to |+\rangle$ and $|1\rangle \to |-\rangle$.

3. The phase gate, which maps $|0\rangle \to |0\rangle$ and $|1\rangle \to i\,|1\rangle$.

In the CFT, it is possible to consider the thermal state, given by the following density matrix:

$$\rho = \frac{1}{Z}\sum_i e^{-\beta E_i} \left|E_i\right\rangle \left\langle E_i\right| . \tag{2.104}$$

In this expression, $\{|E_i\rangle\}_i$ is a basis of energy eigenstates, and Z is the canonical partition function of the system. The state described by (2.104) is, due to its thermal nature, mixed. Then, it is possible to consider different states that purify the system. The most widely used purification in the literature for this state is known as the double thermofield state or TFD, and is given by the following expression:

$$\left|TFD\right\rangle = \frac{1}{\sqrt{Z}}\sum_i e^{-\beta E_i/2} \left|E_i\right\rangle \left|E_i\right\rangle . \tag{2.105}$$

In this case, the auxiliary degrees of freedom, which serve to purify, area a second copy of the same system. The holographic dual of this state is the system described by an eternal black hole [**?**]. This gravitational dual is constituted by two asymptotic regions connected by a smooth geometry. At a given instant of time, the two asymptotic regions are connected by a spatial region known as a wormhole or Einstein-Rosen bridge. The time evolution of the TFD state is given by

$$\left|TDF(t_I, t_D)\right\rangle = \frac{1}{\sqrt{Z}}\sum_i e^{-\beta E_i/2} e^{-iE_i(t_I+t_D)} \left|E_i\right\rangle \left|E_i\right\rangle , \tag{2.106}$$

where $t_{I,D}$ represent a notion of time in the asymptotic regions. For a notion of time evolution in which $t_I \to t_I + \Delta t$ and $t_D \to t_D - \Delta t$, the state remains invariant. On the bulk side, it is therefore observed that the wormhole does not grow under this notion of time. However, if the time flow is chosen to be determined by $t_I + t_D$, the state will evolve non-trivially in time: the interior of the wormhole grows larger as time goes on. Classically, the interior grows without limit; therefore, it is valid to ask: what is the dual in the CFT of the growth of the wormhole? Entanglement entropy or some combination of it cannot be the answer because its growth saturates after relatively short times [199]. In order to specifically answer the previously posed question, it is worth emphasizing other properties of the wormhole. Since entanglement is not a good candidate for measuring the growth of a wormhole interior, it is a bad idea to use the area directly or complicated combinations of it to measure growth. So, it is natural to consider the volume of the spatial region as a measure of the growth of the interior. In analogy with the RT formula, the temporal foliation given by spatial slices that satisfy the property that they have maximum volume is chosen. Calculations of the gravitational side reveal that the volume grows for very long times, reproducing the expected behavior. On the CFT side, the computational complexity of the state $|TDF(t_I, t_D)\rangle$ is a property that does not saturate for short times; even after the system has thermalized, it continues to grow. Because of this, in [**?**] Susskind proposed the following conjecture:

$$C(|TFD(t_I, t_D)\rangle) = \max\left[\frac{\mathcal{V}(t_I, t_D)}{G_N l}\right] . \tag{2.107}$$

That is, the complexity of the TFD state is calculated by determining the maximum volume of the wormhole. In the previous expression, l represents the characteristic length of the system. This prescription for calculating complexity holographically is known as "complexity=volume" or CV. An interesting aspect of this proposal is that for very long times, the time derivative of the complexity, the computation speed, has the following value:

$$\lim_{t_I+t_D\to\infty} \frac{dC_V}{d(t_I + t_D)} = \frac{8\pi M}{d-1}, \tag{2.108}$$

where d is the dimension of spacetime and M is the mass of the black hole. This result interprets the mass of the system as the parameter that measures how high its computation speed is. However, this result was also found by Lloyd when considering the maximum computing speed of a system with energy E. Consequently, it can be inferred that black holes saturate the so-called Lloyd's bound and therefore are the systems that represent the fastest computers in the universe. Although the CV prescription satisfactorily reproduces the known complexity behavior, it has certain associated disadvantages. The first involves the foliation of spacetime into slices of maximum

volume; from a fundamental point of view, the reason for this choice is unclear. The second is the appearance of the characteristic scale l, which can change depending on the context. Emphasizing these observations, a new prescription was constructed where

$$C(|TFD(t_I, t_D)\rangle) = \frac{I_{WdW}(t_I, t_D)}{\pi}. \tag{2.109}$$

Here $I_{WdW}(t_I, t_D)$ refers to the action evaluated in the region encompassed by the Wheeler-DeWitt patch, which in turn is defined as the domain of dependence of a spatial slice that is anchored on times t_I and t_D at the boundary. This prescription is known as "complexity=action" or CA. The Lloyd limit associated with this prescription is given by

$$\lim_{t_I + t_D \to \infty} \frac{dC_A}{d(t_I + t_D)} = \frac{2M}{\pi}. \tag{2.110}$$

Both prescriptions reproduce known behaviors of computational complexity, so there is not yet a definitive criterion that selects one (There is in fact a much larger set of options [200]). This is largely due to the technical difficulty involved in the CFT calculations and the lack of a single formalism to deal with the problem. In recent years, much progress has been made in this regard by implementing Nielsen's geometric formalism in which the problem of finding the optimal circuit is translated to computing a certain geodesic in a metric space [201].

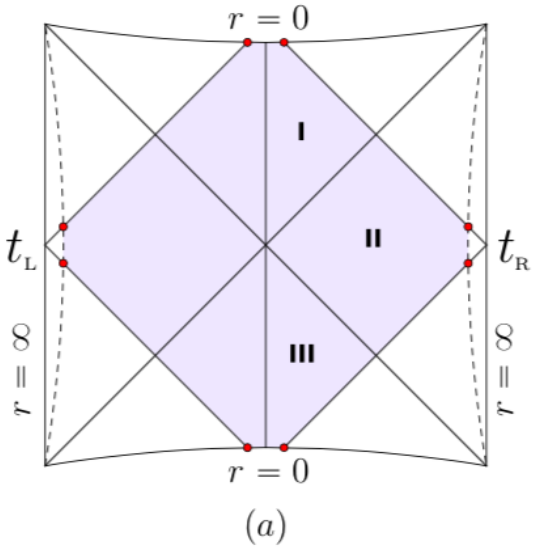

Figure 2.4: WdW patch geometry.

2.7 Manual for the use of the Action

The Wheeler-DeWitt patch is the spacetime region corresponding to the domain of dependence associated with a given spatial slice. The elements that compose its boundary in spacetime are spatial segments, temporal segments, null segments, and all kinds of unions between them; see figure (2.4). The gravitational action in the presence of cosmological constant Λ, from which Einstein's equations are derived, is given by

$$I = \frac{1}{16\pi G_N} \int_{\mathcal{M}} d^{d+1}x \sqrt{-g}(R - 2\Lambda). \tag{2.111}$$

However, when considering a spacetime, $\mathcal{M}$, with boundary $\partial\mathcal{M}$, additional terms associated with the latter have to be considered. The simple variation of the action (2.104) without considering the additional terms generates an ill-defined variational problem due to the appearance of variations in the derivatives of the metric. A detailed analysis reveals the kind of terms that need to be included

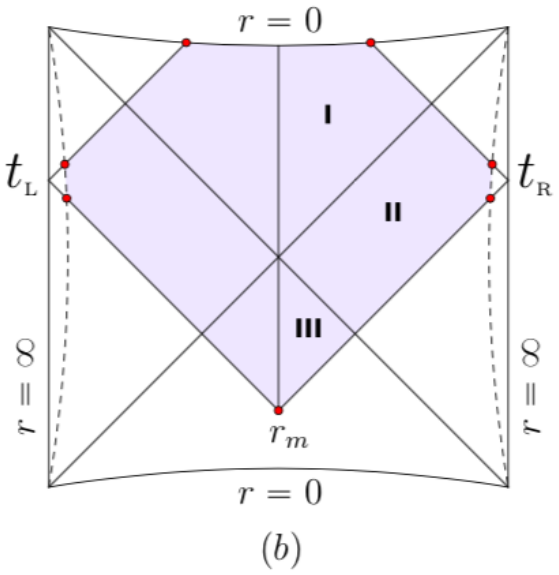

Figure 2.5: WdW patch configuration for times greater than the critical time.

to cancel out unwanted variations [190]. The most general gravitational action that gives rise to Einstein's equations and also has a well-defined variational principle is

$$
\begin{aligned}
I = & \frac{1}{16\pi G_N}\int_{\mathcal{M}} d^dx\sqrt{-g}(R-2\Lambda) \\
& + \frac{1}{8\pi G_N}\left[\sum_{T_i}\int_{\partial\mathcal{M}_{T_i}} d^dx\sqrt{-h}K + \sum_{S_i}\mathrm{sgn}(S_i)\int_{\partial\mathcal{M}_{S_i}} d^dx\sqrt{h}K - \sum_{N_i}\mathrm{sgn}(N_i)\int_{\partial\mathcal{M}_{N_i}} d\lambda d^{d-1}\theta\sqrt{\gamma}\kappa\right] \\
& + \frac{1}{8\pi G_N}\left[\sum_{j_i}\mathrm{sgn}(j_i)\int d^{d-1}x\sqrt{\sigma}\eta_{j_i} + \sum_{m_i}\mathrm{sgn}(m_i)\int d^{d-1}x\sqrt{\sigma}a_{m_i}\right].
\end{aligned}
\tag{2.112}
$$

In the first line of the previous expression, we have the usual Einstein-Hilbert term with cosmological constant evaluated in the bulk. The terms in the second row must be added due to the presence of a boundary. The boundary can be spatial (S_i), temporal (T_i) or null (N_i). For spatial and temporal surfaces, the term to consider is the Gibbons-Hawking action, while in the case of a null surface, a term is added that is the integral on the surface over on affine parameter κ [**?**, **?**]. The sign with which each integral contributes is determined by its orientation. For spatial surfaces, it will be the positive sign if its normal vector points to the future and the minus sign otherwise. Similarly, for null surfaces, the positive sign will be taken if the volume of the region to be integrated is in the future of the null segment and the minus sign is taken otherwise. In the third line, the terms come into play due to the presence of joints between segments. The following list covers all possible cases:

1. **Union between space-like segments ($S \wedge S$).** Let $n^\alpha_{1,2}$ be the normal vector pointing into the future on each surface and $p^\alpha_{1,2}$ be the tangent vector on each surface. Then, the factor η_{j_i} is determined by
$$\eta_{j_i} = \ln|(n_1 + p_1)\cdot n_2|. \tag{2.113}$$

2. **Union between time-like segments ($T \wedge T$).** Let $s^\alpha_{1,2}$ be the spatial unit normal to each surface. Also, let $p^\alpha_{1,2}$ be the tangent vector to each surface. Then, the factor η_{j_i} is determined by
$$\eta_{j_i} = \ln|(s_1 + p_1)\cdot s_2|. \tag{2.114}$$

3. **Union between time-like and space-like segments ($T \wedge S$).** Using the previous definitions of the normal and tangent vectors, we have the following expression

$$\eta_{j_i} = \ln |(n + p) \cdot s|. \tag{2.115}$$

For the cases $(S \wedge S)$ and $(T \wedge S)$, the sign of the integral will be positive if the normal vector, n_1^α, points out of the volume of interest, and negative in the opposite case. In the case $(T \wedge T)$, a positive sign is always obtained. For null segments, there are also three cases that derive from considering the possible unions between surfaces in which one of them is null. The following list summarizes the set of rules to consider for each integral:

1. **Union between null and space-like segments ($N \wedge S$).** Let k_α be the tangent vector pointing to the future of the null surface. Then, the corresponding integral contains the following factor

$$a = \ln |k \cdot n|. \tag{2.116}$$

2. **Union between null and time-like segments ($N \wedge T$).** Let k_α be the tangent vector pointing to the future of the null surface. Then, the corresponding integral contains the following factor

$$a = \ln |k \cdot s|. \tag{2.117}$$

3. **Union between null segments ($N \wedge N$).** Let $k_{1,2}^\alpha$ be the tangent vector pointing into the future of each null surface. Then, the corresponding integral contains the following factor

$$a = \ln |k_1 \cdot k_2|. \tag{2.118}$$

In the case of a Lovelock theory of gravity, a generalization of this manual can be found in [154].

Chapter 3

PhD projects (Objectives, Methods and Results)

The specific objectives outlined before resulted in the following research articles:

- arXiv:1808.00067 [185]. Holographic complexity of anisotropic black branes. Published in Physical Review D in collaboration with Seyed Ali Hosseini Mansoori, Viktor Jahnke and Mohammad M. Qaemmaqami.

- arXiv:1905.07413 [186]. Holographic integral geometry with time dependence. Published in JHEP in collaboration with Bartlomiej Czech and Zi-zhi Wang.

- arXiv:2104.12796 [194] Insensitivity of the complexity rate of change to the conformal anomaly and Lloyd's bound as a possible renormalization condition. Published in Physical Review D in collaboration with Daniel Ávila, César Díaz and Leonardo Patiño.
- arXiv:2201.01786 [187] Holographic Coarse-Graining: Correlators from the Entanglement Wedge and Other Reduced Geometries. Published in JHEP in collaboration with Alberto Güijosa and Juan F. Pedraza.

This section summarizes the results obtained in the previously cited articles.

3.1 Holographic Complexity of Anisotropic Black Branes

Abstract. We use the complexity = action (CA) conjecture to study the full-time dependence of holographic complexity in anisotropic black branes. We find that the time behaviour of holographic complexity of anisotropic systems shares a lot of similarities with the behaviour observed in isotropic systems. In particular, the holographic complexity remains constant for some initial period, and then it starts to change so that the complexity growth rate violates the Lloyd's bound at initial times, and approaches this bound from above at later times. Compared with isotropic systems at the same temperature, the anisotropy reduces the initial period in which the complexity is constant and increases the rate of change of complexity. At late times the difference between the isotropic and anisotropic results is proportional to the pressure difference in the transverse and longitudinal directions.

3.1.1 General aspects of the on-shell action and the WdW patch

The gravitational solution described by the MT model [188] can be extended to an eternal black brane solution. The extended solution is dual to the state $|TFD\rangle$, which is a possible purification resulting from considering the entanglement of two copies of the original theory. The prescription implemented to calculate the complexity involved the evaluation of the on-shell action in the WdW

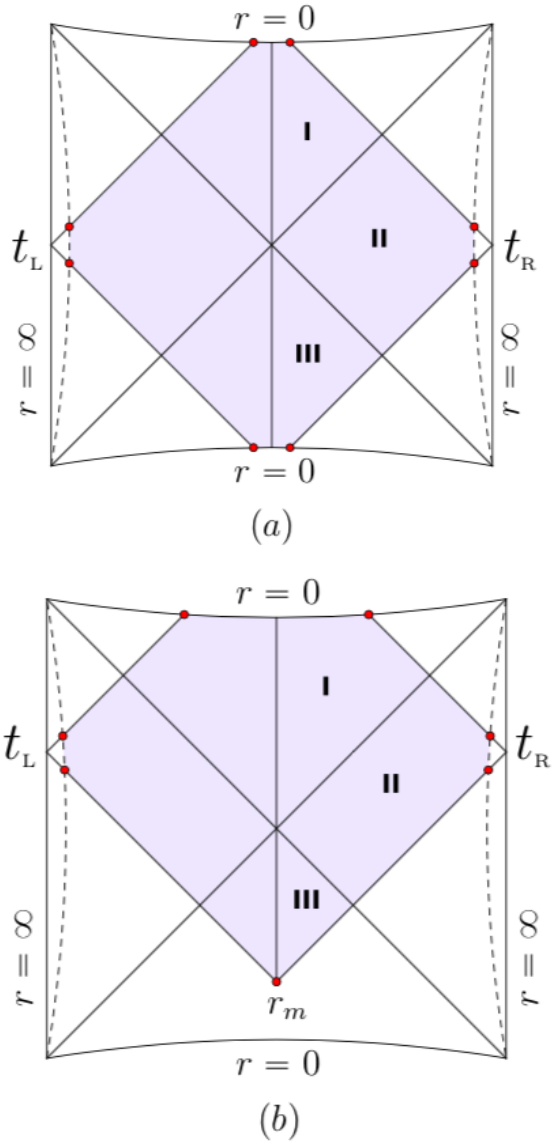

Figure 3.1: Penrose diagram and the WDW patch (blue region) for the two-sided black brane we consider. (a) Configuration at initial times ($t \leq t_c$) in which the WDW patch intersects both the future and the past singularity. (b) Configuration at later times ($t > t_c$) when the WDW patch no longer intersects the past singularity. The dashed lines represent the cutoff surfaces at $r = r_{max}$.

patch. The WdW patch corresponding to this geometry can be seen in figure (3.1). The notion of time on the boundary is taken to be such that $t_I = t_D = t/2$; therefore, the WdW patch is a square figure. The region near the boundaries is regularized using the parameter r_{max} and the regions near the singularities are regularized with the parameter ϵ. The on-shell action has the following form:

$$S = \frac{1}{16\pi G_N}\int_{\mathcal{V}} dV\,(R - 2\Lambda) + \frac{1}{8\pi G_N}\int_{\partial\mathcal{V}} dSK, \tag{3.1}$$

where R is the Ricci scalar evaluated in $\mathcal{V}$, Λ is the cosmological constant and K the extrinsic curvature of $\partial\mathcal{V}$. In order to perform the calculations in the most general way possible, the following form of the metric is assumed:

$$ds^2 = -G_{tt}(r)dt^2 + G_{rr}(r)dr^2 + G_{ij}(r)dx^i dx^j, \tag{3.2}$$

where r is the AdS radial coordinate and (t, x^i) are the gauge theory coordinates with $i = 1, 2, ..., d-1$. The boundary is located at $r \to \infty$ and a horizon is assumed to exist at $r = r_H$, where G_{tt} becomes zero and G_{rr} has a simple pole. We denote the determinant of G_{ij} as G.

In complexity calculations, it is convenient to use coordinates that smoothly cover both sides of the geometry. In this sense, the Eddington-Finkelstein coordinates are used, which are defined as

$$u = t - r^*(r)\,, \quad v = t + r^*(r)\,, \tag{3.3}$$

where the tortoise coordinate is defined as

$$r^*(r) = \mathrm{sgn}(G_{tt}(r)) \int^r dr' \sqrt{\frac{G_{rr}(r')}{G_{tt}(r')}}\,. \tag{3.4}$$

The CA prescription [189] states that the computational complexity of the state $|TFD\rangle$ is given by the gravitational action evaluated in the Wheeler-DeWitt (WdW) patch, in other words,

$$\mathcal{C}_A = \frac{I_{WDW}}{\pi}\,. \tag{3.5}$$

Due to the presence of a boundary, I_{WDW} must be evaluated considering the terms corresponding to each part of the boundary; namely,

$$I_{\mathrm{WDW}} = I_{\mathrm{bulk}} + I_{\mathrm{surface}} + I_{\mathrm{joint}}\,, \tag{3.6}$$

where

$$I_{\mathrm{bulk}} = \frac{1}{16\pi G_N} \int_{\mathcal{V}} dV\,(R - 2\Lambda) \tag{3.7}$$

is the bulk gravitational action and I_{surface}, I_{joint} correspond to the surface and joint terms, respectively. The inclusion of these boundary terms is essential for the correct definition of the gravitational variational principle [190]. The explicit form of the surface and joint terms is given by Eq. (2.112).

The WdW patch boundary is composed of null segments that are shot from the asymptotic boundary at $t_I = t_D = t/2$, timelike segments generated by the presence of the factor r_{max} that regularizes the action, and spatial segments present by the regularization of the singularity with the parameter ϵ. Additionally, there are joints between segments, which make the border not smooth. Conveniently, an affine parameterization of the null surfaces can be used, which makes these terms vanish completely.

The presence of null boundaries and the symmetric configuration of the WdW patch makes it necessary to consider the time range in two stages characterized by a critical time t_c. For times $t < t_c$ the WdW patch overlaps with the past and future singularities because the Penrose diagram does not represent a completely square region [193]. For times $t_c \leq t$, the bottom of the WdW patch is completely separated from the past singularity, so the configuration is now not symmetric. The critical time can be calculated by determining the locus where null geodesics thrown from the boundary toward the past intersect. Then, t_c satisfies the following relation:

$$t_c = 2\,(r^*_\infty - r^*(0))\,, \quad r^*_\infty = \lim_{r\to\infty} r^*(r). \tag{3.8}$$

Figure 3.2 shows the behavior of the critical time as a function of a/T, fixing the temperature. It can be seen that the anisotropy causes a minimal reduction in the critical time. In the following sections, the results of the on-shell action in the aforementioned configurations will be presented.

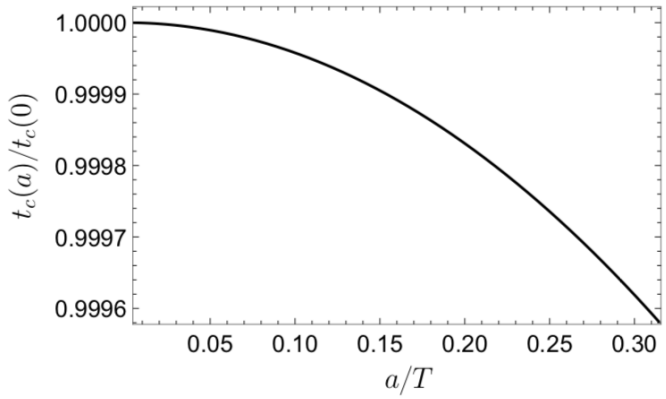

Figure 3.2: Critical time (normalized by isotropic result) versus a/T. We consider increasing values of a, but we choose them r_h in such a way as to keep the temperature fixed as $T = \frac{1}{\pi}$.

3.1.2 Behavior at initial times: $0 \leq t < t_c$

For $t \in [0, t_C)$, the upper and lower corners of the WdW patch are absent due to past and future singularities. The contributions for I_{WdW}, in this case, include the bulk term, two GHY terms for the timelike boundaries at $r = r_{max}$ close to the asymptotic regions, two GHY terms for the spacelike boundaries at $r = \epsilon$ that regularize the region close to the singularities, and the joint terms that correspond to the intersection of the ones mentioned above. Due to the symmetry of the WdW patch configuration, it is possible only to calculate the contributions corresponding to one-half, since the total contribution will be double. Taking this observation into account, the bulk term can be broken down into three parts corresponding to the subregions on the right-hand side. That is

$$I_{\text{bulk}}(t \leq t_c) = 2\left(I^{I}_{bulk} + I^{II}_{bulk} + I^{III}_{bulk}\right) , \tag{3.9}$$

To define regions I, II, and III, reference is made to figure 2.4. The result of adding the three contributions is

$$I_{\text{bulk}} = \frac{1}{2\pi G_N}\int_{\epsilon_0}^{r_{\max}} dr\sqrt{-g}\,\mathcal{L}(r)\Big(r^*_\infty - r^*(r)\Big) . \tag{3.10}$$

It is observed that the result does not depend on time due to the symmetry of the configuration: as time progresses, the region that disappears in the future singularity emerges from the past singularity.

The boundary contribution to the WdW patch shares the exact symmetry as the bulk term; therefore, it is possible to consider the total contribution by only assuming one side and then doubling the result. So, we have

$$I_{\text{surface}}(t \leq t_c) = I^{\text{future}}_{\text{surface}} + I^{\text{past}}_{\text{surface}} + I^{\text{frontera}}_{\text{boundary}}. \tag{3.11}$$

After adding the explicit form of the contributions, the following expression is obtained:

$$I_{\text{sup}}(t \leq t_c) = \frac{V_{d-1}}{4\pi G_N}\mathcal{G}(r)\left(r^*_\infty - r^*(r)\right)\Big|_{r=\epsilon_0} + \frac{V_{d-1}}{8\pi G_N}\mathcal{G}(r)\left(r^*_\infty - r^*(r)\right)\Big|_{r=r_{max}},$$

where

$$\mathcal{G}(r) = \sqrt{\frac{G_{tt}G}{G_{rr}}}\left[\frac{G'_{tt}}{G_{tt}} + \frac{G'}{G}\right] . \tag{3.12}$$

Like the bulk result, the contribution to the action from the boundary region is not time-dependent. Finally, we address the term included in the action due to the presence of non-smooth joints between the boundaries. The type of unions considered corresponds to the intersection of

null boundaries with spacelike boundaries and null with timelike boundaries. The contribution from the joints takes the form

$$I_{\text{joint}} = I_{\text{joint}}^{\text{sing}} + I_{\text{joint}}^{\text{boundary}}\,, \tag{3.13}$$

A detailed analysis reveals that this contribution, like the others, is not time-dependent. In conclusion, the sum of the terms I_{bulk}, I_{surface} and I_{join} does not depend on time, that is

$$\frac{dI_{WDW}}{dt} = 0\,, \quad \text{when } 0 \leq t < t_c\,. \tag{3.14}$$

3.1.3 Behavior at late times: $t_c \leq t$

For $t = t_c$, the lower corner of the WdW patch makes contact with the surface $r = \epsilon$ that regularizes the singularity. For later times the lower corner is completely visible in the Penrose diagram, and therefore we have a configuration that breaks the symmetry of the previous case. On the other hand, the WdW patch is still symmetric about the vertical axis located in the central part of the Penrose diagram. Then, the bulk term and the surface and union terms can be separated in the same way as in the previous case. Then the contribution of the bulk term is

$$I_{\text{bulk}}(t \geq t_c) = 2\left(I_{\text{bulk}}^{\text{I}} + I_{\text{bulk}}^{\text{II}} + I_{\text{bulk}}^{\text{III}}\right)\,, \tag{3.15}$$

whose explicit form turns out to be

$$I_{\text{bulk}}(t \geq t_c) = I_{\text{bulk}}(t < t_c) + \frac{V_{d-1}}{8\pi G_N}\int_{\epsilon_0}^{r_m} dr\sqrt{-g}\,\mathcal{L}(r)\left(\frac{t}{2} - r_\infty^* + r^*(r)\right)\,.$$

In this expression, it can be seen that the term in the action corresponding to the bulk can be separated into two contributions: the contribution of the bulk for early times and a contribution that depends directly on time. The parameter r_m refers to the radial location of the lower corner of the WdW patch, which is also time-dependent and satisfies the following relationship:

$$\frac{t}{2} - r_\infty^* + r^*(r_m) = 0\,. \tag{3.16}$$

The contribution of the surface terms shares the same structure, in other words, we have

$$I_{\text{surface}}(t \geq t_c) = I_{\text{surface}}(t < t_c) + I_{\text{surface}}^{\text{future}}\,, \tag{3.17}$$

where,

$$I_{\text{surface}}^{\text{future}} = \frac{V_{d-1}}{8\pi G_N}\mathcal{G}(r)\left(\frac{t}{2} + r_\infty^* - r^*(r)\right)\Big|_{r=\epsilon}. \tag{3.18}$$

This last term corresponds to the contribution of the surface with $r = \epsilon$.
For late times, the WdW patch contains joints between null and spatial surfaces, as well as joints between null surfaces. Adding all the contributions due to unions gives

$$I_{\text{joints}}(t \geq t_c) = I_{\text{joints}}(t < t_c) - \frac{V_{d-1}}{8\pi G_N}\sqrt{G(r_m)}\log\left|\frac{G_{tt}(r_m)}{\alpha^2}\right|\,. \tag{3.19}$$

The second term represents the WdW patch lower joint contribution in the above expression.

Adding all the terms that contribute to the action and differentiating with respect to time, we finally obtain

$$\frac{dI_{WDW}}{dt} = \frac{V_{d-1}}{16\pi G_N}\left[\int_{\epsilon_0}^{r_m} dr\sqrt{-g}\,\mathcal{L}(r) + \mathcal{G}(r)\Big|_{r=\epsilon} + \left(\frac{1}{2}\sqrt{\frac{G_{tt}}{G_{rr}G}}G'\log\left|\frac{G_{tt}}{\alpha^2}\right| + \sqrt{\frac{G}{G_{rr}G_{tt}}}G'_{tt}\right)\Big|_{r=r_m}\right]\,. \tag{3.20}$$

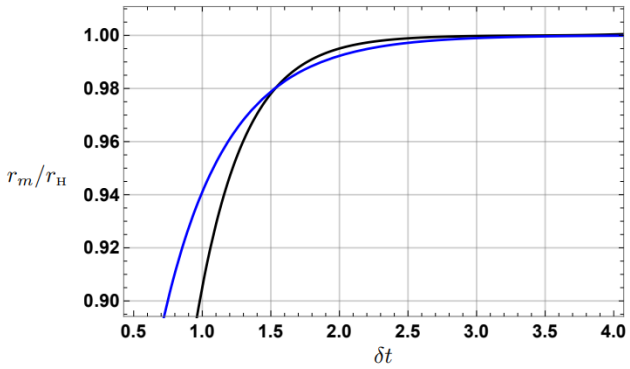

Figure 3.3: $\frac{r_m}{r_h}$ versus δt for the MT model (blue curve) and for the DK model (black curve). Here, for the MT model, we have fixed $r_h = 1$ and $a/T = 0.314$. For the DK model we fixed $B = 3$ and $r_h = 1$. The curves obtained for other values of these parameters are indistinguishable from the above results.

Then, the time derivative of the complexity is obtained simply by using

$$\frac{d\mathcal{C}_A}{dt} = \frac{1}{\pi}\frac{dI_{WDW}}{dt}\,. \tag{3.21}$$

This expression allows calculating the behavior in the complexity growth rate for any time value. In figure (3.1.4), it can be seen that initially, the computation speed remains equal to zero, reflecting that the state does not become more complex. Once the critical time is exceeded, the computation speed increases until it reaches a maximum and then decreases asymptotically to a specific value that coincides with the corresponding Lloyd limit. The behavior is qualitatively similar to the isotropic case.

3.1.4 Late time behavior: $t \to \infty$

The expression for the action evaluated on the on-shell action simplifies dramatically in the limit $t \to \infty$. In this time scale, most of the WdW patch has disappeared due to the presence of the singularity. Consequently, the region's lower joint asymptotically approaches the horizon's radius, that is, $r_m \to r_H$. In figure (3.5) you can see the ratio r_m/r_H as a function of $t - t_c$. The expression that results from taking this limit is

$$\frac{dI_{WDW}}{dt} = \frac{V_{d-1}}{16\pi G_N}\left[\int_\epsilon dr\sqrt{-g}\,\mathcal{L}(r) + \sqrt{\frac{G}{G_{rr}G_{tt}}}G'_{tt}\Big|_{r=r_h} + \sqrt{\frac{G_{tt}G}{G_{rr}}}\left(\frac{G'_{tt}}{G_{tt}} + \frac{G'}{G}\right)\Big|_{r=\epsilon}\right]. \tag{3.22}$$

By substituting the component functions of the metric that characterize the solution of the MT model, the following result is obtained for the computation speed:

$$\frac{dC_A}{dt} = \frac{V_3}{16\pi^2 G_N}\left(6^4 + \frac{^2a^2}{2}\left(5\log(2) - 1\right)\right) = \frac{2M(a)}{\pi}\,. \tag{3.23}$$

The result shows that the computation speed saturates the Lloyd bound for very long times. It is important to highlight that the anisotropy, characterized by a/T, modifies the mass of the isotropic solution to the same extent that it modifies the corresponding computation speed.
In the same way, substituting the functions of the metric that characterize the solution of the DK model, we obtain

$$\frac{d\mathcal{C}_A}{dt} = \frac{1}{\pi}\frac{dI_{WDW}}{dt} = \frac{V_3}{16\pi^2 G_N} \times 6B^{\,2} = \frac{2M_B}{\pi}\,. \tag{3.24}$$

From the above expression it can be seen that the DK model also satisfies the corresponding Lloyd's bound.

3.1.5 Conclusions

This work considers two models that break the $SO(3)$ symmetry in the coordinates (x, y, z). In a perturbative analysis of the anisotropy parameter, the MT model showed a change in its computation speed with respect to the isotropic case. However, the qualitative characteristics of the isotropic case were preserved even in the presence of anisotropy. The computation speed is zero for times below the critical time; it stops being zero from there. The computation speed increases to a maximum value, then decreases and asymptotically saturates the corresponding Lloyd bound. Furthermore, it was found that the maximum value of the computation speed increases as the anisotropy increases, keeping a in the range of validity of the approximation. In the DK model, it was found that the corresponding Lloyd's bound is equally satisfied. The behavior of the complexity shows that it does change in models with broken symmetry under rotations; however, it does so in such a way that the universal characteristics of complexity are not changed.

3.2 Holographic Integral Geometry with Time Dependence

Abstract. We write down Crofton formulas—expressions that compute lengths of spacelike curves in asymptotically AdS_3 geometries as integrals over kinematic space—which apply when the curve and/or the background spacetime is time-dependent. Relative to their static predecessor, the time-dependent Crofton formulas display several new features, whose origin is the local null rotation symmetry of the bulk geometry. In pure AdS_3 where null rotations are global symmetries, the Crofton formulas simplify and become integrals over the null planes, which intersect the bulk curve.

3.2.1 Null alignment condition and local null rotations

The null vector alignment condition, NVA, reviewed in section (2.4.1), states that the differential entropy formula is not only valid using geodesics tangent to the space curve. It is also possible to reproduce the length of the curve using reoriented geodesics using a null vector orthogonal to the vector tangent to the curve. For each point on the spatial curve, a differently reoriented geodesic can be taken; therefore, this additional freedom is local. Because of this, the emergence of a submanifold of codimension one that directly takes this into account is inevitable. The family of all geodesics forms this hypersurface at a given point on the curve. Due to the existence of two null normals at each point on the curve, there are two hypersurfaces tangent to the curve. These tangent hypersurfaces are nothing more than null leaves that emanate tangentially from the point of the curve. Locally, these geodesics are related to each other by implementing a null rotation, which has the property of fixing a null vector.

3.2.2 Crofton formula

The differential entropy formula correctly calculates the length of a closed curve in the bulk using NVA geodesics to the curve. This calculation employs a one-dimensional integral to sum all the NVA geodesic in the curve. In the static case, this formula was promoted to a double integral using Stokes' theorem, giving rise to Crofton's formula and the correct identification of the Crofton form as the double derivative of the entanglement entropy [**?**]. The previous statement allowed us to identify the space where the double integral is performed as the kinematic space [186]. For closed space curves with non-trivial dependence on time, in general, the set of tangent or NVA geodesics will have endpoints described by the coordinates $x_L^\mu = (\tau_L, \theta_L)$ and $x_R^\mu = (\tau_R, \theta_R)$. Then, the differential entropy formula takes the form

$$L[\gamma] = \int_{\mathcal{M}_{\text{NVA}}} dx_R^\mu \frac{\partial S(x_L^\mu, x_R^\mu)}{\partial x_R^\mu}. \tag{3.25}$$

In this expression $\mathcal{M}_{\text{NVA}}$ is the set of all NVA geodesics that define the curve in the bulk. On the other hand, using Stokes' theorem, we get

$$\int_{\mathcal{K}} dx_L^\nu \wedge dx_R^\mu \frac{\partial^2 S(x_L^\mu, x_R^\mu)}{\partial x_L^\nu \partial x_R^\mu} = \int_{\mathcal{K}} d\left(\frac{\partial S(x_L^\mu, x_R^\mu)}{\partial x_R^\mu} dx_R^\mu\right) = \int_{\partial\mathcal{K}} dx_R^\mu \frac{\partial S(x_L^\mu, x_R^\mu)}{\partial x_R^\mu}, \tag{3.26}$$

where for consistency with the differential entropy formula $\mathcal{M}_{\text{NVA}} = \partial\mathcal{K}$ is identified. Therefore, the integration region $\mathcal{K}$ in the kinematic space must have a boundary in which all points are NVA geodesics. The previous argument allows us to identify Crofton's formula for the covariant case,

$$\frac{L[\gamma]}{4G} = \frac{1}{4}\int_K \omega \times n, \tag{3.27}$$

where

$$\begin{aligned}\omega &= \frac{\partial^2 S}{\partial x_L^\mu \partial x_R^\mu} dx_L^\mu \wedge dx_R^\nu \\ &= \frac{\partial^2 S}{\partial\theta_L \partial\theta_R} d\theta_L \wedge d\theta_R + \frac{\partial^2 S}{\partial\theta_L \partial\tau_R} d\theta_L \wedge d\tau_R + \frac{\partial^2 S}{\partial\tau_L \partial\theta_R} d\tau_L \wedge d\theta_R + \frac{\partial^2 S}{\partial\tau_L \partial\tau_R} d\tau_L \wedge d\tau_R\end{aligned} \tag{3.28}$$

and n represents the intersection number of the null plane with the spatial curve. For a convex curve, this factor is 2. As a consistency check for this formula, the case of spatial curves in AdS_3 was analyzed [186]. The first curve considered is a circumference of radius R centered at the origin of AdS_3. This curve has no time dependence; however, its use is justified as an example of consistency. The Crofton form was found to reproduce the length of this curve correctly. As a second example, the same circumference was used, now with a slight temporary oscillatory disturbance, so it does not alter its causal structure. The parameterization of this curve is given by

$$R(\theta) = R_0, \tag{3.29}$$

$$\tau(\theta) = \frac{R_0}{2\sqrt{1+R_0^2}} \epsilon \sin(2\theta). \tag{3.30}$$

Using Crofton's formula Eq. (3.27) was found to exactly reproduce the gravitational result.

3.2.3 Conclusions

The differential entropy formula applied in the covariant context allowed Crofton's formula to be generalized to the same scenario. The crucial step in the correct definition of the formula and identification of the Crofton form was the application of Stokes' theorem. This procedure also allowed us to identify the corresponding region in the kinematic space: the set of all points whose boundary can be understood as the NVA geodesics of the spatial curve in the bulk. The NVA condition allowed us to identify the geometric object, the tangent null sheet, which encodes the extra degree of freedom that exists when choosing the geodesics that reproduce the length of the curve in the differential entropy formula. Because all NVA geodesics are related to each other by a null rotation that keeps them on the same null sheet, this object provides us with a tool in which a single geometric entity describes an infinite number of possibilities when choosing NVA geodesics.

3.3 Insensitivity of the complexity rate of change to the conformal anomaly and Lloyd's bound as a possible renormalization condition

Abstract. We determine the effect on the computational complexity of a conformal anomaly using the Complexity=Action prescription of the gauge/gravity correspondence. To allow the involvement of said anomaly, we extend previous studies to include arbitrary values for the anisotropic parameter and the magnetic field respectively on the Mateos-Trancanelli and the D'Hoker-Kraus

holographic models. Our main result is that the rate of change of the computational complexity is independent of the conformal anomaly in both cases. In addition, this allows us to also show that, if so desired, the saturation of Lloyd's bound at infinite time can be used as a renormalization condition.

3.3.1 Conformal anomaly in the Mateos-Trancanelli and D'Hoker-Kraus models

The traditional treatment of quantum field theories implies starting with a classical action described in terms of classical fields. Later, those classical fields go through a standard procedure called "quantization" to obtain a quantum description of the classical system. The classical system sometimes possesses symmetries that must be preserved after quantization. This consideration applies especially in the case of a gauge symmetry. A gauge symmetry is an over-description of the system in which more than one possible field configuration exists for the same physical description. It is not a property of Nature but rather a property of how we choose to describe Nature. This type of symmetry must survive the quantization procedure in the sense that the symmetry must be also a symmetry of the quantum system. Otherwise, the quantum system might become mathematically inconsistent. On the other hand, *global* symmetries are actual symmetries, intrinsic to the system and with real physical consequences. They can sometimes be lost upon quantization, without inconsistency. Generically, the absence in a quantum theory of a symmetry that was present classically is known as an 'anomaly'.

The conformal anomaly is a particular case of interest that can be present in a CFT. As explained before, CFTs are quantum theories with an infinite number of degrees of freedom which have the conformal group as a symmetry group. In particular, they are invariant under a local rescaling of the metric that is

$$\delta g_{\alpha\beta} = \epsilon(x) g_{\alpha\beta}, \tag{3.31}$$

where $\epsilon(x)$ is an infinitesimal parameter controlling the transformation. Under this transformation, the action changes as follows:

$$\delta S = \int d^D x \frac{\delta S}{\delta g_{\alpha\beta}} \delta g_{\alpha\beta}. \tag{3.32}$$

It is possible to express the previous formula in a way that looks more familiar. This step involves the identification of $\frac{\delta S}{\delta g_{\alpha\beta}}$ as the energy-momentum tensor, omitting some proportionality factors involving the metric. The result of this identification is

$$T^{\alpha}_{\alpha} = 0, \tag{3.33}$$

namely, the trace of the energy-momentum tensor must be equal to zero if the theory respects the symmetry at the classical level. At the quantum level, the story can be very different. Hence, a conformal anomaly will exist if

$$\langle T^{\alpha}_{\alpha} \rangle \neq 0. \tag{3.34}$$

Holographically, it is conceivable to compute the exact form of the previous relation. Given a holographic pair of theories, gravitational theory on AdS and a CFT, it is possible to calculate the CFT energy-momentum tensor from a gravitational calculation using the GKPW prescription and the holographic renormalization procedure. The holographic dictionary states that operators in the bulk are into one-to-one correspondence with local gauge invariant operators in the CFT. Specifically, the CFT energy-momentum tensor is related to the metric in the gravitational theory. Most of the time, integrating quantities on AdS involves dealing with IR divergencies. Therefore, a renormalization procedure in the bulk is needed in which the action is regularized to obtain finite quantities of physical meaning. Taking into account the previous statement, the holographic dictionary states that to compute the CFT energy-momentum, one must perform the following calculation:

$$\langle T_{ij}(x) \rangle = \frac{2}{\sqrt{g_{(0)}(x)}} \frac{\delta S_{\text{ren}}}{\delta g_{(0)}(x)}, \tag{3.35}$$

where S_{ren} is the renormalized action and $g_{(0)}(x)$ is the boundary condition for the metric. In the case of the MT model, explicit calculation reveals

$$\langle T_i^i \rangle = \frac{V_x}{96\pi G_5} a^4, \tag{3.36}$$

where V_x denotes the spatial volume and a measures the amount of anisotropy in the system. In the case of the DK model, the same procedure reveals

$$\langle T_i^i \rangle = -\frac{V_x}{8\pi G_5} b^2, \tag{3.37}$$

where b measures the magnetic field present in the system. Notice the role of the anisotropy and the magnetic field in the previous two expressions. They can be seen as parameters that break the conformal symmetry. In both cases, the parameters a, b, and T characterize a specific theory giving rise to a family of solutions. For the MT model, the dimensionless parameter is a/T, whereas for the DK model, it is b/T^2. Therefore, if the conformal symmetry is preserved, it is expected that every dimensionless physical quantity is a function of the dimensionless parameters. Otherwise, the conformal anomaly would be present.

As stated before, both models, MT and DK, exhibit a conformal anomaly introduced by the anisotropy and the magnetic field, respectively. The trace of the energy-momentum tensor depends, in both cases, on a specific power of the symmetry breaking parameter, a, and b. In the case of the MT model, the trace is proportional to a^4, whereas, in the DK model, it is proportional to b^2. In [185] the late-time rate of computation was determined up to second order in the anisotropy. This result was equal to the expected Lloyd's bound at the corresponding order, $2M/\pi$. Nevertheless, the final result did not reflect the conformal anomaly of the system, because this effect was expected to be present in the next order of perturbation theory, $O(a^4)$. That is why, in out work it was important to calculate the late-time rate of computation in both models to all orders in the parameters a and b.

3.3.2 Computational Speed

Counterterms and the renormalization scheme

From (3.20), we can see that all the terms that diverge in the $r_{\text{max}} \to \infty$ limit were eliminated by the time derivative, rendering $\frac{dI_{WDW}}{dt}$ finite. This is because the r_{max} surfaces only undergo a time translation, and given that both families of solutions are static, any boundary integral evaluated at this surface will be time-independent. This is true for the counterterm actions, so they were omitted in the evaluation of I_{WdW}. It should be noted, though, that I_{WdW} itself is a divergent quantity. The counterterms necessary to remove said divergences were computed in [191] and later applied in [192] for a BTZ black hole. These counterterms do not modify the late time behavior of the complexity rate of change; thus, we omitted them from the previous computation.

Usually, when computing thermodynamic quantities such as the state's free energy, the gravitational action is evaluated in the exterior region. The boundary of this region is constituted by the surfaces at $r = r_{\text{max}}$ and $r = r_{\text{h}}$, but the counterterms vanish when evaluated at the horizon. However, as the WdW patch boundary includes the $r = r_{\text{min}}$ surfaces, the counterterms also need to be evaluated there. In our work, it was explicitly checked numerically that, for any solution in both models, the contribution from this vanishes when the limit $r_{\text{max}} \to r_{\text{s}}$ is taken. This means that I_{WdW}, and the complexity of the TFD state, is independent of the finite term determined by C_{sch}, namely, the renomalization constant.

Behavior at initial times: $0 \leq t < t_c$

In [185] were found general expressions for the computational speed, namely, the time derivative of the complexity. As previously explained, the holographic calculation in the CA prescription involves the evaluation of the action in the region known as the WdW patch. As the boundary

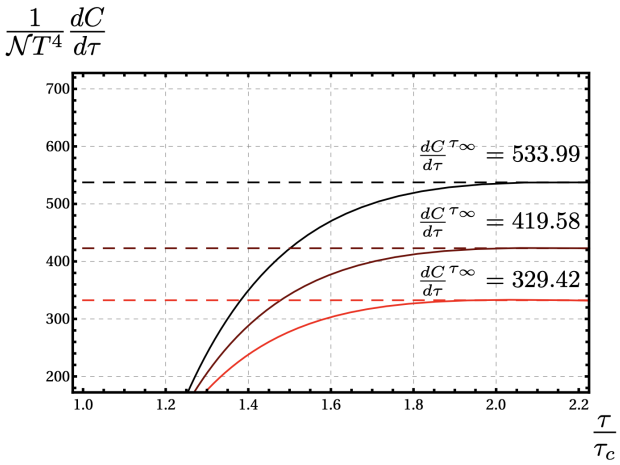

Figure 3.4: Rate of change of the complexity $dC/d\tau$ in units of $\mathcal{N}T^4$ as a function of τ for the MT model. Each curve corresponds to a different value for the anisotropic parameter, being $a/T = 19.57, 41.14, 85.46$ from bottom to top respectively. The horizontal dashed lines correspond to the late time behavior of each curve, with the precise values being $dC/d\tau^{\infty} = 329.42, 419.58, 533.99$, respectively. For all cases we fixed $l_{\text{null}} = L = 1$.

time passes, the interior of the WdW patch changes. For this reason, separating the calculation into three stages is suitable. The first stage involves a configuration of the WdW patch in which the lower corner is hidden behind the past singularity. The second stage involves a configuration in which some of the interior of the WdW patch desappears behind the future singularity. Finally, the third stage consists of a configuration in which the lower corner gets too close to the future singularity. For the first stage, the computational rate is zero in general, reflecting the fact that initially, the state keeps its complexity constant.

Behavior at later times: $t_c \leq t$

For the case of the MT model, it is possible to evaluate eq. (3.20) numerically, which allows the computation of the rate of change of the complexity of the TFD state as a function of time for any value of the anisotropic parameter. The result of the evaluation is presented in Fig. (3.3.2) for $l_{\text{null}} = L = 1$ and the three values of the anisotropy $a/T = 19.57, 41.14, 85.46$, displayed from bottom to top. This shows that the general effect of the anisotropy is to increase the value of dC/dt for any given t. It is also possible to see that, for any a/T, at t shortly after t_c the rate of change of the complexity decreases as time passes, reaches a minimum, and then it increases to a constant value, that we will denote as $\frac{dC^{t\infty}}{dt}$, for late times.

The dashed horizontal lines in Fig. (3.3.2) mark the asymptotic values and are plotted as a continuous function of a/T displayed as a red line in Fig. (3.3.2). While the early-time behavior can be modified by changing l_{null}, the late time behavior is independent of this arbitrary constant. It is also important to note that, for a given t, the rate of change of the complexity only depends on the dimensionless parameter a/T. A check was done numerically by varying a and T independently. The conclusion from this is that $\frac{dC^{t\infty}}{dt}$ is independent of the energy scale and thus is unaffected by the conformal anomaly.

For the case of the DK model, it was possible also to employ a numerical analysis. The result of the evaluation is presented in Fig. (3.3.2) for $l_{\text{null}} = L = 1$ with three different values of the magnetic field intensity being, from bottom to top, $b/T^2 = 40.59, 47.56, 56.62$ respectively. As in the case of the MT model, in this system, the magnetic field tends to increase the value of dC/dt for any given t. In general, the same behavior was found for the computational speed at any magnetic field strength value. For later times, the computational speed increases by passing the corresponding Lloyd's bound. Then, it reaches a maximum and goes down again, decreasing its value asymptotically, reaching the expected Lloyd's bound.

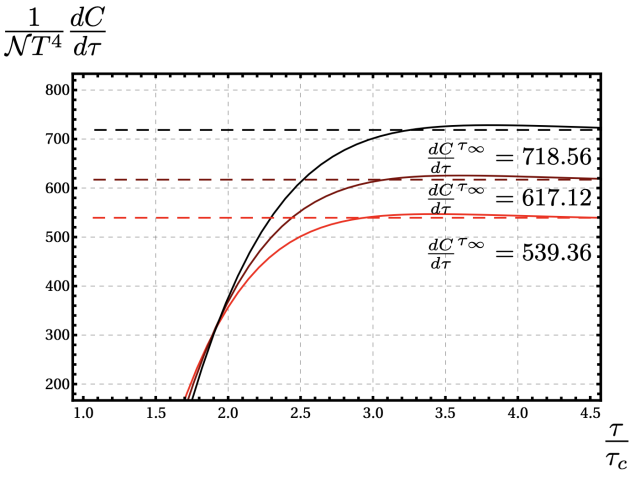

Figure 3.5: Rate of change of the complexity $dC/d\tau$ in units of $\mathcal{N}T^4$ as a function of τ for the DK model. Each curve corresponds to a different magnetic intensity, being $a/T = 19.57, 41.14, 85.46$ from bottom to top respectively. The horizontal dashed lines correspond to the late time behavior of each curve, with the precise values being $dC/d\tau^\infty = 329.42, 419.58, 533.99$, respectively. For all cases we fixed $l_{\text{null}} = L = 1$.

3.3.3 Conclusions

The results presented in this paper coincide with the previous results obtained via a perturbative analysis. In the process, it was possible to get novel features from the studied models. The main result demonstrates that the time derivative of the complexity is unaffected by the presence of a conformal anomaly. The first of two reasons why this is the case is that $(1/T^4)dC/dt$, which is a dimensionless quantity, only depends on a and T through the dimensionless ratio a/T, proving that such derivative is independent of the energy scale, which was fixed to unity throughout this paper. The second reason is that the counterterm action, which contains the scheme dependent coefficient C_{sch}, does not contribute to the derivative with respect to t, as the integral over the boundary regulator is constant and the integral near the singularity vanishes as the regulator is removed.

The other main result is in regards to Lloyd's bound. It is expected, when using the CA prescription, that Lloyd's bound will be violated for any finite time, only to be saturated when an infinite amount of time has passed. Knowing that this was the case for $a = 0$ and $b = 0$, the validity of this result was studied for arbitrary values of the anisotropic parameter and the magnetic field. The energy of the system, which appears on the right-hand side of Lloyd's bound, depends on both the energy scale and the coefficient C_{sch}. However, as just stated, dC/dt does not depend on any of these quantities. While at first sight, this could be interpreted as an inconsistency for Lloyd's bound when a conformal anomaly is present, that is not what it is. The role of C_{sch} is to keep the physical quantities scheme-independent, and in particular, for the energy, this means to absorb any modification that it could suffer when the value of the energy scale is changed, once, of course, a renormalization condition has been imposed. Thus, the results above demonstrate that, if so desired, the saturation of Lloyd's bound at an infinite time can be used as a renormalization condition and let C_{sch} be adjusted to satisfy it for any given $, a, T$ or $, b, T$, depending on the model.

3.4 Holographic Coarse-Graining: Correlators from the Entanglement Wedge and Other Reduced Geometries

Abstract. There is some tension between two well-known ideas in holography. On the one hand, subregion duality asserts that the reduced density matrix associated with a limited region of the boundary theory is dual to a correspondingly limited region in the bulk, known as the entanglement wedge. On the other hand, correlators that in the boundary theory can be computed solely with that density matrix are calculated in the bulk via the GKPW or BDHM prescriptions, which require

input from beyond the entanglement wedge. We show that this tension is resolved by recognizing that the reduced state is only fully identified when the entanglement wedge is supplemented with a specific infrared boundary action, associated with an end-of-the-world brane. This action is obtained by coarse-graining through a variant of Wilsonian integration, a procedure that we call holographic rememorization, which can also be applied to define other reduced density or transition matrices, as well as more general reduced partition functions. We find an interesting connection with AdS/BCFT, and, in this context, we are led to a simple example of an equivalence between an ensemble of theories and a single theory, as discussed in recent studies of the black hole information problem.

3.4.1 Subregion duality and bulk reconstruction

The RT surface played a prominent role in (2.44) that eventually led to the proposal of subregion duality. In more detail, the seminal works [21, 22, 40] conjectured that the reduced density matrix ρ is dual to the entanglement wedge of A, denoted $\mathcal{E}$ and defined as the domain of dependence of any codimension-one bulk spacelike region extending between A and Γ.

The bulk-to-boundary translation is known as 'bulk reconstruction', and seeks to identify the region in the bulk that can be fully reconstructed with the information in ρ. Building on important insights gained over the years in [41, 42, 43, 44, 21, 22, 45, 46, 40], this question was definitively answered in [47, 48, 49, 50, 51, 52, 53], which showed that, indeed, all local bulk operators in $\mathcal{E}$ are fully reconstructible within A. Crucial for this achievement was the realization that holography works as a special type of code for quantum error correction (QEC) [54, 55, 56], and bulk reconstruction is meaningful only within a 'code subspace' of the QFT, where bulk effective field theory is approximately valid.

A crucial property of ρ is the fact that it allows the correct determination of all correlators of local or extended operators $\mathcal{O}_i$ placed within A:

$$\mathrm{tr}_A(\rho\,\mathcal{O}_1\cdots\mathcal{O}_n) = \langle\Psi|\,\mathcal{O}_1\cdots\mathcal{O}_n\,|\Psi\rangle\ . \tag{3.38}$$

On the flip side, ρ would not know about correlators of operators that are inserted *outside* of A. From the subsystem perspective, the insertion of such operators amounts to a change of the reduced state, and would require recomputation of ρ.

The starting point for this project is the observation that the GKPW prescription seemingly contradicts (3.38), because even when the sources $J_l(x)$ are turned off in A^{c}, so that operator insertions are purely within A, $Z_{\rm Grav}[J_l]$ still requires information from $\mathcal{E}^{\mathsf{c}}$, the bulk region *beyond* the entanglement wedge. This is true even for basic two-point functions of simple operators, well within the confines of the relevant code subspace in the QFT. This contradiction reveals that, by itself, the identification of $\mathcal{E}$ is not equivalent to a complete specification of ρ.

What we need then is a reformulation of the bulk recipe for correlators in A, that makes reference *only* to the entanglement wedge. Given that the issue is tracing out some of the degrees of freedom contributing to the (bulk or boundary) path integral, the natural tool at our disposal is Wilsonian integration, whose holographic implementation was developed in [70, 71, 72]. For our purposes, we will seek to apply it in a nonstandard manner: instead of tracing over a UV region, as is done in standard Wilsonian renormalization, we will trace over the bulk region $\mathcal{E}^{\mathsf{c}}$, which includes the IR region as well as what amounts to the UV in A^{c}.

The net result of this approach will be a boundary action $I_{\rm IR}$ defined at the IR end of the entanglement wedge, whose inclusion guarantees that correlators within A are correctly reproduced. Its presence is analogous to the counterterm action $I_{\rm UV}$ prescribed by holographic renormalization, but whereas the latter serves to cancel the divergences in $I_{\rm bulk}$, the former is needed to keep the memory of the portion of the state encoded by $\mathcal{E}^{\mathsf{c}}$. For this reason, we refer to our procedure as *holographic rememorization*.

Conceptually, the issue is that the reduced density matrix ρ specifies not only the subset A of degrees of freedom that remain untraced, but also their state. In the bulk, the identification of $\mathcal{E}$ goes along with the choice of A, but the specification of the state is not complete until the boundary action $I_{\rm IR}$ is provided. The full association is therefore not $\rho \leftrightarrow \mathcal{E}$, but $\rho \leftrightarrow (\mathcal{E}, I_{\rm IR})$.

In completing the statement of subregion duality, the results stated here also relate to a puzzle raised recently in [82]. It was noted there that in some situations the bulk metric can be

reconstructed far beyond the entanglement wedge, by applying the prescription of [83] to two-dimensional minimal surfaces that reach outside $\mathcal{E}$ despite being anchored within A. These surfaces can be spanned by string worldsheets that, according to the standard holographic dictionary [84, 85], compute expectation values of Wilson loops that are certainly encoded in ρ. The authors of [82] inferred from this that either there exist data in ρ that determine the metric parametrically far outside $\mathcal{E}$, conflicting with the standard intuition about subregion duality, or the information of such surfaces is not contained in ρ, indicating that there is something wrong with the holographic recipe for Wilson loops. Our perspective is more in line with the first option: by definition, ρ does contain data about the state in A^{c}, and therefore $\mathcal{E}^{\mathsf{c}}$. However, *it does not fully and uniquely determine that state*. In particular, many states lead to the same reduced density matrix ρ and, hence, the same infrared action I_{IR}.[1] Wilson loops whose dual worldsheets exit $\mathcal{E}$ are directly analogous to the correlators of local operators considered throughout this paper, which are likewise inferred from field profiles that lie partly beyond $\mathcal{E}$.

The results presented here show that the boundary term I_{IR}, which is needed to fully specify ρ, encodes the external portions of the field profiles, and of the worldsheets relevant to [82], thereby resolving the tension with subregion duality.

3.4.2 Holographic rememorization

In a Poincaré-invariant d-dimensional QFT with spacetime coordinates $x^\mu \equiv (t, \vec{x})$ and fields $\Phi(x)$, the standard Wilsonian effective action at floating cutoff Λ, I^Λ_{QFT} , is obtained [137] by integrating out the Fourier modes $\Phi(p)$ with momentum $p > \Lambda$,

$$\exp\left(iI^\Lambda_{\text{QFT}}[\Phi_{p<\Lambda}]\right) \equiv \int \mathcal{D}\Phi_{p>\Lambda} \exp\left(iI_{\text{QFT}}[\Phi]\right) \ , \tag{3.39}$$

so that the partition function can be reexpressed as

$$Z_{\text{QFT}} = \int \mathcal{D}\Phi \exp\left(iI_{\text{QFT}}[\Phi]\right) = \int \mathcal{D}\Phi_{p\leq\Lambda} \exp\left(iI^\Lambda_{\text{QFT}}[\Phi_{p\leq\Lambda}]\right) \ . \tag{3.40}$$

Let us now briefly review the holographic implementation of Wilsonian integration [70, 71, 72]. For simplicity, we consider a bulk scalar field ϕ on a fixed $(d+1)$-dimensional asymptotically AdS geometry. In Poincaré coordinates $(x, z) \equiv (t, \vec{x}, z)$, the pure AdS metric is

$$ds^2 = \frac{L^2}{z^2}\left(-dt^2 + d\vec{x}^2 + dz^2\right) \ , \tag{3.41}$$

so we have in mind a geometry that approaches (3.41) as $z \to 0$, possibly with non-normalizable falloff. Extensions can be made to any locally asymptotically AdS geometry, possibly tensored or warped with an accompanying compact manifold, as well as to other types of bulk fields (including the metric itself), with or without interactions. The limit $G_N \to 0$ where backreaction is suppressed corresponds to considering large central charge at the UV fixed point of the QFT, $c \to \infty$.

The well-known UV-IR connection [138, 140] relates the bulk radial direction z to an energy scale $1/z$ in the QFT. This is naturally taken to refer to a resolution scale in the sense of the renormalization group (RG) [141, 142, 143, 117, 118], and attempts have been made to derive holography directly from this connection [144, 145, 146, 155]. For the specific case of the Wilsonian RG, the floating UV cutoff Λ is translated into a radial position $z_\Lambda \equiv 1/\Lambda$ in the bulk, and the dual description of (3.40) then involves integrating out the UV region of the geometry, $z < z_\Lambda$ [70, 71].[2] In more detail, the path integral that computes the partition function on the gravity side is separated in the following form:

$$\begin{aligned} Z_{\text{Grav}}[\underline{\phi}] &= \int \mathcal{D}\phi \exp\left(i(I_{\text{bulk}}[\phi] + I_{\text{UV}}[\underline{\phi}])\right) \\ &= \int \mathcal{D}\phi_{z<z_\Lambda} \mathcal{D}\bar{\phi} \mathcal{D}\phi_{z>z_\Lambda} \exp\left(i(I_{\text{bulk}}[\phi_{z<z_\Lambda}] + I_{\text{UV}}[\underline{\phi}])\right) \exp\left(iI_{\text{bulk}}[\phi_{z>z_\Lambda}]\right) \\ &\equiv \int \mathcal{D}\bar{\phi} \mathcal{D}\phi_{z>z_\Lambda} \exp\left(i(I_{\text{bulk}}[\phi_{z>z_\Lambda}] + I^{z_\Lambda}_{\text{UV}}[\bar{\phi}, \underline{\phi}])\right) \ . \end{aligned} \tag{3.42}$$

[1] Put the other way around, given a reduced state ρ, there are infinitely many ways to purify it. Adding to this, one may even consider global states that are mixed to begin with.

[2] More precisely, a bulk radial cutoff z_Λ corresponds *not* to a sharp cutoff in momentum space, but to a smooth cutoff akin to [156].

Since we are using the Lorentzian version of the correspondence [157, 158], the path integral includes a specification of the initial and final states, which are left implicit for now. In the first line of (3.42), we have taken into account the usual UV counterterms $I_{\rm UV}$ needed for holographic renormalization [65, 66, 67, 68, 69], which are defined at the original cutoff surface $z = \epsilon$. It is implicitly understood that for the time being we are working with the standard boundary condition $\phi(x, z) \to z^{d-\Delta}\underline{\phi}(x)$ as $z \to 0$, where $\underline{\phi}(x)$ is to be equated with the QFT source $J(x)$ that couples linearly to the local operator $\mathcal{O}(x)$ of interest, and Δ is the scaling dimension of $\mathcal{O}$. In the second line of (3.42), $\bar{\phi}$ denotes the value of the field at the floating cutoff surface $z = z_\Lambda$. In the final line, the new boundary term $I_{\rm UV}^{z_\Lambda}$ has been generated by the UV integration.

Contemplating the split path integral in the second line of (3.42), it is evident that we can exchange the roles of the UV and IR, so that we instead choose to integrate out the IR region, $z > z_\Lambda$. Upon doing so, we arrive at

$$Z_{\rm Grav}[\underline{\phi}] = \int \mathcal{D}\bar{\phi}\mathcal{D}\phi_{z<z_\Lambda} \exp\left(i(I_{\rm bulk}[\phi_{z<z_\Lambda}] + I_{\rm IR}[\bar{\phi}] + I_{\rm UV}[\underline{\phi}])\right) \ , \tag{3.43}$$

where we now have an *infrared* boundary term $I_{\rm IR}$. Evidently, the QFT interpretation is that we are now defining an upward Wilsonian RG flow, integrating out the field modes with $p < \Lambda$.[3] In (3.43) we have no longer labeled $I_{\rm UV}$ with the location $z = \epsilon$ of the UV cutoff surface, which is now held fixed. For the same reason, in the remainder of the paper we will omit the label in all mention of the UV counterterms.

In both (3.42) and (3.43), we are carrying out the path integral up to a constant radial depth $z = z_\Lambda$. This cutoff surface can be turned into a more general timelike surface via an x-dependent reparametrization of z, which is known to correspond to a Weyl transformation in the QFT [159]. So if we carry out the path integral up to an x-dependent depth, $z = \bar{z}(x)$, we will be considering a spacetime-dependent RG flow, as in [160, 161].

Reducing to the entanglement wedge

The preceding observation suggests a natural way to address the challenge described in the Introduction. To obtain a generalization of the GKPW recipe that is defined purely within the entanglement wedge $\mathcal{E}$ associated with a spatial region A in the QFT, we ought to integrate out the entire complementary region $\mathcal{E}^{\rm c}$.

To spell this out, let D refer to the causal diamond of A in the QFT, and denote the profile of the source in D as $J_D(x)$, with $J_{D^{\rm c}}(x)$ standing then for the source in the complement $D^{\rm c}$. All correlators within D in a given global state $|\Psi\rangle$ are encoded in $Z_{\rm QFT}[J_D, J_{D^{\rm c}}{=}0]$, so in the bulk we are interested in $Z_{\rm Grav}[\underline{\phi}_D, \underline{\phi}_{D^{\rm c}}{=}0]$.[4] These boundary conditions are implicitly understood to hold in the expressions below. We will define

$$\exp\left(i(I_{\rm IR}[\bar{\phi}])\right) \equiv \int \mathcal{D}\phi_{\mathcal{E}^{\rm c}} \exp\left(i(I_{\rm bulk}[\phi_{\mathcal{E}^{\rm c}}])\right) \ , \tag{3.44}$$

where $\bar{\phi}(x) \equiv \phi(x, \bar{z}(x))$ is the value of the bulk field on $\overline{\mathcal{E}}$, the interface between $\mathcal{E}$ and $\mathcal{E}^{\rm c}$. Notice that the counterterm action $I_{\rm UV}[\underline{\phi}_{D^{\rm c}}]$ drops out, since we have turned off the source in that region, and the subleading behaviour $\phi \propto z^\Delta$ is the normalizable mode that leads to a finite bulk action. The source within D, $\underline{\phi}_D = J_D$, plays no role in the right-hand side of (3.44), so by construction $I_{\rm IR}$ is independent of it.

Our prescription for computing correlators within subregion duality is to employ the partition function

$$Z_{\rm Grav}[\underline{\phi}] = \int \mathcal{D}\bar{\phi}\mathcal{D}\phi_{\mathcal{E}} \exp\left(i(I_{\rm bulk}[\phi_{\mathcal{E}}] + I_{\rm IR}[\bar{\phi}] + I_{\rm UV}[\underline{\phi}])\right) \ , \tag{3.45}$$

where it is understood from now on that $\underline{\phi}$ refers solely to a source within D. Eq. (3.45) is thus the generating functional for correlators within D. The presence here of the IR boundary action is absolutely crucial to comply with (3.38), which is a defining property of the reduced density

[3] See the previous footnote.

[4] Nothing stops us from turning on the sources $J_{D^{\rm c}}$, but that calculation would amount to having an adjustable reduced state, and the infrared action (3.44) would naturally be a functional of $J_{D^{\rm c}}$. We would then be able to compute *all* correlators, independently of whether the operators are inserted in D or $D^{\rm c}$. That is *not* the case when we only have access to a specific reduced density matrix ρ describing the state on D, which is situation of main interest in this paper.

matrix. We thus see that *the information encoded in ρ is dual not merely to the entanglement wedge, but to $\mathcal{E}$ equipped with the specific IR boundary term I_{IR}.*[5] Physically, the point is that, after tracing over $\mathcal{E}^c$, the IR boundary of the entanglement wedge, $\overline{\mathcal{E}}$, becomes an actual edge of spacetime, with very specific dynamics for the end-of-the-world (EOW) brane that resides there. This point will become clearer towards the end of the following section.

The preceding construction has been formulated for simplicity in terms of a single bulk scalar field $\phi(x,z)$, which is what we need if we restrict attention solely to correlators of its dual scalar operator $\mathcal{O}(x)$. The same reduction can be performed singly or jointly on other bulk fields, including the metric itself (dealing appropriately with the associated diffeomorphism invariance, see, e.g., [127, 128, 129, 130, 131, 132, 133, 134]). A combined analysis of our scalar field and the metric is necessary if we are not working in the limit of strictly infinite central charge, and need then to consider how ϕ backreacts on the geometry.

3.5 Rememorization of generic scalar correlators

A standard scenario where we can illustrate our general rememorization procedure is in the computation of correlators of a single scalar operator $\mathcal{O}(x)$ in a large-c CFT$_d$ on Minkowski spacetime, which is dual to a free scalar field $\phi(x,z)$ on Poincaré AdS$_{d+1}$, Eq. (3.41). As recalled in the Introduction, the GKPW recipe [3, 4] equates the partition functions on both sides as in (3.45), identifying the external source $J(x)$ of $\mathcal{O}(x)$ in the CFT with the asymptotic boundary condition $\underline{\phi}(x)$ of the dual field.

Working in Euclidean signature, the bulk partition function is given by

$$Z_{\rm Grav}[\underline{\phi}] = \int_{\phi(x,\epsilon)=\epsilon^{d-\Delta}\underline{\phi}(x)} \mathcal{D}\phi \, \exp\big(-I_{\rm bulk}[\phi] - I_{\rm UV}[\underline{\phi}]\big) \ , \tag{3.46}$$

where $z=\epsilon$ is the UV radial cutoff, and Δ denotes the scaling dimension of $\mathcal{O}(x)$. The bulk action is

$$I_{\rm bulk}[\phi] = \frac{1}{2}\int d^{d+1}x\sqrt{g}\,\left[g^{mn}\partial_m\phi\partial_n\phi + M^2\phi^2\right] \ , \tag{3.47}$$

with $M^2L^2=\Delta(\Delta-d)$. As always, $I_{\rm UV}[\underline{\phi}]$ denotes the counterterm boundary action for holographic renormalization [68, 69], whose explicit form will not be needed here.

3.5.1 A simple example: wall at constant z

The most obvious way to separate the bulk spacetime is by means of a wall at $z=\bar{z}$. The regions below and above the wall correspond respectively to the UV and IR of the CFT. Contrary to the standard Wilsonian elimination of the UV region, here we want to integrate out the IR component. This reduction will generate a contribution to the effective action of the remaining geometry that encodes the information of the IR.

Specifically, in analogy with (3.44) we need to calculate

$$\exp\big(-I_{\rm IR}[\bar{\phi}]\big) = \int_{\phi(x,\bar{z})=\bar{\phi}(x)} \mathcal{D}\phi_{z>\bar{z}} \, \exp\left(-I_{\rm bulk}[\phi]\right), \tag{3.48}$$

where $\bar{\phi}(x)$ is the boundary condition for the fields on the resulting EOW brane at $\bar{z}$. Since the path integral is quadratic, the saddle-point approximation is exact. For the on-shell evaluation of (3.48), we need the classical solution of the KG equation in the (Wick-rotated version of the) metric (3.41),

$$z^{d+1}\partial_z\left(\frac{\partial_z\phi}{z^{d-1}}\right) + z^2\delta^{\mu\nu}\partial_\mu\phi\partial_\nu\phi - M^2L^2\phi = 0 \ . \tag{3.49}$$

As usual, due to translational symmetry, it is useful to decompose into Fourier modes, $\phi(x,z) = \int \frac{d^dp}{(2\pi)^d}\,\tilde{\phi}(p,z)e^{ip\cdot x}$. The general solution is then found to be [3, 4]

$$\tilde{\phi}(p,z) = z^{\frac{d}{2}}\left(C_1(p)I_{\Delta-\frac{d}{2}}(pz) + C_2(p)K_{\Delta-\frac{d}{2}}(pz)\right) \ . \tag{3.50}$$

[5] In the partition function (3.45) or the correlators it encodes, one has the reduced density matrix inside a trace, as in (3.38). To obtain ρ directly, one must cut open the path integral across the time slice $t=t_0$ on which A resides. Strictly speaking, this will only yield a density matrix if the configuration is symmetric under time reversal about t_0.

The coefficients $C_1(p)$ and $C_2(p)$ take specific forms depending on the boundary conditions imposed. For the standard time-ordered correlators, we impose regularity as $z \to \infty$, which sets $C_1(p) = 0 \ \forall p$. At the wall, we must enforce the Dirichlet condition

$$\phi(p, \bar{z}) = \bar{\tilde{\phi}}(p) \ , \quad \text{with} \quad \bar{\tilde{\phi}}(p) \equiv \int d^d x \, \bar{\phi}(x) e^{-ip\cdot x} \ . \tag{3.51}$$

This determines $C_2(p)$, singling out the momentum-space solution

$$\tilde{\phi}^{\rm cl}(p, z) = \left(\frac{z}{\bar{z}}\right)^{\frac{d}{2}} \frac{K_{\Delta-\frac{d}{2}}(pz)}{K_{\Delta-\frac{d}{2}}(p\bar{z})} \bar{\tilde{\phi}}(p) \ . \tag{3.52}$$

With this solution, we can evaluate the on-shell action. The result can be expressed as a surface term at $z = \bar{z}$,

$$I_{\rm IR}[\bar{\phi}] = \frac{1}{2} \int_{\partial \mathcal{R}} d^d x \sqrt{h} \, n^m \phi^{\rm cl} \partial_m \phi^{\rm cl} \ , \tag{3.53}$$

with h the induced metric and n the outward unit normal. In momentum space, this is

$$I_{\rm IR}[\bar{\phi}] = -\frac{L^{d-1}}{2\bar{z}^{d-1}} \int \frac{d^d p}{(2\pi)^d} \, \tilde{\phi}^{\rm cl}(-p, z) \partial_z \tilde{\phi}^{\rm cl}(p, z)\Big|_{z=\bar{z}} \ . \tag{3.54}$$

The derivative in the integrand can be evaluated explicitly, obtaining

$$\partial_z \tilde{\phi}^{\rm cl}\Big|_{z=\bar{z}} = \partial_z \left(\left(\frac{z}{\bar{z}}\right)^{\frac{d}{2}} \frac{K_{\Delta-\frac{d}{2}}(pz)}{K_{\Delta-\frac{d}{2}}(p\bar{z})} \right)\Bigg|_{z=\bar{z}} \bar{\tilde{\phi}}(p) \ . \tag{3.55}$$

At this point, it is convenient to define

$$\hat{\mathcal{W}} \bar{\phi}(x) \equiv -\frac{\bar{z}}{L} \int \frac{d^d p}{(2\pi)^d} \, \partial_z \left(\left(\frac{z}{\bar{z}}\right)^{\frac{d}{2}} \frac{K_{\Delta-\frac{d}{2}}(pz)}{K_{\Delta-\frac{d}{2}}(p\bar{z})} \right)\Bigg|_{z=\bar{z}} \bar{\tilde{\phi}}(p) e^{ip\cdot x} \ . \tag{3.56}$$

Using this in (3.53), we are left with

$$I_{\rm IR}[\bar{\phi}] = \frac{1}{2} \int_{z=\bar{z}} d^d x \sqrt{h} \, \bar{\phi}(x) \hat{\mathcal{W}} \bar{\phi}(x) \ . \tag{3.57}$$

Note that this is a nonlocal expression, because, as seen in (3.56), the operator $\hat{\mathcal{W}}$ acts on $\bar{\phi}(x)$ with an infinite series of spacetime derivatives.

The boundary term (3.57) encodes the information of the classical profile of the scalar field in the IR region of the bulk, $z > \bar{z}$. As explained in the previous section, this term supplements the action in the UV region, and determines the suitable boundary condition for the field ϕ at $z = \bar{z}$. This guarantees the coincidence between correlators computed with the reduced geometry and those obtained from the complete spacetime.

To see this explicitly, notice that variation of the effective action for the UV region, $I_{\rm eff} \equiv I_{\rm bulk}[\phi] + I_{\rm IR}[\bar{\phi}] + I_{\rm UV}[\underline{\phi}]$, yields the following boundary terms at $z = \bar{z}$:

$$\delta I_{\rm eff} \supset \int_{z=\bar{z}} d^d x \sqrt{h} n^m \partial_m \phi \delta\phi + \frac{1}{2} \int_{z=\bar{z}} d^d x \sqrt{h} \delta\phi \hat{\mathcal{W}} \phi + \frac{1}{2} \int_{z=\bar{z}} d^d x \sqrt{h} \phi \hat{\mathcal{W}} \delta\phi \ . \tag{3.58}$$

We then need to integrate by parts the final term, but the nonlocal nature of the operator $\hat{\mathcal{W}}$ makes this a bit nontrivial in the position-space representation. We will return to this point in the next subsection. Here, it is simplest to change to the momentum-space representation, $\phi(x, z) = \int \frac{d^d p}{(2\pi)^d} \tilde{\phi}(p, z) e^{ip\cdot x}$. Using (3.56), we see then that the vanishing of (3.58) implies that one of the following two boundary conditions must hold:

$$\text{Dirichlet (IR)} \qquad \tilde{\phi}(p, z)|_{z=\bar{z}} = \bar{\tilde{\phi}}(p) \ , \tag{3.59}$$

$$\text{Neumann (IR)} \qquad \partial_z \tilde{\phi}(p, z)\Big|_{z=\bar{z}} = \partial_z \left(\left(\frac{z}{\bar{z}}\right)^{\frac{d}{2}} \frac{K_{\Delta-\frac{d}{2}}(pz)}{K_{\Delta-\frac{d}{2}}(p\bar{z})} \right)\Bigg|_{z=\bar{z}} \tilde{\phi}(p, \bar{z}) \ . \tag{3.60}$$

These two alternatives are appropriate before and after performing the $\mathcal{D}\bar{\phi}$ path integral, respectively. Since one can exchance the order of the integrals, one find an equivalence between the Dirichlet and Neumann approaches for the case of a free bulk scalar field on a general background. In our pure AdS_{d+1} analysis here, we will focus on illustrating the Neumann approach, which is the more efficient of the two. Our task is then to enforce (3.60) at the wall, together with the standard Dirichlet condition at the AdS boundary,

$$\text{Dirichlet (UV)} \qquad \tilde{\phi}(p,z)|_{z=\epsilon} = \epsilon^{d-\Delta}\tilde{\underline{\phi}}(p) \ . \tag{3.61}$$

A general momentum-space solution to (3.49) is given by (3.50). Applying it in conjunction with (3.60) and (3.61), we deduce that

$$\phi(x,z) = \int \frac{d^d p}{(2\pi)^d} \left(\frac{z}{\epsilon}\right)^{\frac{d}{2}} \frac{K_{\Delta-\frac{d}{2}}(pz)}{K_{\Delta-\frac{d}{2}}(p\epsilon)} \tilde{\underline{\phi}}(p) e^{ip\cdot x} \ , \tag{3.62}$$

which as expected, is exactly equal to the solution in the entire spacetime with the same boundary condition at $z=\epsilon$ and the regularity condition at the Poincaré horizon. This result confirms that the role of the boundary term, obtained via the Wilsonian reduction of the IR, is to keep the memory of the information of that region, by supplying the correct boundary conditions at the interface.

3.5.2 General recipe

In the preceding subsection, we performed a reduction to a region of the spacetime delimited by a wall at $z=\bar{z}$ (which becomes then the location of the EOW brane that arises from the reduction). In that example, translational symmetry greatly simplifies the task of finding an explicit solution of the Klein-Gordon equation with the prescribed boundary conditions. Nevertheless, our rememorization procedure can be applied to more general regions in the bulk. The example that was the initial motivation for this work is the entanglement wedge $\mathcal{E}$ associated with a spatial region A in the CFT, described in Section 3.4.2. In that context, the reduction is performed over the exterior of the entanglement wedge, $\mathcal{E}^{\mathsf{c}}$.

In the most general case, one reduces to some spacetime region $\mathcal{R}$ in the bulk of an asymptotically locally AdS spacetime, which delineates some spacetime region R in the boundary. At large c, the saddle point evaluation translates into a linear PDE problem with arbitrary Dirichlet boundary conditions on the specified interface.

In more detail, within $\mathcal{R}^{\mathsf{c}}$ we ought to solve

$$\left(\Box - M^2\right)\phi(x^m) = 0 \ , \tag{3.63}$$

with boundary condition

$$\phi(x,z) = \bar{\phi}(x) \qquad \text{if} \qquad (x,z) \in \overline{\partial\mathcal{R}} \ , \tag{3.64}$$

where $\overline{\mathcal{R}}$ denotes the interface between $\mathcal{R}$ and $\mathcal{R}^{\mathsf{c}}$ (the eventual location of the EOW brane), and $\bar{\phi}$ is a specific but arbitrary profile. If the boundary of $\mathcal{R}^{\mathsf{c}}$ has other components aside from $\overline{\mathcal{R}}$, appropriate boundary conditions must be specified there as well. For instance, if $\mathcal{R}=\mathcal{E}$ is the entanglement wedge in Poincaré AdS associated with a causal diamond D in the CFT, then we must turn off the source $J(x)$ in D^{c}, and pick boundary conditions at the Poincaré horizon (e.g., regularity in the Euclidean description, which is appropriate if we wish to compute the time-ordered correlators).

We can obtain a general solution to the problem if we first tackle the problem of finding the associated Green's function

$$\left(\Box - M^2\right)G(x^m, x'^m) = \frac{1}{\sqrt{|g|}}\delta(x^m - x'^m) \ , \tag{3.65}$$

with the requirement that

$$G(x^m, x'^m) = 0 \qquad \text{if} \qquad x^m \in \partial(\mathcal{R}^{\mathsf{c}}) \ . \tag{3.66}$$

In the following, we will specify the prescription to compute $\phi(x^m)$ given $G(x^m, x'^m)$.

With the help of Green's identities, we can prove the following modification that incorporates the Klein-Gordon operator [215]:

$$\int_{\mathcal{M}} d^D x' \sqrt{|g|} \left\{ v \left(\Box - M^2 \right) u - u \left(\Box - M^2 \right) v \right\} = \int_{\partial \mathcal{M}} d^{D-1} x' \sqrt{|h|} \left(v n^m \partial_m u - u n^m \partial_m v \right), \quad (3.67)$$

where u and v are two smooth functions defined in $\mathcal{M}$, h_{ab} is the induced metric on the boundary $\partial\mathcal{M}$ and n^m is the outward-pointing normal to $\partial\mathcal{M}$. The previous expression is stated in general notation, but for our purposes, we identify $\mathcal{M}$ with $\mathcal{R}^{\mathsf{c}}$, and set the dimension to $d+1$. If we replace $u = \phi$ and $v = G$, then Eq. (3.67) simplifies enormously. The first term in the left-hand side gives zero contribution since ϕ is assumed to be a solution to (3.63), while the second term gives the value of the field at x'. In the right-hand side, the boundary conditions of the Green's function make the first term vanish. Therefore, we obtain[6]

$$\phi(x^m) = \int_{\overline{\mathcal{R}}} d^d x' \sqrt{h(x')}\, \bar{\phi}(x') n^m \partial_m G(x', x) \ . \quad (3.68)$$

This expression is convenient, since its dependence on the boundary condition is manifest, and the evaluation of the Green's function can at least be carried out numerically.

Substitution of (3.68) in (3.53) gives

$$I_{\text{IR}}[\bar{\phi}] = \int_{\overline{\mathcal{R}}} d^d x d^d x' \sqrt{h(x)} \sqrt{h(x')} n^l(x) n^m(x') \partial_l \partial_m G(x, x') \bar{\phi}(x) \bar{\phi}(x'). \quad (3.69)$$

Note here that the crucial information of the region that has been integrated out, $\mathcal{R}^{\mathsf{c}}$, is encoded in the Green's function G, because the profile $\bar{\phi}$ is arbitrary. The resulting effective action in $\mathcal{R}$ is thus

$$I^{\mathcal{R}}_{\text{eff}} = I_{\text{bulk}}[\phi_{\mathcal{R}}] + I_{\text{IR}}[\bar{\phi}] + I_{\text{UV}}[\underline{\phi}] \ . \quad (3.70)$$

Consider now the variational principle based on $I^{\mathcal{R}}_{\text{eff}}$. As usual, variation of the bulk term gives rise to a term that is proportional to the EOM and a term that is related to the normal derivative of the field at the interface. Variation of I_{IR} gives

$$\delta I_{\text{IR}}[\bar{\phi}] = \int_{\overline{\mathcal{R}}} d^d x d^d x' \sqrt{h(x)} \sqrt{h(x')} n^l(x) n^m(x') \left[\partial_l \partial_m G(x, x') + \partial_l \partial_m G(x', x) \right] \bar{\phi}(x') \delta\bar{\phi}(x) \ . \quad (3.71)$$

Based on the form of this expression, it is convenient to define the nonlocal operator

$$\hat{\mathcal{W}} \phi(x) \equiv \int_{\overline{\mathcal{R}}} d^d x' \sqrt{h(x')} n^l(x) n^m(x') \left[\partial_l \partial_m G(x, x') + \partial_l \partial_m G(x', x) \right] \phi(x') \ . \quad (3.72)$$

Using this, we can rewrite the variation of the infrared action as

$$\delta I_{\text{IR}}[\bar{\phi}] = \int_{\partial \mathcal{E}_A} d^d x \sqrt{h} \hat{\mathcal{W}} \bar{\phi} \delta\bar{\phi} \ . \quad (3.73)$$

The boundary variation (3.73), supplemented with the variation of the bulk term, gives rise again to (3.58), now with a more general definition for the operator $\hat{\mathcal{W}}$. From this line of reasoning, we see then that $\hat{\mathcal{W}}$ is a key piece of information of the reduction. In the end, we deduce the following two alternative boundary conditions for the field:

$$\text{Dirichlet (IR)} \qquad \phi(x)|_{\overline{\mathcal{R}}} = \bar{\phi}(x) \ , \quad (3.74)$$

$$\text{Neumann (IR)} \qquad n^m_m \phi(x)|_{\overline{\mathcal{R}}} = \hat{\mathcal{W}} \phi(x) \ . \quad (3.75)$$

The former is called for prior to carrying out the $\mathcal{D}\bar{\phi}$ path integral, and the latter is enforced as a result of that integral. Eq. (3.75) it shows that through (3.72), the determination of the

[6] For brevity, we assume here that ϕ is meant to have vanishing boundary conditions on $(\mathcal{R}^{\mathsf{c}}) \setminus \overline{\mathcal{R}}$. Were this not the case, there would be an additional, $\bar{\phi}$-independent term in (3.68). This would not change anything essential in what follows.

appropriate Neumann boundary condition and the resulting IR action for general $\mathcal{R}$ has been reduced to finding the Green's function G satisfying (3.66). The compact form of our notation should not obscure the fact that (3.75) is a *nonlocal* boundary condition, because $\hat{\mathcal{W}}$ denotes the convolution (3.72).

The geometric interpretation of (3.75) is as follows. In the saddle-point approximation, the full partition function (3.46) is entirely determined by the solution $\phi^{\rm cl}$ that interpolates between the prescribed UV boundary condition $\underline{\phi}(x)$ and the appropriate IR condition (e.g., in Euclidean AdS, regularity at what would have been the Poincaré horizon). After rememorizing, the role of $I_{\rm IR}$ is to pick out the *same* solution $\phi^{\rm cl}$ purely within $\mathcal{R}$. Across $\overline{\mathcal{R}}$, this solution is continuous, and its normal derivative is also continuous. But when we split the path integral into the portions on $\mathcal{R}$ and $\mathcal{R}^{\mathsf{c}}$, and prior to carrying out the integral over $\bar{\phi}$, the normal derivatives of the inner and outer saddles do not match. The net result of the $\mathcal{D}\bar{\phi}$ integral is to enforce the boundary condition (3.75), which is precisely the statement that the two normal derivatives match. This ensures that we have found $\phi^{\rm cl}$. Since this solution was originally picked out by standard boundary conditions at the IR and UV ends of the full geometry, it naturally does not satisfy any simple requirement on the intermediate surface $\overline{\mathcal{R}}$. This explains the nonlocal nature of (3.75): the correct normal derivative at any given point depends on the value of $\bar{\phi}$ all over $\overline{\partial\mathcal{R}}$.

3.5.3 Conclusions

In this project, we dive into the problem of finding the correct prescription for computing holographically CFT correlators using the gravitational information inside the entanglement wedge. We emphasized that the GKPW prescription is insufficient to calculate those correlators because the path integral required for that computation involves the sum over field configuration whose domain is outside the entanglement wedge. Therefore, it was necessary to implement the Wilsonian renormalization technique in a non-standard way to replace the previously mentioned path integral with an equivalent calculation considering the sum of field configurations supported inside the desired region. The result of applying this procedure generates a boundary term, $I_{\rm IR}$, that keeps the memory of whatever is included in the entanglement wedge complement. This opens the possibility of interpreting $I_{\rm IR}$ as the remnant of a possible purification.

Our application of the Wilsonian renormalization technique involved the computation of the path integral for fields supported in the complement of the desired region. At first for simplicity, we considered the Wilsonian reduction for computing CFT correlators considering a wall at $z = \bar{z}$. This type of reduction can be understood as a density matrix reduction in momentum space given the fact that $z = \bar{z}$ is related to the energy cutoff in the CFT [140]. Additionally, in [187] we analyzed the two-point function for operators with large conformal dimensions, namely $\Delta \gg d$. Holographically, it is possible to calculate the two-point function using the length of a geodesic in the bulk that has both of its endpoints located on the AdS boundary. The two-point function can be calculated by exponentiating the length of that geodesic. Our now 'rememorization' technique has much wider applicability than what was observed in [187]. In particular, it would be interesting to apply it in the context of black hole geometries, to obtain an effective description of the exterior region in the spirit of the membrane paradigm [139].

Bibliography

[1] A. Einstein, B. Podolsky and N. Rosen, Phys. Rev. **47** (1935), 777-780 doi:10.1103/PhysRev.47.777

[2] J. M. Maldacena, "The large N limit of superconformal field theories and supergravity," Adv. Theor. Math. Phys. **2**, 231 (1998) [Int. J. Theor. Phys. **38**, 1113 (1999)] [arXiv:hep-th/9711200].

[3] S. S. Gubser, I. R. Klebanov and A. M. Polyakov, "Gauge theory correlators from non-critical string theory," Phys. Lett. B **428**, 105 (1998) [arXiv:hep-th/9802109].

[4] E. Witten, "Anti-de Sitter space and holography," Adv. Theor. Math. Phys. **2**, 253 (1998) [arXiv:hep-th/9802150].

[5] J. M. Maldacena, "Eternal black holes in anti-de Sitter," JHEP **04** (2003), 021 doi:10.1088/1126-6708/2003/04/021 [arXiv:hep-th/0106112 [hep-th]].

[6] M. Van Raamsdonk, "Comments on quantum gravity and entanglement," arXiv:0907.2939 [hep-th];
"A patchwork description of dual spacetimes in AdS/CFT," Class. Quant. Grav. **28** (2011) 065002.

[7] B. Swingle, "Entanglement Renormalization and Holography," Phys. Rev. D **86** (2012) 065007 [arXiv:0905.1317 [cond-mat.str-el]];
"Constructing holographic spacetimes using entanglement renormalization," arXiv:1209.3304 [hep-th].

[8] J. Maldacena and L. Susskind, "Cool horizons for entangled black holes," Fortsch. Phys. **61** (2013), 781-811 [arXiv:1306.0533 [hep-th]].

[9] E. Witten, "Notes on some entanglement properties of quantum field theory," Rev. Mod. Phys. **90** (2018) no.4, 045003 [arXiv:1803.04993 [hep-th]].

[10] S. Ryu and T. Takayanagi, "Holographic derivation of entanglement entropy from AdS/CFT," Phys. Rev. Lett. **96** (2006) 181602 [hep-th/0603001].

[11] V. E. Hubeny, M. Rangamani and T. Takayanagi, "A Covariant holographic entanglement entropy proposal," JHEP **0707** (2007) 062 [arXiv:0705.0016 [hep-th]].

[12] D. Garfinkle, G. T. Horowitz and A. Strominger, Phys. Rev. D **43** (1991), 3140 [erratum: Phys. Rev. D **45** (1992), 3888] doi:10.1103/PhysRevD.43.3140

[13] A. Lewkowycz and J. Maldacena, "Generalized gravitational entropy," JHEP **1308** (2013) 090 [arXiv:1304.4926 [hep-th]].

[14] M. Headrick, R. C. Myers and J. Wien, JHEP **10** (2014), 149 doi:10.1007/JHEP10(2014)149 [arXiv:1408.4770 [hep-th]].

[15] X. Dong, A. Lewkowycz and M. Rangamani, "Deriving covariant holographic entanglement," JHEP **1611** (2016) 028 [arXiv:1607.07506 [hep-th]].

[16] T. Barrella, X. Dong, S. A. Hartnoll and V. L. Martin, "Holographic entanglement beyond classical gravity," JHEP **1309** (2013) 109 [arXiv:1306.4682 [hep-th]].

[17] T. Faulkner, A. Lewkowycz and J. Maldacena, "Quantum corrections to holographic entanglement entropy," JHEP **1311** (2013) 074 [arXiv:1307.2892 [hep-th]].

[18] N. Engelhardt and A. C. Wall, "Quantum Extremal Surfaces: Holographic Entanglement Entropy beyond the Classical Regime," JHEP **1501** (2015) 073 [arXiv:1408.3203 [hep-th]].

[19] X. Dong, "Holographic Entanglement Entropy for General Higher Derivative Gravity," JHEP **1401** (2014) 044 [arXiv:1310.5713 [hep-th]].

[20] J. Camps, "Generalized entropy and higher derivative Gravity," JHEP **1403** (2014) 070 [arXiv:1310.6659 [hep-th]].

[21] B. Czech, J. L. Karczmarek, F. Nogueira and M. Van Raamsdonk, "The Gravity Dual of a Density Matrix," Class. Quant. Grav. **29** (2012) 155009 [arXiv:1204.1330 [hep-th]].

[22] A. C. Wall, "Maximin Surfaces, and the Strong Subadditivity of the Covariant Holographic Entanglement Entropy," Class. Quant. Grav. **31** (2014) no.22, 225007 [arXiv:1211.3494 [hep-th]].

[23] S. Sachdev, Phys. Rev. Lett. **105** (2010), 151602 doi:10.1103/PhysRevLett.105.151602 [arXiv:1006.3794 [hep-th]].

[24] A. Almheiri and J. Polchinski, JHEP **11** (2015), 014 doi:10.1007/JHEP11(2015)014 [arXiv:1402.6334 [hep-th]].

[25] F. A. Smirnov and A. B. Zamolodchikov, Nucl. Phys. B **915** (2017), 363-383 doi:10.1016/j.nuclphysb.2016.12.014 [arXiv:1608.05499 [hep-th]].

[26] L. McGough, M. Mezei and H. Verlinde, JHEP **04** (2018), 010 doi:10.1007/JHEP04(2018)010 [arXiv:1611.03470 [hep-th]].

[27] K. Skenderis, Class. Quant. Grav. **19** (2002), 5849-5876 doi:10.1088/0264-9381/19/22/306 [arXiv:hep-th/0209067 [hep-th]].

[28] D. Mateos and D. Trancanelli, JHEP **07** (2011), 054 doi:10.1007/JHEP07(2011)054 [arXiv:1106.1637 [hep-th]].

[29] V. Jahnke, A. S. Misobuchi and D. Trancanelli, JHEP **01** (2015), 122 doi:10.1007/JHEP01(2015)122 [arXiv:1411.5964 [hep-th]].

[30] E. D'Hoker and P. Kraus, JHEP **10** (2009), 088 doi:10.1088/1126-6708/2009/10/088 [arXiv:0908.3875 [hep-th]].

[31] A. C. Wall, Class. Quant. Grav. **31** (2014) no.22, 225007 doi:10.1088/0264-9381/31/22/225007 [arXiv:1211.3494 [hep-th]].

[32] T. Nishioka, Rev. Mod. Phys. **90** (2018) no.3, 035007 doi:10.1103/RevModPhys.90.035007 [arXiv:1801.10352 [hep-th]].

[33] M. Rangamani and T. Takayanagi, Lect. Notes Phys. **931** (2017), pp.1-246 Springer, 2017, doi:10.1007/978-3-319-52573-0 [arXiv:1609.01287 [hep-th]].

[34] P. H. Ginsparg, [arXiv:hep-th/9108028 [hep-th]].

[35] B. Czech, J. L. Karczmarek, F. Nogueira and M. Van Raamsdonk, Class. Quant. Grav. **29** (2012), 155009 doi:10.1088/0264-9381/29/15/155009 [arXiv:1204.1330 [hep-th]].

[36] D. Harlow, Commun. Math. Phys. **354** (2017) no.3, 865-912 doi:10.1007/s00220-017-2904-z [arXiv:1607.03901 [hep-th]].

[37] A. W. Peet and J. Polchinski, Phys. Rev. D **59** (1999), 065011 doi:10.1103/PhysRevD.59.065011 [arXiv:hep-th/9809022 [hep-th]].

[38] V. Balasubramanian, B. D. Chowdhury, B. Czech, J. de Boer and M. P. Heller, Phys. Rev. D **89** (2014) no.8, 086004 doi:10.1103/PhysRevD.89.086004 [arXiv:1310.4204 [hep-th]].

[39] L. Susskind and E. Witten, [arXiv:hep-th/9805114 [hep-th]].

[40] M. Headrick, V. E. Hubeny, A. Lawrence and M. Rangamani, "Causality & holographic entanglement entropy," JHEP **1412** (2014) 162 [arXiv:1408.6300 [hep-th]].

[41] I. Bena, "On the construction of local fields in the bulk of AdS(5) and other spaces," Phys. Rev. D **62** (2000) 066007 [hep-th/9905186].

[42] A. Hamilton, D. N. Kabat, G. Lifschytz and D. A. Lowe, "Local bulk operators in AdS/CFT: A Boundary view of horizons and locality," Phys. Rev. D **73** (2006) 086003 [hep-th/0506118];
"Holographic representation of local bulk operators," Phys. Rev. D **74** (2006) 066009 [hep-th/0606141];
"Local bulk operators in AdS/CFT: A Holographic description of the black hole interior," Phys. Rev. D **75** (2007) 106001 Erratum: [Phys. Rev. D **75** (2007) 129902] [hep-th/0612053].

[43] I. Heemskerk, D. Marolf, J. Polchinski and J. Sully, "Bulk and Transhorizon Measurements in AdS/CFT," JHEP **1210** (2012) 165 [arXiv:1201.3664 [hep-th]].

[44] R. Bousso, S. Leichenauer and V. Rosenhaus, "Light-sheets and AdS/CFT," Phys. Rev. D **86** (2012) 046009 [arXiv:1203.6619 [hep-th]].

[45] K. Papadodimas and S. Raju, "An Infalling Observer in AdS/CFT," JHEP **10** (2013), 212 [arXiv:1211.6767 [hep-th]];
"State-Dependent Bulk-Boundary Maps and Black Hole Complementarity," Phys. Rev. D **89** (2014) no.8, 086010 [arXiv:1310.6335 [hep-th]];
"Black Hole Interior in the Holographic Correspondence and the Information Paradox," Phys. Rev. Lett. **112** (2014) no.5, 051301 [arXiv:1310.6334 [hep-th]];
"Remarks on the necessity and implications of state-dependence in the black hole interior," Phys. Rev. D **93** (2016) no.8, 084049 [arXiv:1503.08825 [hep-th]].

[46] I. A. Morrison, "Boundary-to-bulk maps for AdS causal wedges and the Reeh-Schlieder property in holography," JHEP **1405** (2014) 053 [arXiv:1403.3426 [hep-th]].

[47] D. L. Jafferis, A. Lewkowycz, J. Maldacena and S. J. Suh, "Relative entropy equals bulk relative entropy," JHEP **1606** (2016) 004 [arXiv:1512.06431 [hep-th]].

[48] X. Dong, D. Harlow and A. C. Wall, "Reconstruction of Bulk Operators within the Entanglement Wedge in Gauge-Gravity Duality," Phys. Rev. Lett. **117** (2016) no.2, 021601 [arXiv:1601.05416 [hep-th]].

[49] T. Faulkner and A. Lewkowycz, "Bulk locality from modular flow," JHEP **1707** (2017) 151 [arXiv:1704.05464 [hep-th]].

[50] J. Cotler, P. Hayden, G. Penington, G. Salton, B. Swingle and M. Walter, "Entanglement Wedge Reconstruction via Universal Recovery Channels," Phys. Rev. X **9** (2019) no.3, 031011 [arXiv:1704.05839 [hep-th]].

[51] J. W. Kim, "Explicit reconstruction of the entanglement wedge," JHEP **1701** (2017) 131 [arXiv:1607.03605 [hep-th]].

[52] A. Almheiri, T. Anous and A. Lewkowycz, "Inside out: meet the operators inside the horizon. On bulk reconstruction behind causal horizons," JHEP **01** (2018), 028 [arXiv:1707.06622 [hep-th]].

[53] C. F. Chen, G. Penington and G. Salton, "Entanglement Wedge Reconstruction using the Petz Map," JHEP **01** (2020), 168 [arXiv:1902.02844 [hep-th]].

[54] A. Almheiri, X. Dong and D. Harlow, "Bulk Locality and Quantum Error Correction in AdS/CFT," JHEP **1504** (2015) 163 [arXiv:1411.7041 [hep-th]].

[55] D. Harlow, "The Ryu–Takayanagi Formula from Quantum Error Correction," Commun. Math. Phys. **354** (2017) no.3, 865-912 [arXiv:1607.03901 [hep-th]].

[56] C. Akers and G. Penington, "Quantum minimal surfaces from quantum error correction," [arXiv:2109.14618 [hep-th]].

[57] D. Harlow, "TASI Lectures on the Emergence of the Bulk in AdS/CFT," arXiv:1802.01040 [hep-th].

[58] T. De Jonckheere, "Modave lectures on bulk reconstruction in AdS/CFT," PoS Modave **2017** (2018) 005 [arXiv:1711.07787 [hep-th]].

[59] N. Kajuri, "Lectures on Bulk Reconstruction," SciPost Phys. Lect. Notes **22** (2021), 1 [arXiv:2003.00587 [hep-th]].

[60] B. Chen, B. Czech and Z. z. Wang, "Quantum Information in Holographic Duality," [arXiv:2108.09188 [hep-th]].

[61] T. Kibe, P. Mandayam and A. Mukhopadhyay, "Holographic spacetime, black holes and quantum error correcting codes: A review," [arXiv:2110.14669 [hep-th]].

[62] C. Akers, J. Koeller, S. Leichenauer and A. Levine, "Geometric Constraints from Subregion Duality Beyond the Classical Regime," [arXiv:1610.08968 [hep-th]].

[63] E. Cáceres, A. S. Misobuchi and J. F. Pedraza, "Constraining higher order gravities with subregion duality," JHEP **11**, 175 (2019) [arXiv:1907.08021 [hep-th]].

[64] I. Heemskerk, J. Penedones, J. Polchinski and J. Sully, "Holography from Conformal Field Theory," JHEP **10** (2009), 079 [arXiv:0907.0151 [hep-th]].

[65] M. Henningson and K. Skenderis, "The Holographic Weyl anomaly," JHEP **07** (1998), 023 [arXiv:hep-th/9806087 [hep-th]].

[66] V. Balasubramanian and P. Kraus, "A Stress tensor for Anti-de Sitter gravity," Commun. Math. Phys. **208** (1999), 413-428 [arXiv:hep-th/9902121 [hep-th]].

[67] R. Emparan, C. V. Johnson and R. C. Myers, "Surface terms as counterterms in the AdS / CFT correspondence," Phys. Rev. D **60** (1999), 104001 [arXiv:hep-th/9903238 [hep-th]].

[68] S. de Haro, S. N. Solodukhin and K. Skenderis, "Holographic reconstruction of space-time and renormalization in the AdS / CFT correspondence," Commun. Math. Phys. **217** (2001), 595-622 [arXiv:hep-th/0002230 [hep-th]].

[69] K. Skenderis, "Lecture notes on holographic renormalization," Class. Quant. Grav. **19** (2002), 5849-5876 [arXiv:hep-th/0209067 [hep-th]].

[70] I. Heemskerk and J. Polchinski, 'Holographic and Wilsonian Renormalization Groups," JHEP **06** (2011), 031 doi:10.1007/JHEP06(2011)031 [arXiv:1010.1264 [hep-th]].

[71] T. Faulkner, H. Liu and M. Rangamani, "Integrating out geometry: Holographic Wilsonian RG and the membrane paradigm," JHEP **08** (2011), 051 doi:10.1007/JHEP08(2011)051 [arXiv:1010.4036 [hep-th]].

[72] V. Balasubramanian, M. Guica and A. Lawrence, "Holographic Interpretations of the Renormalization Group," JHEP **01** (2013), 115 doi:10.1007/JHEP01(2013)115 [arXiv:1211.1729 [hep-th]].

[73] T. Banks, M. R. Douglas, G. T. Horowitz and E. J. Martinec, "AdS dynamics from conformal field theory," hep-th/9808016.

[74] V. Balasubramanian, P. Kraus, A. E. Lawrence and S. P. Trivedi, "Holographic probes of anti-de Sitter space-times," Phys. Rev. D **59** (1999), 104021 [arXiv:hep-th/9808017 [hep-th]].

[75] D. Harlow and D. Stanford, "Operator Dictionaries and Wave Functions in AdS/CFT and dS/CFT," [arXiv:1104.2621 [hep-th]].

[76] R. Espíndola, A. Güijosa and J. F. Pedraza, "Entanglement Wedge Reconstruction and Entanglement of Purification," Eur. Phys. J. C **78** (2018) no.8, 646 [arXiv:1804.05855 [hep-th]].

[77] V. Balasubramanian, B. D. Chowdhury, B. Czech, J. de Boer and M. P. Heller, "Bulk curves from boundary data in holography," Phys. Rev. D **89** (2014) no.8, 086004 [arXiv:1310.4204 [hep-th]].

[78] B. M. Terhal, M. Horodecki, D. W. Leung, D. P. DiVincenzo, "The entanglement of purification," J. Math. Phys. **43**, 4286–4298 (2002) [arXiv:quant-ph/0202044].

[79] T. Takayanagi and K. Umemoto, "Holographic Entanglement of Purification," arXiv:1708.09393 [hep-th].

[80] T. Nishioka, S. Ryu and T. Takayanagi, J. Phys. A **42** (2009), 504008 doi:10.1088/1751-8113/42/50/504008 [arXiv:0905.0932 [hep-th]].

[81] P. Nguyen, T. Devakul, M. G. Halbasch, M. P. Zaletel and B. Swingle, "Entanglement of purification: from spin chains to holography," JHEP **1801** (2018) 098 [arXiv:1709.07424 [hep-th]].

[82] N. Bao, A. Chatwin-Davies, B. E. Niehoff and M. Usatyuk, "Bulk Reconstruction Beyond the Entanglement Wedge," Phys. Rev. D **101** (2020) no.6, 066011 [arXiv:1911.00519 [hep-th]].

[83] N. Bao, C. Cao, S. Fischetti and C. Keeler, "Towards Bulk Metric Reconstruction from Extremal Area Variations," Class. Quant. Grav. **36** (2019) no.18, 185002 [arXiv:1904.04834 [hep-th]];
N. Bao, C. Cao, S. Fischetti, J. Pollack and Y. Zhong, "More of the Bulk from Extremal Area Variations," Class. Quant. Grav. **38** (2021) no.4, 047001 [arXiv:2009.07850 [hep-th]].

[84] S. J. Rey and J. T. Yee, "Macroscopic strings as heavy quarks in large N gauge theory and anti-de Sitter supergravity," Eur. Phys. J. C **22** (2001) 379 [arXiv:hep-th/9803001].

[85] J. M. Maldacena, "Wilson loops in large N field theories," Phys. Rev. Lett. **80** (1998) 4859 [arXiv:hep-th/9803002].

[86] N. Engelhardt and A. C. Wall, "Decoding the Apparent Horizon: Coarse-Grained Holographic Entropy," Phys. Rev. Lett. **121** (2018) no.21, 211301 [arXiv:1706.02038 [hep-th]];
"Coarse Graining Holographic Black Holes," JHEP **05** (2019), 160 [arXiv:1806.01281 [hep-th]].

[87] N. Engelhardt and S. Fischetti, "Losing the IR: a Holographic Framework for Area Theorems," Class. Quant. Grav. **36** (2019) no.3, 035008 [arXiv:1805.08891 [hep-th]].

[88] Y. Nomura, P. Rath and N. Salzetta, "Pulling the Boundary into the Bulk," Phys. Rev. D **98** (2018) no.2, 026010 [arXiv:1805.00523 [hep-th]];
C. Murdia, Y. Nomura and P. Rath, "Coarse-Graining Holographic States: A Semiclassical Flow in General Spacetimes," Phys. Rev. D **102** (2020) no.8, 086001 [arXiv:2008.01755 [hep-th]].

[89] B. Czech, J. De Boer, D. Ge and L. Lamprou, "A modular sewing kit for entanglement wedges," JHEP **11** (2019), 094 [arXiv:1903.04493 [hep-th]].

[90] B. Chen, B. Czech and Z. z. Wang, "Query complexity and cutoff dependence of the CFT_2 ground state," Phys. Rev. D **103** (2021) no.2, 026015 [arXiv:2004.11377 [hep-th]].

[91] A. Karch and L. Randall, "Locally localized gravity," JHEP **05** (2001), 008 [arXiv:hep-th/0011156 [hep-th]];
"Localized gravity in string theory," Phys. Rev. Lett. **87** (2001), 061601 [arXiv:hep-th/0105108 [hep-th]].

[92] A. Karch and L. Randall, "Open and closed string interpretation of SUSY CFT's on branes with boundaries," JHEP **06** (2001), 063 [arXiv:hep-th/0105132 [hep-th]].

[93] T. Takayanagi, "Holographic Dual of BCFT," Phys. Rev. Lett. **107** (2011), 101602 [arXiv:1105.5165 [hep-th]];
M. Fujita, T. Takayanagi and E. Tonni, "Aspects of AdS/BCFT," JHEP **11** (2011), 043 doi:10.1007/JHEP11(2011)043 [arXiv:1108.5152 [hep-th]];
M. Nozaki, T. Takayanagi and T. Ugajin, "Central Charges for BCFTs and Holography," JHEP **06** (2012), 066 [arXiv:1205.1573 [hep-th]].

[94] R. X. Miao, C. S. Chu and W. Z. Guo, "New proposal for a holographic boundary conformal field theory," Phys. Rev. D **96** (2017) no.4, 046005 [arXiv:1701.04275 [hep-th]];
"On New Proposal for Holographic BCFT," JHEP **04** (2017), 089 [arXiv:1701.07202 [hep-th]];
R. X. Miao, "Holographic BCFT with Dirichlet Boundary Condition," JHEP **02** (2019), 025 [arXiv:1806.10777 [hep-th]].

[95] M. Miyaji and T. Takayanagi, "Surface/State Correspondence as a Generalized Holography," PTEP **2015** (2015) no.7, 073B03 [arXiv:1503.03542 [hep-th]];
M. Miyaji, T. Numasawa, N. Shiba, T. Takayanagi and K. Watanabe, "Continuous Multiscale Entanglement Renormalization Ansatz as Holographic Surface-State Correspondence," Phys. Rev. Lett. **115** (2015) no.17, 171602 [arXiv:1506.01353 [hep-th]].

[96] B. Grado-White, D. Marolf and S. J. Weinberg, "Radial Cutoffs and Holographic Entanglement," JHEP **01** (2021), 009 [arXiv:2008.07022 [hep-th]].

[97] P. Caputa, N. Kundu, M. Miyaji, T. Takayanagi and K. Watanabe, "Anti-de Sitter Space from Optimization of Path Integrals in Conformal Field Theories," Phys. Rev. Lett. **119** (2017) no.7, 071602 [arXiv:1703.00456 [hep-th]];
P. Caputa, N. Kundu, M. Miyaji, T. Takayanagi and K. Watanabe, "Liouville Action as Path-Integral Complexity: From Continuous Tensor Networks to AdS/CFT," JHEP **11** (2017), 097 [arXiv:1706.07056 [hep-th]];
H. A. Camargo, M. P. Heller, R. Jefferson and J. Knaute, "Path integral optimization as circuit complexity," Phys. Rev. Lett. **123** (2019) no.1, 011601 [arXiv:1904.02713 [hep-th]];
J. Boruch, P. Caputa and T. Takayanagi, "Path-Integral Optimization from Hartle-Hawking Wave Function," Phys. Rev. D **103** (2021) no.4, 046017 [arXiv:2011.08188 [hep-th]];
J. Boruch, P. Caputa, D. Ge and T. Takayanagi, "Holographic Path-Integral Optimization," [arXiv:2104.00010 [hep-th]].

[98] T. Takayanagi, "Holographic Spacetimes as Quantum Circuits of Path-Integrations," JHEP **12** (2018), 048 [arXiv:1808.09072 [hep-th]];
T. Shimaji, T. Takayanagi and Z. Wei, "Holographic Quantum Circuits from Splitting/Joining Local Quenches," JHEP **03** (2019), 165 [arXiv:1812.01176 [hep-th]];
A. R. Chandra, J. de Boer, M. Flory, M. P. Heller, S. Hörtner and A. Rolph, "Spacetime as a quantum circuit," JHEP **21** (2020), 207 [arXiv:2101.01185 [hep-th]].

[99] X. L. Qi, "Exact holographic mapping and emergent space-time geometry," arXiv:1309.6282 [hep-th].

[100] F. Pastawski, B. Yoshida, D. Harlow and J. Preskill, "Holographic quantum error-correcting codes: Toy models for the bulk/boundary correspondence," JHEP **1506** (2015) 149 [arXiv:1503.06237 [hep-th]].

[101] P. Hayden, S. Nezami, X. L. Qi, N. Thomas, M. Walter and Z. Yang, "Holographic duality from random tensor networks," JHEP **1611** (2016) 009 [arXiv:1601.01694 [hep-th]].

[102] N. Bao, G. Penington, J. Sorce and A. C. Wall, "Beyond Toy Models: Distilling Tensor Networks in Full AdS/CFT," JHEP **11** (2019), 069 [arXiv:1812.01171 [hep-th]].

[103] D. Marolf and H. Maxfield, "Transcending the ensemble: baby universes, spacetime wormholes, and the order and disorder of black hole information," JHEP **08** (2020), 044 [arXiv:2002.08950 [hep-th]].

[104] K. Langhoff and Y. Nomura, "Ensemble from Coarse Graining: Reconstructing the Interior of an Evaporating Black Hole," Phys. Rev. D **102** (2020) no.8, 086021 [arXiv:2008.04202 [hep-th]];
Y. Nomura, "Black Hole Interior in Unitary Gauge Construction," Phys. Rev. D **103** (2021) no.6, 066011 [arXiv:2010.15827 [hep-th]].

[105] D. Neuenfeld, "Double Holography as a Model for Black Hole Complementarity," [arXiv:2105.01130 [hep-th]].

[106] G. Penington, "Entanglement Wedge Reconstruction and the Information Paradox," JHEP **09** (2020), 002 [arXiv:1905.08255 [hep-th]].

[107] A. Almheiri, N. Engelhardt, D. Marolf and H. Maxfield, "The entropy of bulk quantum fields and the entanglement wedge of an evaporating black hole," JHEP **12** (2019), 063 [arXiv:1905.08762 [hep-th]].

[108] A. Almheiri, R. Mahajan, J. Maldacena and Y. Zhao, "The Page curve of Hawking radiation from semiclassical geometry," JHEP **03** (2020), 149 [arXiv:1908.10996 [hep-th]].

[109] A. Almheiri, T. Hartman, J. Maldacena, E. Shaghoulian and A. Tajdini, "Replica Wormholes and the Entropy of Hawking Radiation," JHEP **05** (2020), 013 [arXiv:1911.12333 [hep-th]].

[110] G. Penington, S. H. Shenker, D. Stanford and Z. Yang, "Replica wormholes and the black hole interior," [arXiv:1911.11977 [hep-th]].

[111] J. F. Pedraza, A. Svesko, W. Sybesma and M. R. Visser, "Microcanonical Action and the Entropy of Hawking Radiation," [arXiv:2111.06912 [hep-th]].

[112] J. McNamara and C. Vafa, "Baby Universes, Holography, and the Swampland," [arXiv:2004.06738 [hep-th]].

[113] J. J. Heckman, A. P. Turner and X. Yu, "Disorder Averaging and its UV (Dis)Contents," [arXiv:2111.06404 [hep-th]].

[114] V. Balasubramanian, M. B. McDermott and M. Van Raamsdonk, "Momentum-space entanglement and renormalization in quantum field theory," Phys. Rev. D **86** (2012), 045014 [arXiv:1108.3568 [hep-th]].

[115] V. Balasubramanian and S. F. Ross, "Holographic particle detection," Phys. Rev. D **61**, 044007 (2000) [arXiv:hep-th/9906226 [hep-th]].

[116] J. Louko, D. Marolf and S. F. Ross, "On geodesic propagators and black hole holography," Phys. Rev. D **62**, 044041 (2000) [arXiv:hep-th/0002111 [hep-th]].

[117] S. Grozdanov, "Wilsonian Renormalisation and the Exact Cut-Off Scale from Holographic Duality," JHEP **06** (2012), 079 [arXiv:1112.3356 [hep-th]].

[118] E. Kiritsis, W. Li and F. Nitti, "Holographic RG flow and the Quantum Effective Action," Fortsch. Phys. **62** (2014), 389-454 [arXiv:1401.0888 [hep-th]].

[119] C. A. Agón, A. Güijosa and J. F. Pedraza, "Radiation and a dynamical UV/IR connection in AdS/CFT," JHEP **06** (2014), 043 [arXiv:1402.5961 [hep-th]].

[120] L. Randall and R. Sundrum, "An Alternative to compactification," Phys. Rev. Lett. **83** (1999), 4690-4693 [arXiv:hep-th/9906064 [hep-th]].

[121] H. L. Verlinde, "Holography and compactification," Nucl. Phys. B **580** (2000), 264-274 [arXiv:hep-th/9906182 [hep-th]].

[122] S. S. Gubser, "AdS / CFT and gravity," Phys. Rev. D **63** (2001), 084017 doi:10.1103/PhysRevD.63.084017 [arXiv:hep-th/9912001 [hep-th]].

[123] H. Geng and A. Karch, "Massive islands," JHEP **09** (2020), 121 [arXiv:2006.02438 [hep-th]].

[124] H. Z. Chen, R. C. Myers, D. Neuenfeld, I. A. Reyes and J. Sandor, "Quantum Extremal Islands Made Easy, Part I: Entanglement on the Brane," JHEP **10** (2020), 166 [arXiv:2006.04851 [hep-th]];
"Quantum Extremal Islands Made Easy, Part II: Black Holes on the Brane," JHEP **12** (2020), 025 [arXiv:2010.00018 [hep-th]].

[125] H. Omiya and Z. Wei, "Causal Structures and Nonlocality in Double Holography," [arXiv:2107.01219 [hep-th]].

[126] H. Geng, A. Karch, C. Perez-Pardavila, S. Raju, L. Randall, M. Riojas and S. Shashi, "Information Transfer with a Gravitating Bath," SciPost Phys. **10** (2021) no.5, 103, [arXiv:2012.04671 [hep-th]];
"Inconsistency of Islands in Theories with Long-Range Gravity," [arXiv:2107.03390 [hep-th]].

[127] D. Harlow, "Wormholes, Emergent Gauge Fields, and the Weak Gravity Conjecture," JHEP **01** (2016), 122 [arXiv:1510.07911 [hep-th]].

[128] W. Donnelly and L. Freidel, "Local subsystems in gauge theory and gravity," JHEP **09** (2016), 102 [arXiv:1601.04744 [hep-th]].

[129] D. L. Jafferis, "Bulk reconstruction and the Hartle-Hawking wavefunction," [arXiv:1703.01519 [hep-th]].

[130] H. Gomes, F. Hopfmüller and A. Riello, "A unified geometric framework for boundary charges and dressings: non-Abelian theory and matter," Nucl. Phys. B **941** (2019), 249-315 [arXiv:1808.02074 [hep-th]].

[131] X. Dong, D. Harlow and D. Marolf, "Flat entanglement spectra in fixed-area states of quantum gravity," JHEP **10** (2019), 240 [arXiv:1811.05382 [hep-th]].

[132] C. Akers and P. Rath, "Holographic Renyi Entropy from Quantum Error Correction," JHEP **05** (2019), 052 doi:10.1007/JHEP05(2019)052 [arXiv:1811.05171 [hep-th]].

[133] S. B. Giddings and A. Kinsella, "Gauge-invariant observables, gravitational dressings, and holography in AdS," JHEP **11** (2018), 074 [arXiv:1802.01602 [hep-th]];
W. Donnelly and S. B. Giddings, "Gravitational splitting at first order: Quantum information localization in gravity," Phys. Rev. D **98** (2018) no.8, 086006 [arXiv:1805.11095 [hep-th]];
S. B. Giddings, "Gravitational dressing, soft charges, and perturbative gravitational splitting," Phys. Rev. D **100** (2019) no.12, 126001 [arXiv:1903.06160 [hep-th]];
S. Giddings and S. Weinberg, "Gauge-invariant observables in gravity and electromagnetism: black hole backgrounds and null dressings," Phys. Rev. D **102** (2020) no.2, 026010 [arXiv:1911.09115 [hep-th]];
S. B. Giddings, "Gravitational dressing, soft charges, and perturbative gravitational splitting," Phys. Rev. D **100** (2019) no.12, 126001 [arXiv:1903.06160 [hep-th]].

[134] L. Freidel, M. Geiller and D. Pranzetti, "Edge modes of gravity. Part I. Corner potentials and charges," JHEP **11** (2020), 026 [arXiv:2006.12527 [hep-th]];
"Edge modes of gravity. Part II. Corner metric and Lorentz charges," JHEP **11** (2020), 027 [arXiv:2007.03563 [hep-th]];
"Edge modes of gravity. Part III. Corner simplicity constraints," JHEP **01** (2021), 100 [arXiv:2007.12635 [hep-th]];
W. Donnelly, L. Freidel, S. F. Moosavian and A. J. Speranza, "Gravitational edge modes, coadjoint orbits, and hydrodynamics," JHEP **09** (2021), 008 [arXiv:2012.10367 [hep-th]];
L. Freidel, R. Oliveri, D. Pranzetti and S. Speziale, "Extended corner symmetry, charge bracket and Einstein's equations," JHEP **09** (2021), 083 [arXiv:2104.12881 [hep-th]];
L. Freidel, "A canonical bracket for open gravitational system," [arXiv:2111.14747 [hep-th]].

[135] A. Laddha, S. G. Prabhu, S. Raju and P. Shrivastava, "The Holographic Nature of Null Infinity," SciPost Phys. **10** (2021) no.2, 041 [arXiv:2002.02448 [hep-th]];
C. Chowdhury, O. Papadoulaki and S. Raju, "A physical protocol for observers near the boundary to obtain bulk information in quantum gravity," SciPost Phys. **10** (2021) no.5, 106 [arXiv:2008.01740 [hep-th]];
C. Chowdhury, V. Godet, O. Papadoulaki and S. Raju, "Holography from the Wheeler-DeWitt equation," [arXiv:2107.14802 [hep-th]];
S. Raju, "Failure of the split property in gravity and the information paradox," [arXiv:2110.05470 [hep-th]].

[136] S. B. Giddings, "On the questions of asymptotic recoverability of information and subsystems in quantum gravity," [arXiv:2112.03207 [hep-th]].

[137] K. G. Wilson and J. B. Kogut, "The Renormalization group and the epsilon expansion," Phys. Rept. **12** (1974), 75-199

[138] L. Susskind and E. Witten, "The Holographic bound in anti-de Sitter space," [arXiv:hep-th/9805114 [hep-th]].

[139] T. Damour, Phys. Rev. D **18** (1978), 3598-3604 doi:10.1103/PhysRevD.18.3598

[140] A. W. Peet and J. Polchinski, "UV / IR relations in AdS dynamics," Phys. Rev. D **59** (1999), 065011 [arXiv:hep-th/9809022 [hep-th]].

[141] E. T. Akhmedov, "A Remark on the AdS / CFT correspondence and the renormalization group flow," Phys. Lett. B **442** (1998), 152-158 [arXiv:hep-th/9806217 [hep-th]].

[142] V. Balasubramanian and P. Kraus, "Space-time and the holographic renormalization group," Phys. Rev. Lett. **83** (1999), 3605-3608 [arXiv:hep-th/9903190 [hep-th]].

[143] J. de Boer, E. P. Verlinde and H. L. Verlinde, "On the holographic renormalization group," JHEP **08** (2000), 003 [arXiv:hep-th/9912012 [hep-th]].

[144] S. S. Lee, "Holographic description of quantum field theory," Nucl. Phys. B **832** (2010), 567-585 [arXiv:0912.5223 [hep-th]].

[145] M. R. Douglas, L. Mazzucato and S. S. Razamat, "Holographic dual of free field theory," Phys. Rev. D **83** (2011), 071701 [arXiv:1011.4926 [hep-th]].

[146] V. Shyam, "General Covariance from the Quantum Renormalization Group," Phys. Rev. D **95** (2017) no.6, 066003 [arXiv:1611.05315 [gr-qc]].

[147] E. Witten, Adv. Theor. Math. Phys. **2** (1998), 505-532 doi:10.4310/ATMP.1998.v2.n3.a3 [arXiv:hep-th/9803131 [hep-th]].

[148] S. Ryu and T. Takayanagi, Phys. Rev. Lett. **96** (2006), 181602 doi:10.1103/PhysRevLett.96.181602 [arXiv:hep-th/0603001 [hep-th]].

[149] R. Abt, J. Erdmenger, H. Hinrichsen, C. M. Melby-Thompson, R. Meyer, C. Northe and I. A. Reyes, Fortsch. Phys. **66** (2018) no.6, 1800034 doi:10.1002/prop.201800034 [arXiv:1710.01327 [hep-th]].

[150] N. Engelhardt and A. C. Wall, JHEP **03** (2014), 068 doi:10.1007/JHEP03(2014)068 [arXiv:1312.3699 [hep-th]].

[151] V. E. Hubeny, JHEP **07** (2012), 093 doi:10.1007/JHEP07(2012)093 [arXiv:1203.1044 [hep-th]].

[152] T. Takayanagi and K. Umemoto, Nature Phys. **14** (2018) no.6, 573-577 doi:10.1038/s41567-018-0075-2 [arXiv:1708.09393 [hep-th]].

[153] P. Nguyen, T. Devakul, M. G. Halbasch, M. P. Zaletel and B. Swingle, JHEP **01** (2018), 098 doi:10.1007/JHEP01(2018)098 [arXiv:1709.07424 [hep-th]].

[154] P. A. Cano, R. A. Hennigar and H. Marrochio, Phys. Rev. Lett. **121** (2018) no.12, 121602 doi:10.1103/PhysRevLett.121.121602 [arXiv:1803.02795 [hep-th]].

[155] K. S. Kim, S. Ryu and K. Lee, "Emergent dual holographic description as a non-perturbative generalization of the Wilsonian renormalization group," [arXiv:2112.06237 [hep-th]].

[156] J. Polchinski, "Renormalization and Effective Lagrangians," Nucl. Phys. B **231** (1984), 269-295.

[157] V. Balasubramanian, P. Kraus and A. E. Lawrence, "Bulk versus boundary dynamics in anti-de Sitter space-time," Phys. Rev. D **59** (1999), 046003 [arXiv:hep-th/9805171 [hep-th]].

[158] K. Skenderis and B. C. van Rees, "Real-time gauge/gravity duality," Phys. Rev. Lett. **101** (2008), 081601 doi:10.1103/PhysRevLett.101.081601 [arXiv:0805.0150 [hep-th]];
"Real-time gauge/gravity duality: Prescription, Renormalization and Examples," JHEP **05** (2009), 085 [arXiv:0812.2909 [hep-th]].

[159] C. Imbimbo, A. Schwimmer, S. Theisen and S. Yankielowicz, "Diffeomorphisms and holographic anomalies," Class. Quant. Grav. **17** (2000), 1129-1138 [arXiv:hep-th/9910267 [hep-th]].

[160] H. Osborn, "Weyl consistency conditions and a local renormalization group equation for general renormalizable field theories," Nucl. Phys. B **363** (1991), 486-526.

[161] J. F. Melo and J. E. Santos, "Developing local RG: quantum RG and BFSS," JHEP **05** (2020), 063 [arXiv:1910.09559 [hep-th]].

[162] E. D'Hoker, J. Estes and M. Gutperle, "Exact half-BPS Type IIB interface solutions. I. Local solution and supersymmetric Janus," JHEP **06** (2007), 021 [arXiv:0705.0022 [hep-th]];
"Exact half-BPS Type IIB interface solutions. II. Flux solutions and multi-Janus," JHEP **06** (2007), 022 [arXiv:0705.0024 [hep-th]].

[163] O. Aharony, L. Berdichevsky, M. Berkooz and I. Shamir, "Near-horizon solutions for D3-branes ending on 5-branes," Phys. Rev. D **84** (2011), 126003 [arXiv:1106.1870 [hep-th]];
L. Berdichevsky and B. e. Dahan, "Local gravitational solutions dual to M2-branes intersecting and/or ending on M5-branes," JHEP **08** (2013), 061 [arXiv:1304.4389 [hep-th]].

[164] B. Assel, C. Bachas, J. Estes and J. Gomis, "Holographic Duals of D=3 N=4 Superconformal Field Theories," JHEP **08** (2011), 087 [arXiv:1106.4253 [hep-th]];
C. Bachas, E. D'Hoker, J. Estes and D. Krym, "M-theory Solutions Invariant under $D(2,1;\gamma) \oplus D(2,1;\gamma)$," Fortsch. Phys. **62** (2014), 207-254 [arXiv:1312.5477 [hep-th]].

[165] M. Chiodaroli, E. D'Hoker and M. Gutperle, "Simple Holographic Duals to Boundary CFTs," JHEP **02** (2012), 005 [arXiv:1111.6912 [hep-th]];
"Holographic duals of Boundary CFTs," JHEP **07** (2012), 177 [arXiv:1205.5303 [hep-th]].

[166] P. Hayden, M. Headrick and A. Maloney, "Holographic Mutual Information is Monogamous," Phys. Rev. D **87** (2013) no.4, 046003 [arXiv:1107.2940 [hep-th]].

[167] N. Bao, S. Nezami, H. Ooguri, B. Stoica, J. Sully and M. Walter, "The Holographic Entropy Cone," JHEP **09** (2015), 130 [arXiv:1505.07839 [hep-th]].

[168] S. Hernández Cuenca, "Holographic entropy cone for five regions," Phys. Rev. D **100** (2019) no.2, 2 [arXiv:1903.09148 [hep-th]].

[169] T. He, M. Headrick and V. E. Hubeny, "Holographic Entropy Relations Repackaged," JHEP **10** (2019), 118 [arXiv:1905.06985 [hep-th]];
T. He, M. Headrick and V. E. Hubeny, "Holographic Entropy Relations Repackaged," JHEP **10** (2019), 118 [arXiv:1905.06985 [hep-th]];
T. He, V. E. Hubeny and M. Rangamani, "Superbalance of Holographic Entropy Inequalities," JHEP **07** (2020), 245 [arXiv:2002.04558 [hep-th]].

[170] W. Reeves, M. Rozali, P. Simidzija, J. Sully, C. Waddell and D. Wakeham, "Looking for (and not finding) a bulk brane," JHEP **12** (2021), 002 [arXiv:2108.10345 [hep-th]].

[171] K. Parattu, S. Chakraborty, B. R. Majhi and T. Padmanabhan, "A Boundary Term for the Gravitational Action with Null Boundaries," Gen. Rel. Grav. **48** (2016) no.7, 94 [arXiv:1501.01053 [gr-qc]].
L. Lehner, R. C. Myers, E. Poisson and R. D. Sorkin, "Gravitational action with null boundaries," Phys. Rev. D **94** (2016) no.8, 084046 [arXiv:1609.00207 [hep-th]].

[172] I. R. Klebanov and E. Witten, "AdS / CFT correspondence and symmetry breaking," Nucl. Phys. B **556** (1999), 89-114 [arXiv:hep-th/9905104 [hep-th]].

[173] E. Witten, "Multitrace operators, boundary conditions, and AdS / CFT correspondence," [arXiv:hep-th/0112258 [hep-th]].

[174] M. Berkooz, A. Sever and A. Shomer, "'Double trace' deformations, boundary conditions and space-time singularities," JHEP **05** (2002), 034 [arXiv:hep-th/0112264 [hep-th]].

[175] A. Sever and A. Shomer, "A Note on multitrace deformations and AdS/CFT," JHEP **07** (2002), 027 [arXiv:hep-th/0203168 [hep-th]].

[176] A. Ishibashi and R. M. Wald, "Dynamics in nonglobally hyperbolic static space-times. 3. Anti-de Sitter space-time," Class. Quant. Grav. **21** (2004), 2981-3014 doi:10.1088/0264-9381/21/12/012 [arXiv:hep-th/0402184 [hep-th]].

[177] D. Marolf and S. F. Ross, "Boundary Conditions and New Dualities: Vector Fields in AdS/CFT," JHEP **11** (2006), 085 [arXiv:hep-th/0606113 [hep-th]].

[178] G. Compere and D. Marolf, "Setting the boundary free in AdS/CFT," Class. Quant. Grav. **25** (2008), 195014 [arXiv:0805.1902 [hep-th]].

[179] C. Ecker, W. van der Schee, D. Mateos and J. Casalderrey-Solana, "Holographic Evolution with Dynamical Boundary Gravity," [arXiv:2109.10355 [hep-th]].

[180] L. Brink and M. Henneaux, *Principles of String Theory*, Plenum Press, 1988.

[181] H. Casini and M. Huerta, "Remarks on the entanglement entropy for disconnected regions," JHEP **03** (2009), 048 [arXiv:0812.1773 [hep-th]].

[182] Y. Nakata, T. Takayanagi, Y. Taki, K. Tamaoka and Z. Wei, "New holographic generalization of entanglement entropy," Phys. Rev. D **103** (2021) no.2, 026005 [arXiv:2005.13801 [hep-th]].

[183] R. C. Myers, J. Rao and S. Sugishita, "Holographic Holes in Higher Dimensions," JHEP **1406** (2014) 044 [arXiv:1403.3416 [hep-th]].

[184] B. Czech, X. Dong and J. Sully, "Holographic Reconstruction of General Bulk Surfaces," JHEP **1411** (2014) 015 [arXiv:1406.4889 [hep-th]].

[185] S. A. Hosseini Mansoori, V. Jahnke, M. M. Qaemmaqami and Y. D. Olivas, Phys. Rev. D **100** (2019) no.4, 046014 doi:10.1103/PhysRevD.100.046014 [arXiv:1808.00067 [hep-th]].

[186] B. Czech, Y. D. Olivas and Z. z. Wang, JHEP **12** (2020), 063 doi:10.1007/JHEP12(2020)063 [arXiv:1905.07413 [hep-th]].

[187] A. Guijosa, Y. D. Olivas and J. F. Pedraza, JHEP **08** (2022), 118 doi:10.1007/JHEP08(2022)118 [arXiv:2201.01786 [hep-th]].

[188] D. Mateos and D. Trancanelli, JHEP **07** (2011), 054 doi:10.1007/JHEP07(2011)054 [arXiv:1106.1637 [hep-th]].

[189] A. R. Brown, D. A. Roberts, L. Susskind, B. Swingle and Y. Zhao, Phys. Rev. Lett. **116** (2016) no.19, 191301 doi:10.1103/PhysRevLett.116.191301 [arXiv:1509.07876 [hep-th]].

[190] L. Lehner, R. C. Myers, E. Poisson and R. D. Sorkin, Phys. Rev. D **94** (2016) no.8, 084046 doi:10.1103/PhysRevD.94.084046 [arXiv:1609.00207 [hep-th]].

[191] A. Akhavan and F. Omidi, JHEP **11** (2019), 054 doi:10.1007/JHEP11(2019)054 [arXiv:1906.09561 [hep-th]].

[192] F. Omidi, JHEP **07** (2020), 020 doi:10.1007/JHEP07(2020)020 [arXiv:2004.11628 [hep-th]].

[193] L. Fidkowski, V. Hubeny, M. Kleban and S. Shenker, JHEP **02** (2004), 014 doi:10.1088/1126-6708/2004/02/014 [arXiv:hep-th/0306170 [hep-th]].

[194] D. Ávila, C. Díaz, Y. D. Olivas and L. Patiño, Phys. Rev. D **104** (2021) no.6, 066011 doi:10.1103/PhysRevD.104.066011 [arXiv:2104.12796 [hep-th]].

[195] V. E. Hubeny, "Covariant Residual Entropy," JHEP **1409** (2014) 156 [arXiv:1406.4611 [hep-th]].

[196] M. Headrick, R. C. Myers and J. Wien, "Holographic Holes and Differential Entropy," JHEP **1410** (2014) 149 [arXiv:1408.4770 [hep-th]].

[197] B. Czech and L. Lamprou, "Holographic definition of points and distances," Phys. Rev. D **90** (2014) 106005 [arXiv:1409.4473 [hep-th]].

[198] B. Czech, P. Hayden, N. Lashkari and B. Swingle, "The Information Theoretic Interpretation of the Length of a Curve," JHEP **1506** (2015) 157 [arXiv:1410.1540 [hep-th]].

[199] T. Hartman and J. Maldacena, JHEP **05** (2013), 014 doi:10.1007/JHEP05(2013)014 [arXiv:1303.1080 [hep-th]].

[200] A. Belin, R. C. Myers, S. M. Ruan, G. Sárosi and A. J. Speranza, Phys. Rev. Lett. **128** (2022) no.8, 081602 doi:10.1103/PhysRevLett.128.081602 [arXiv:2111.02429 [hep-th]].

[201] R. Jefferson and R. C. Myers, JHEP **10** (2017), 107 doi:10.1007/JHEP10(2017)107 [arXiv:1707.08570 [hep-th]].

[202] B. Czech, L. Lamprou, S. McCandlish and J. Sully, "Integral Geometry and Holography," JHEP **1510** (2015) 175 [arXiv:1505.05515 [hep-th]].

[203] R. Espíndola, A. Güijosa, A. Landetta and J. F. Pedraza, "What's the point? Hole-ography in Poincaré AdS," Eur. Phys. J. C **78** (2018) no.1, 75 [arXiv:1708.02958 [hep-th]].

[204] V. Balasubramanian and C. Rabideau, "The dual of non-extremal area: differential entropy in higher dimensions," JHEP **09** (2020), 051 [arXiv:1812.06985 [hep-th]].

[205] B. Czech, Y. D. Olivas and Z. z. Wang, "Holographic integral geometry with time dependence," JHEP **12** (2020), 063 [arXiv:1905.07413 [hep-th]].

[206] B. Czech, L. Lamprou, S. McCandlish, B. Mosk and J. Sully, "A Stereoscopic Look into the Bulk," JHEP **1607** (2016) 129 [arXiv:1604.03110 [hep-th]].

[207] J. de Boer, F. M. Haehl, M. P. Heller and R. C. Myers, "Entanglement, holography and causal diamonds," JHEP **1608** (2016) 162 [arXiv:1606.03307 [hep-th]].

[208] M. J. Donald, "On the relative entropy," Commun. Math. Phys. **105**, 13 (1986).

[209] N. Bao and I. F. Halpern, "Holographic Inequalities and Entanglement of Purification," JHEP **1803** (2018) 006 [arXiv:1710.07643 [hep-th]];
"Conditional and Multipartite Entanglements of Purification and Holography," Phys. Rev. D **99** (2019) no.4, 046010 [arXiv:1805.00476 [hep-th]].

[210] K. Umemoto and Y. Zhou, "Entanglement of Purification for Multipartite States and its Holographic Dual," JHEP **10** (2018), 152 [arXiv:1805.02625 [hep-th]].

[211] J. Kudler-Flam and S. Ryu, "Entanglement negativity and minimal entanglement wedge cross sections in holographic theories," Phys. Rev. D **99** (2019) no.10, 106014 [arXiv:1808.00446 [hep-th]];
Y. Kusuki, J. Kudler-Flam and S. Ryu, "Derivation of Holographic Negativity in AdS_3/CFT_2," Phys. Rev. Lett. **123** (2019) no.13, 131603 [arXiv:1907.07824 [hep-th]].

[212] K. Tamaoka, "Entanglement Wedge Cross Section from the Dual Density Matrix," Phys. Rev. Lett. **122** (2019) no.14, 141601 [arXiv:1809.09109 [hep-th]].

[213] S. Dutta and T. Faulkner, "A canonical purification for the entanglement wedge cross-section," JHEP **03** (2021), 178 [arXiv:1905.00577 [hep-th]].

[214] P. Caputa, M. Miyaji, T. Takayanagi and K. Umemoto, "Holographic Entanglement of Purification from Conformal Field Theories," Phys. Rev. Lett. **122** (2019) no.11, 111601 [arXiv:1812.05268 [hep-th]].

[215] R. Haberman, *Applied Partial Differential Equations with Fourier Series and Boundary Value Problems*, Pearson, 2012.

[216] J. Kastikainen and S. Shashi, "Structure of Holographic BCFT Correlators from Geodesics," [arXiv:2109.00079 [hep-th]].

[217] M. Headrick, "Entanglement Renyi entropies in holographic theories," Phys. Rev. D **82** (2010), 126010 [arXiv:1006.0047 [hep-th]].

[218] C. Agón and T. Faulkner, "Quantum Corrections to Holographic Mutual Information," JHEP **08**, 118 (2016) [arXiv:1511.07462 [hep-th]].